Dottorato di Ricerca in Ingegneria dei Prodotti e dei Processi Industriali

Safe production of nitrated intermediates of industrial interest using traditional batch reactors and innovative microdevices

Thesis by

Danilo Russo

Degree of Doctor of Philosophy

in

INDUSTRIAL PRODUCT AND PROCESS ENGINEERING (XXX)

University of Naples "Federico II"

School of Polytechnic and Basic Sciences

Department of Chemical Engineering, Materials and Industrial Production (DICMAPI)

2014 - 2017

Safe production of nitrated intermediates of industrial interest using traditional batch reactors and innovative microdevices

by

Danilo Russo

Tutor: Prof. R. Andreozzi, Prof. S. Guido, Prof. R. Marotta

Co-Tutor: Dr. Ing. I. Di Somma

Course coordinator: Prof. G. Mensitieri

INDEX

List of Figures

List of Tables

List of Symbols

Symbol	Units	Meaning
$[i]$	$mol \cdot L^{-1}$	Molar concentration of the species *i*
T	K	Absolute temperature
γ_i	[-]	Activity coefficient of the species *i*
a_i	$mol \cdot L^{-1}$	Activity of the species *i*
ρ_i	$g \cdot cm^{-3}$	Density of the species *i*
MW_i	$g \cdot mol^{-1}$	Molar weight of the species *i*
X_i	[-]	Molar fraction of the species *i*
τ	s	Residence time
k_{int}	$L \cdot s^{-1} \cdot mol^{-1}$	Intrinsic kinetic constant of nitration
$N\%$	[-]	Nitric acid molar percentage
$S\%$	[-]	Sulfuric acid molar percentage
m_i	$mol \cdot Kg^{-1}$	Molality of the species *i*
N_i	mol	Moles of the species *i*
N_i^{aq}	mol	Moles of the species *i* dissolved in the acidic aqueous phase
V	L	Volume
V^{aq}	L	Volume of the homogeneous acidic aqueous phase
V^{mix}	L	Volume of the aqueous mixture of acids
V_{diss}^{Ar}	L	Volume of the organics dissolved in the acidic aqueous phase
K_i	$mol^n \cdot L^{-n}$	General equilibrium constant
ΔH_i	$J \cdot mol^{-1} \cdot K^{-1}$	General enthalpy change
ΔS_i	$J \cdot mol^{-1}$	General entropy change
K	$mol^2 \cdot L^{-2}$	Equilibrium constant of nitric acid ionization to nitronium ion
K_C	$mol \cdot L^{-1}$	Equilibrium constant of aldehydes coordination with nitronium ion
K_N	$mol \cdot L^{-1}$	Nitric acid dissociation constant
r_i	$mol \cdot L^{-1} \cdot s^{-1}$	General reaction rate
$r_{N,i}$	$mol \cdot L^{-1} \cdot s^{-1}$	Rate of nitration of the species *i*
$r_{ox,i}$	$mol \cdot L^{-1} \cdot s^{-1}$	Rate of oxidation of the species *i*
k'	s^{-1}	Pseudo first-order kinetic constant
$k_{N,i}$	$L \cdot s^{-1} \cdot mol^{-1}$	Intrinsic kinetic constant of nitration of the species *i*
$k_{OX,i}$	s^{-1}	Intrinsic kinetic constant of oxidation of the species *i*

k_N^g	$L \cdot s^{-1} \cdot mol^{-1}$	Global kinetic constant of nitration
$k_{N,i}^0$	$L \cdot s^{-1} \cdot mol^{-1}$	Pre-exponential factor of nitration of the species *i*
$k_{OX,i}^0$	s^{-1}	Pre-exponential factor of oxidation of the species *i*
k_N^{0*}	$L \cdot s^{-1} \cdot mol^{-1}$	Pre-exponential factor of the global kinetic constant of nitration
k'_0	s^{-1}	Pre-exponential factor of pseudo first-order kinetic constant
k_N^0	$L \cdot s^{-1} \cdot mol^{-1}$	Pre-exponential factor of the intrinsic kinetic constant of nitration
E_a	$J \cdot mol^{-1}$	General activation energy
$E_{a,Ni}$	$J \cdot mol^{-1}$	Activation energy of nitration of the species *i*
$E_{a,OXi}$	$J \cdot mol^{-1}$	Activation energy of oxidation of the species *i*
$E_{a,N}$	$J \cdot mol^{-1}$	Activation energy of the intrinsic nitration reaction
H_R	[-]	Acidity function
M_C	[-]	Marziano Acidity Function
n_i	[-]	Factor of proportionality between Marziano Acidity Functions
H_0	[-]	Hammett Acidity Function
A	m^2	Exchange surface
U	$W \cdot m^2 \cdot K^{-1}$	Global heat transfer coefficient
c_P	$J \cdot g^{-1} \cdot K^{-1}$	Mean specific heat of the reacting mixture
P_G	W	Generated thermal power
P_D	W	Dissipated thermal power
Φ	[-]	Thermal inertia
C	$J \cdot g^{-1} \cdot K^{-1}$	Mean specific heat of the reactor material
ΔT_{ad}	K	Adiabatic temperature rise
m_{mix}	g	Mass of the reacting mixture
m_{Ar}	g	Mass of the aromatic species

Abstract

2 and 3- nitrobenzaldehydes are two isomers involved in a wide range of fine chemicals production, from dyes to pesticides. They are also employed in highly priced materials production such as pharmaceuticals, photo-removable protecting groups, and non-linear optical materials. Direct fed-batch nitration of benzaldehyde for their production suffers from different drawbacks such as the difficulties in controlling the two isomers yields at different nitrating agent compositions and the possibility of thermal runaway of the system. Moreover, adopting the traditional processes of production of benzaldehyde, it is impossible to obtain chlorine-free benzaldehyde and high temperatures and pressures are required. In this thesis, the possibility of synthesizing 2 and 3-nitrobenzaldehyde, using both benzyl alcohol and benzaldehyde as a row material, is investigated in concentrated mixtures of nitric and sulfuric acids, i.e. mixed acid. In fact, despite the new interest for innovative and alternative nitrating agents, mixed acid still represents the most used and effective reaction media in nitration processes. The adoption of benzyl alcohol as an alternative organic substrate is attractive since it is a lower priced material obtainable in high purity. In this work a successful attempt of conducting tandem oxidation-nitration reaction in a one step process is shown, highlighting the advantages and the drawbacks of this process and proposing some possible alternative reactor design solutions.

A first investigation was devoted to clarify some aspects concerning nitric acid speciation in concentrated ternary mixture of nitric acid, sulfuric acid and water and the relative influence of the acids concentrations on their dissociation. As a result, different semi-empirical and empirical correlations were proposed to predict nitronium ion concentrations at varying conditions, defining and overcoming the limitations of the conflicting theories proposed in the literature. Moreover, the study of the influence of sulfuric acid on nitric acid dissociation helped in developing more reliable kinetic models.

A kinetic modeling of tandem oxidation-nitration of benzyl alcohol to nitrobenzaldehydes was developed in order to successfully predict the behavior of the reacting system at varying process conditions and clarify the mechanisms of reaction. Specifically, the influence of temperature and composition of the reaction media was clarified. The developed kinetic model elucidated the mechanism of formation of important intermediates such as the coordinated form of nitronium ion with the aldehydic group of benzaldehyde to form ortho-nitrobenzaldehyde.

The intensification of nitrobenzaldehydes synthesis was studied using a commercially available microreactor, which allowed to carry out the process under harsher conditions. As a result, it was possible to produce the two isomers with the highest yields obtained so far.

Finally an extension of the developed model to investigate benzaldehyde nitration kinetics under heterogeneous liquid-liquid conditions was provided.

1. Background

1.1. Nitration processes

1.1.1. Importance of nitration processes

Nitration processes are among the oldest and more common processes in the chemical industry. They are carried out to produce a wide range of bulk and fine chemicals involved in the synthesis of a great variety of chemical products, from the high-throughput production of explosives, fertilizers, pesticides, and dyes to the finest highly priced pharmaceuticals and innovative materials for research and innovation purposes (Urbanski, 1964; Wang et al., 1988; Chen et al., 1998; Kockmann et al., 2009; Kulkarni et al., 2009; Kulkarni, 2014).

All the reactions of addition of an $-NO_2$ group to an organic substrate (often aromatic) are usually included (Hoggett et al., 1971; Olah et al., 1989) under the broad definition of nitration processes. The first reported nitration reaction was the nitration of benzene in red fuming nitric acid, in the first half of the XIX century, by Mitscherlich (1834). Since then, the importance of this class of reactions was rapidly recognized by chemists and academics, leading to several studies to investigate the reaction mechanisms and alternative nitrating agents. In this respect, nitration reactions also played a key-role in the development of theoretical organic chemistry and, specifically, in the electrophilic aromatic substitution mechanisms and in the evaluation of the effects of different substituents on its orientation (Stock, 1976; de Queiroz et al., 2006; Galabov et al., 2016).

1.1.2. Nitration reactions

Nitration reactions can proceed via a free radical and an ionic mechanism (Olah et al., 1989). The first mechanism is by far the less studied and it is generally carried out in gaseous phase for the nitration of aliphatic compounds (Markofsky et al., 2003). It proceeds through a radical chain reaction pattern initiated by the thermal, photolytic, or radiolytic homolysis of N_2O_4 to generate NO_2 radicals.

Nitrations of aromatic substrates proceed by an ionic mechanism (Hughes, 1950; Olah, 1971). In this case, the nitrating agent is nitronium ion that is formed by an acid catalyzed mechanism resulting in the de-hydration of nitric acid. The equilibrium of nitronium anion generation can be generally written as

$$HNO_3 + HA \rightleftarrows NO_2^+ + A^- + H_2O \qquad \text{r.1.1}$$

In reaction r.1.1 nitric acid acts as a base. As a result, in order to give nitronium ion at significant concentration a very strong acid HA must be used. Since its first adoption by Hoffmann and Muspratt in 1845 (Booth, 2003), sulfuric acid was usually used as a nitrating homogeneous catalyst and homogeneous mixtures of concentrated nitric and sulfuric acid are nowadays the most studied and known nitrating agent (Kulkarni, 2014), also named mixed acid. In this case, equilibrium r.1.1 is usually reported as

$$HNO_3 + H_2SO_4 \rightleftarrows NO_2^+ + HSO_4^- + H_2O \qquad \text{r.1.2}$$

Organic substrates also undergo nitration processes in pure or highly concentrated aqueous nitric acid. In this case, the self-ionization reaction is

$$HNO_3 + HNO_3 \rightleftarrows NO_2^+ + NO_3^- + H_2O \qquad \text{r.1.3}$$

However, nitronium ion concentrations formed according to r.1.3 is significant only for nitric acid weight percentage higher than 95% (Schofield, 1981) and is superseded by r.1.2, when sulfuric acid is present. Although several attempts were made to investigate alternative nitrating systems, mixed acid is the most adopted nitrating mixture, so far.

According to the most reported reaction mechanism, once formed, electrophilic nitronium ions can attack the electrons of organic substrates aromatic ring to form a high-energetic ionic reaction intermediate, namely σ-complex or Wheland intermediate (Wheland, 1942; Koleva et al., 2015). It regains its aromaticity by loss of the proton on the sp^3 carbon, leading to the formation of the substituted nitrated product (Fig. 1.1)

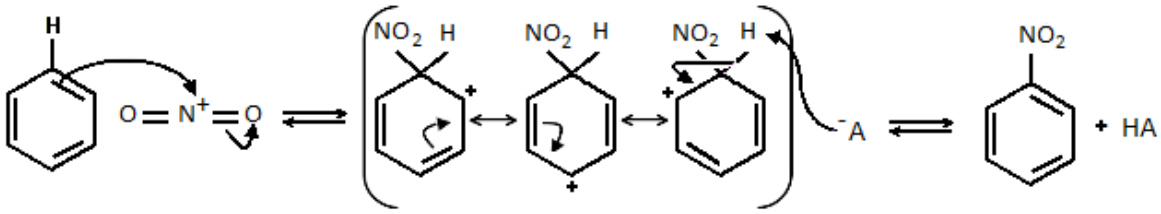

Fig.1.1. Aromatic electrophilic nitration mechanism.

Aromatic mono-nitrated products can be nitrated several times to give poly-nitrated compounds. However, the first nitro substituent is usually strongly deactivating so that harsher conditions, i.e. more acidic media and higher temperatures, are usually necessary to carry out poly-nitration reactions. As a result, dangerous side reactions could be triggered. As an example, although 1,3,5-trinitrobenzene could be produced through the further nitration of 1,3-dinitrobenzene, the decarboxylation of 2,4,6-trinitrobenzoic acid is usually preferred to avoid the extensive occurrence of side reactions and low yields (Booth, 2003).

From a thermodynamic point of view, nitration reactions are strongly exothermic; in fact, the mono-nitration of benzene has a ΔH of - 117 kJ/mol (Booth, 2003). For this reason, thermal control is fundamental when running nitration reactions and a loss in the thermal exchange or a mistake in the reactants loading can easily cause an increase in the reacting system temperature, with the consequent trigger of even higher exothermic side reactions and the formation of gaseous products that can pressurize reactors and lead to a thermal explosion scenario. According to Barton et al. (1997), fifteen industrial incidents were reported in nitration plants, second in number only to polymerization plants (65 incidents), demonstrating that nitrations are among the most hazardous chemical processes carried out in the chemical industry, since polymerization plants are by far more prevalent.

Electrophilic aromatic nitration kinetics have been widely investigated during the last century and their understanding is of crucial importance in defining the most convenient and safe conditions under which running the processes. Nitration kinetics are strongly dependent on the mechanisms presented in reaction r.1.1 and Scheme 1. They can be summarized as

$$HNO_3 + HA \xrightarrow{k_{dir}} NO_2^+ + A^- + H_2O \qquad \text{r.1.4}$$

$$NO_2^+ + A^- + H_2O \xrightarrow{k_{inv}} HNO_3 + HA \qquad \text{r.1.5}$$

$$Ar + NO_2^+ \xrightarrow{k_{int}} ArNO_2^+ \xrightarrow{-H^+} ArNO_2 \qquad \text{r.1.6}$$

where r.1.4 and r.1.5 are the direct and inverse reactions of equilibrium r.1.1, and r.1.6 represents the formation of the σ-complex and the successive nitrated product formation (Hoggett et al., 1971). The rate determining step could be both the nitronium ion or the Wheland intermediate formation depending on the adopted reaction conditions and the possible presence of solvents. In the absence of sulfuric acid or much water, the reaction rate was observed to be independent on the aromatic concentration suggesting that in this case the rate determining step is the formation of nitronium ion, since $k_{int}[Ar] \gg k_{inv}[H_2O]$. However, in most practical cases, the solubility of aromatics in the aqueous nitrating mixtures is fairly low and water is present at sufficiently high concentration so that the equilibrium condition expressed by reaction r.1.1 is reached much faster than the attack of the nitronium ion to the aromatic ring (Hoggett et al., 1971). A typical nitrating agent for large-scale aromatic mono-nitrations is reported to be 20% w/w nitric acid, 60% w/w sulfuric acid, and 20% w/w water (Booth, 2003), namely standard mixed acid. In this case, the reaction rate is first-order in the concentration of the aromatic species and the following expression can be adopted

$$r = k_{int}[Ar][NO_2^+] \qquad \text{eq.1.1}$$

1.1.3. Nitration processes in the chemical industry

The first developed nitration process, started in 1856, was the aniline production, that was firstly employed in dyes and pigments synthesis (Booth, 2003). Nowadays, the production of dyes and colorants is still one the most important manufacturing sectors to depend on nitration productive units. However, with the ever-growing demand for food industry products, and as a result of the mass-production applied to the technology of warfare during the XX century, bulk chemical productions of explosives and agrochemicals (fertilizers, pesticides, herbicides, *et cetera*) are the main industrial applications of nitration processes. But nevertheless, at present, nitration processes are also developed for the production of highly priced fine chemicals with important applications in pharmaceutical drugs and new materials synthesis. Almost all of the nitrated products of industrial interest are produced *via* aromatic direct nitration. Together with the above-mentioned aniline, other nitrated key-intermediates in the

industry are nitrobenzene, nitrotoluene and nitrochlorobenzenes. Fig. 1.2 summarizes the fundamental products of nitration processes and their applications.

A general scheme of a mixed acid-based nitration plant is presented in Fig.1.3. The nitrating mixture and the organic substrate are fed to the reactor. Nitration reactors are both continuous or batch, depending on the required productivity of the specific process. For low-tonnage productions batch or fed-batch enamel lined mild steel reactors are usually preferred. Major requirements to be met in the design of reactors are connected with the high exchange surface and the efficient mixing system needed for a precise temperature control and an effective mass transfer between the partially miscible liquid organic and acid phases. Thermal control is usually operated coupling a cooling jacket with an internal cooling system. In order to enhance the exchange of generated thermal power and the contact between the immiscible phases without overloading and overdimensioning the mixing system, the vessel volume is generally limited to 6000 L (Booth, 2003). Other issues to be taken into account are related to the required excess of nitrating agent, which occupies a significant volume, and the prolonged reaction times, resulting from low adopted temperatures to reduce the generated heating power (Kulkarni, 2014).

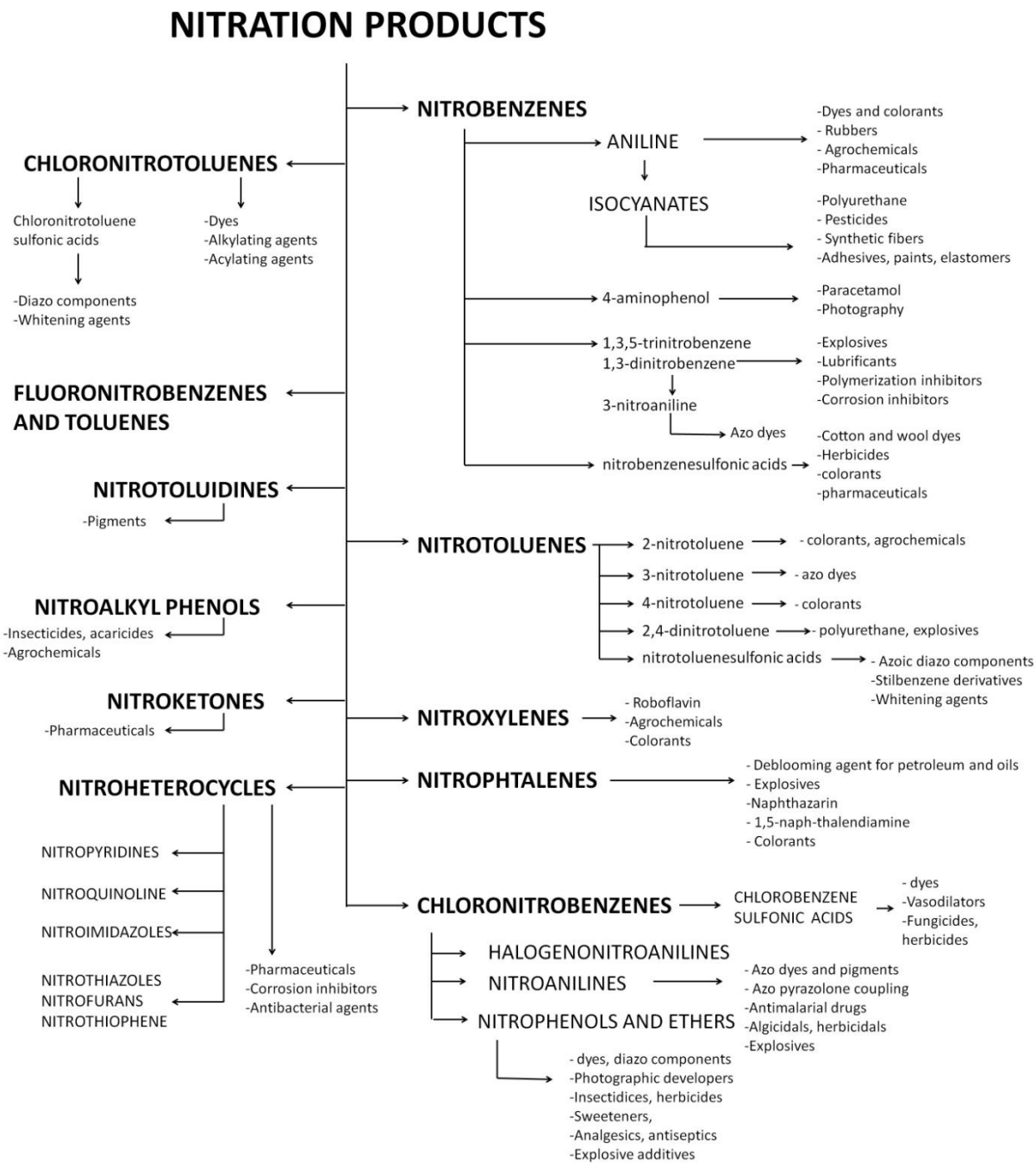

Fig. 1.2. Main industrial nitrated products.

For higher tonnage productions, such as nitrobenzenes, nitrotoluenes and nitrochlorobenzenes, continuous reactors have been adopted on a commercial scale.

The output stream usually consists of spent acids, with an increased amount of water generated during the nitration process by reaction r.1.1, unreacted organics, by-products and a mixture of nitrated isomers, as a result of the different selectivity towards the different nitro

group positions on the aromatic ring (Kulkarni, 2014). As a consequence, a first separator is provided after the reactor to recover spent acids, mostly sulfuric acid, that are successively concentrated and recycled into the reactor. The crude organic mixture is then washed to remove residual acids and distilled/separated/purified to obtain the desired isomers. The unconverted organic substrate is separated and recycled into the reactor.

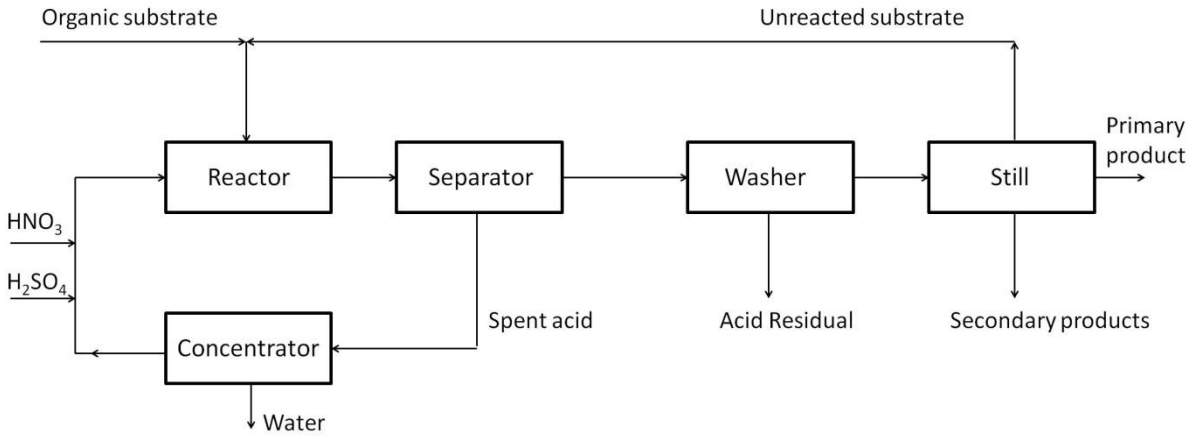

Fig. 1.3. General scheme of an industrial nitration plant.

1.1.4. Nitrating agents

As previously stated, nitronium ion is the real nitrating agent in electrophilic aromatic nitrations. Its formation in the reaction mixture is traditionally related to the acid catalyzed ionization of nitric acid. For reasons of convenience and economics, the acid catalyzed dissociation is usually carried out using sulfuric acid. However, several drawbacks are associated with the adoption of mixed acid as a nitrating mixtures, linked to the continuous acid residual formation and the dilution of the system due to water formation as the nitration of the organic substrate occurs. For these reasons, in the last 50 years, several studies focused on the adoption of new nitrating systems. The innovative studied nitrating mixtures are based on different approaches:

- adoption of a solvent in order to carry out nitrations in a homogeneous phase and to influence the ionization of nitric acid. To this regard, no easy correlations can be

inferred between the solvent polarity and the effect on the reactivity (Hoggett, 1971), probably because of the formation of aggregates of molecules of nitric acid;

- substitution of sulfuric acid with other strong acids such as $HClO_4$ or nitric acid itself;
- substitution of nitric acid with alternative $X - NO_2$ molecules to generate nitronium ions; in this regard, more electronegative X groups correspond to stronger nitrating agents, since higher concentrations of NO_2^+ are generated in a shorter time. In this case, nitronium tetrafluoroborate, BF_4NO_2, and acetyl nitrate, $CH_3COO - NO_2$, are the most studied and adopted. However, a study (Andreozzi et al., 2002) involving nitrating mixtures containing acetyl nitrate revealed a high hazard related to the gaseous product generation as a result of its thermal decomposition.

Although several studies have been conducted on alternative nitrating mixtures, mixed acid, aqueous nitric acid and red fuming nitric acid are still considered the most convenient ones, and the adoption of alternative compounds is often limited to supporting studies rather than to practical applications in nitration plants. Fig. 1.4. shows the relative percentage of published papers investigating the different nitrating mixtures in the last 50 years, as shown by Kulkarni (2014).

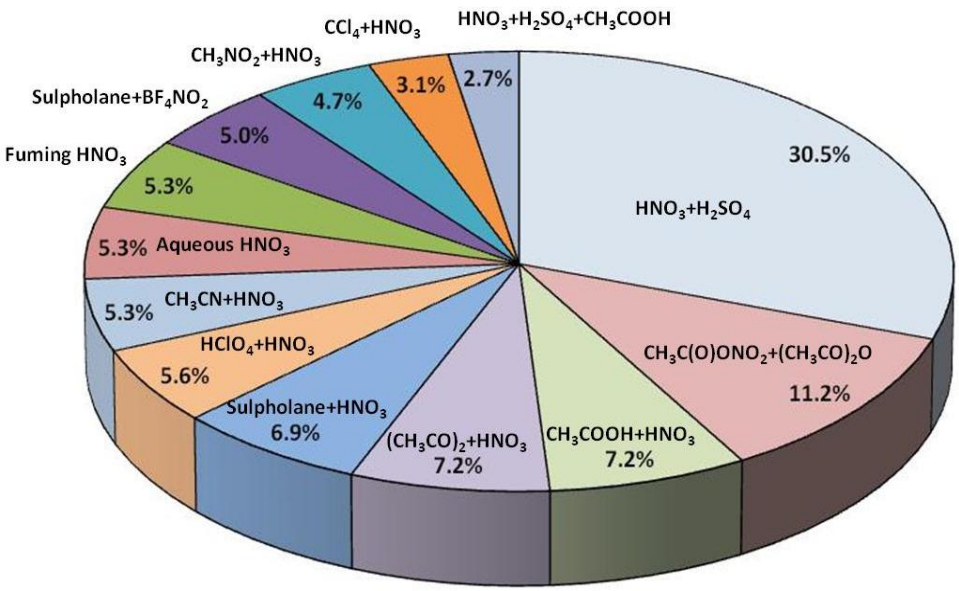

Fig. 1.4. Relative incidence of different nitrating mixtures over the last 50 years literature (adapted from Kulkarni, 2014).

1.2. Thermal explosion hazard

1.2.1. Thermal runaway and thermal explosions

A thermal runaway is defined as the unconstrained increase of temperature, as a result of the loss of thermal control of an exothermic reaction. The most common incidents due to thermal runaway scenarios were caused by conditions in which the heat generation of a chemical reactive system exceeded the heat dissipation capacity of the thermal exchange system (Gygax, 1988). This scenario may be generally due to accidental changes of the operating conditions, such as the refrigerant flow rate, the reactants loading, and an inadequate mixing.
A traditional simplified approach in describing the thermal power balance in a refrigerated jacketed vessel is presented in Fig. 1.5.
In the hypothesis of an exothermic reaction with a heat of reaction of ΔH, with an Arrhenius dependence on the temperature T, operated in an ideally stirred tank reactor of volume V, the generated thermal power P_{G1}, at the initial reagent concentration c_0, is

$$P_{G1} = V \cdot (-\Delta H) \cdot k_0 \cdot exp\left(-\frac{E}{RT}\right) c_0^n \qquad \text{eq.1.2}$$

where n is the order of reaction. On the other hand, the dissipated thermal power P_{D1} is

$$P_{D1} = Q \int_{T_{in}}^{T_{out}} c_p dT = UA\,(T - T_E) \qquad \text{eq.1.3}$$

where Q is the refrigerant flow rate, T_{in} and T_{out} the inlet and outlet temperature of the refrigerant stream, respectively, c_p the specific heat of the refrigerant, U the global heat transfer coefficient, A the exchange surface, and T_E the mean integral temperature along the cooling circuit. Typical profiles of P_{G1} and P_{D1} as a function of the temperature are shown in Fig. 1.5. An operational reactor is usually maintained in an unstable equilibrium (Gygax, 1988) state where $P_{G1} = P_{D1}$, represented by point A in Fig. 1.5. Under those condition, an increase in temperature, leads to a generated power higher than the dissipation capacity of the system with a consequent further temperature rise. On the contrary, a decrease in temperature

drives the system toward a stable equilibrium represented by the low temperature point B in Fig. 4.

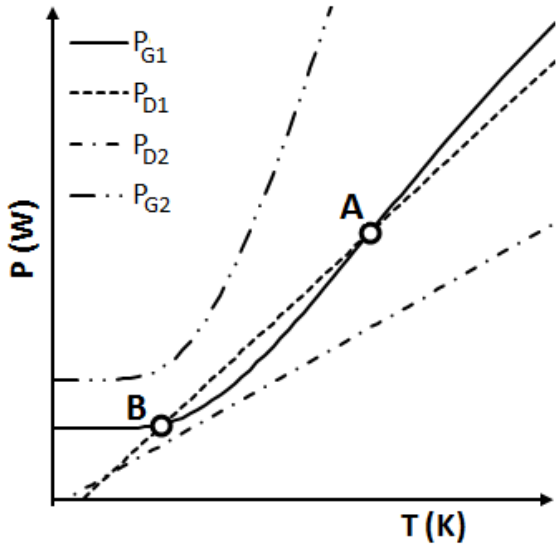

Fig. 1.5. Generated (P_G) and dissipated (P_D) thermal power in a refrigerated tank reactor as a function of temperature.

However, an error in the operating conditions can change the relative position of the functions in Fig. 1.5. For example, a failure in the refrigerant fluid pumping or an undesired fouling of the heat exchanger surfaces can reduce the dissipated thermal power from P_{D1} to P_{D2} in a condition under which the generated thermal power is always higher than the dissipation capacity of the cooling system with a consequent uncontrolled increase in temperature. An increase in temperature results in a higher reaction rate and generated thermal power. Fig. 1.6 summarizes the uncontrolled positive feedback mechanism.

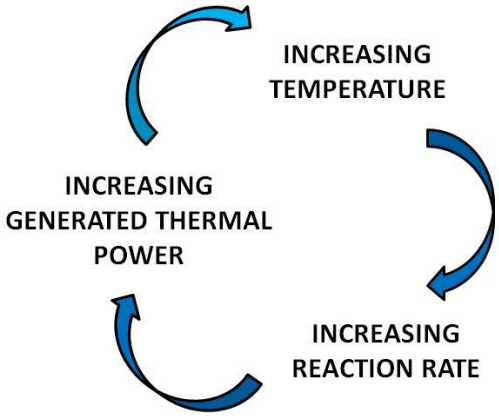

Fig. 1.6. Positive feedback mechanism in thermal runaway.

Although a theoretical stable condition at higher temperature exists, these conditions, in the absence of an adequate control systems, easily lead to a thermal runaway, since the increase in temperature can trigger secondary exothermic reactions and decompositions of the generated compounds to form gaseous products. Undesired secondary reactions, that are generally absent or very slow under normal operating conditions, can assume a significant role in the generation of an additional thermal power, since they usually are highly exothermic. The generated power expression, eq. 1.2, changes as follow

$$P_{G2} = P_{G1} + P_{G,und}(T) \qquad \text{eq.1.4}$$

where $P_{G,und}(T)$ is the additional generated thermal power due to the undesired secondary reactions. Fig. 1.5 shows the absence of stable operating conditions, seeing that $P_{G2} > P_{D2}$ at every T. It must be specified that eq.1.2 does not take into account the consume of the substrate that results in a decrement in the generated thermal power as the reaction proceeds.
A conservative general criterion to establish whether a thermal runaway can set off a chain reaction-caused explosion, is the evaluation of the adiabatic temperature rise ΔT_{ad} defined as the increase in temperature of a reacting mixture as a result of an exothermal reaction under the assumption of no heat transfer to or from the environment. In a batch reactor it can be estimated as

$$\Delta T_{ad} = \frac{(-\Delta H) \cdot n}{m_{mix} \cdot c_p} \qquad \text{eq. 1.5}$$

where n are the moles of reactant, m_{mix} the mixture mass, and c_p its mean specific heat capacity. If the maximum adiabatic temperature T_{max}

$$T_{max} = T_0 + \Delta T_{ad} \qquad \text{eq. 1.6}$$

is higher than the onset temperature of secondary reactions a serious risk for secondary reactions to take place exists.

To summarize, in order to turn a thermal runaway in a thermal explosion scenario additional conditions must be met:

- the reacting system must be strongly self-accelerating, i.e. a small increase in temperature shall determine a significant increase in the reaction rate that will rapidly cause a further temperature increase and trigger secondary reactions;
- pressurization of the reactor. This is generally caused by high-temperature-activated decomposition reactions with formation of gaseous products that can pressurize a confined reactor. If gas formation is sufficiently fast, bursting discs and venting valves cannot prevent the mechanical burst of the vessel.

Some of the most famous incidents in the chemical industry, i.e. Seveso and Bhopal disasters, were caused by thermal runaways. 189 incidents, in which runaway in batch reactors have occurred, have been reported during the period 1962-1987 (Barton et al., 1989) whereas a recent study (Saada et al., 2015) analyzes 30 new incidents reported between 1988 and 2013. In this last study, it is shown that, although the number of incidents was drastically reduced, the number of fatalities and injuries have more than quadruplicated and triplicated, respectively. Among the most probable technical causes, most authors proposed the mischarging of the reactants in their relative amounts or their order, the failure of the agitation system, the presence of impurities capable of dramatically affecting the reactivity of the systems, and the poor understanding of thermo-reaction chemistry (Etchells, 1997; Westerterp et al., 2006).
Therefore, the need of assessing and predicting the hazard connected with processes in which a thermal explosion scenario is possible has arisen.
In this regard, a first screening to indentify the possible violent and explosive decomposition of key products and by-products is based on different empirical and semi-empirical approaches (Gustin, 1993). Lists of hazardous reactions (Bretherick, 1990) and processes associated with a high probability of thermal runaway and explosion (Barton et al., 1989) are nowadays available. Moreover, explosophoric group methods can be adopted to evaluate potential risk connected with the presence of highly likely explosive functional groups in the molecules involved in the process. Finally, a preliminary evaluation can be carried out adopting the Chetah method (Chemical Thermodynamics and Hazard evaluation), proposed by the ASTM International. This method is based on the calculation of four indices related to the maximum heat of decomposition, the heat of combustion, the oxygen content, and a fourth semi-empirical index. The simultaneous evaluation of the four indices can be indicative of an intrinsic hazard related to the deliberate adoption, and the desired or undesired formation of a

specific compound in a chemical process. In the event that one of the above-mentioned screening criteria suggested a likely hazard, further investigations need to be conducted. Ideally, experimental investigations should be devoted to a complete thermo-kinetic characterization of the reactive system under normal operating conditions and as a result of deviations from the optimum design conditions. In this regard, several works were published about by-products identification in a thermal runaway (Lunghi et al., 2002), dynamic processes evolution (Ball et al., 2013), kinetics characterizations (Andreozzi et al., 2006; Di Somma et al., 2012), thermal decompositions and calorimetric investigations (Westerterp et al., 2006; Chen et al., 2012; Gustin, 1993; Das et al., 2011; Patil et al., 2012), simulations of runaway phaenomena (Kotoyori, 1991; van Woezik et al., 2001; Copelli et al., 2014; Chen et al., 1996) and new general runaway criterions (Zaldivar et al., 2003).

1.2.2. Explosion hazard in nitration processes

Nitrations are among the most hazardous industrial processes. Available analyses (Barton et al., 1989; Saada et al., 2015) reported 17 serious incidents related to thermal runaways of nitrating reactive systems in the last 50 years. This number is second only to the incidents occurred in polymerization processes, but it is extremely significant if one considers that polymerization processes are by far more prevalent.

Nitrations meet all the requirements for the onset of a thermal explosion. They are strongly exothermic with a heat of reaction ΔH ranging from -73 to -253 KJ·mol^{-1} (Kulkarni, 2014). They are usually carried out in mixed acid or concentrated nitric acid and their reaction rate is very sensitive to small variations in the acid mixture composition and operating temperature, so that an accidental increase in the temperature can easily lead to a self-accelerating reactive system. Several secondary exothermic reactions can be activated as a result of a deviation from the design operating conditions:

- nitric acid decomposition: red fuming nitric acid continuously decomposes into gaseous nitrogen oxides (NO_x). The decomposition is also present in aqueous nitric acid and it is accelerated in the presence of sulfuric acid; the amount of nitrogen oxides increases at higher temperatures (Di Somma et al., 2014a);
- oxidation reactions: nitric acid is a strong oxidizing agent and the exothermic oxidation of organics is possible in mixed acids. This can decrease selectivity towards desired products

under normal operating conditions and generate a significant amount of additional thermal power in a thermal runaway;

- poly-nitrations: they often occur under harsher conditions than mono-nitrations; poly-nitrated products are formed during the uncontrolled increase in temperature;
- nitro-compounds decomposition: nitrated organic or aliphatic compounds are commonly used as explosives. This is due to the fact that, under heating, pure nitro-compounds usually remain stable up to 250-350 °C (Gustin, 1998). Beyond their onset temperature, their decomposition is rapid, violent, and exothermic with a decomposition heat of about 1000 J/g. However, in a nitration plant, nitro-compounds are always present as a reaction mixture of different isomers, acids, and impurities. Under these conditions, their thermal stability is much lower than in pure compounds and explosive decompositions can be possible at lower temperature (Bretheric; 1990; Booth, 2003). For example, a mixture of nitric acid, sulfuric acid, and di-nitrotoluene was reported to explode at 130°C, although pure di-nitrotoluene is stable until 250°C (Gustin, 1998).

All the reported secondary reactions are strongly exothermic and some of them proceed with the formation of gaseous products so that the pressurization of the reactor can be very likely.

It is worth noting that the nitration reactor is not the only hazardous unit in a nitration plant. In distillation and purification units of Fig. 1.3, a mixture of nitrated compounds is usually heated in order to separate the different fractions. Moreover, particular attention must be paid to washing operations of acid mixtures at the outlet of the reactor, that could contaminate nitro-compounds with alkali, capable of further reduce their thermal stability (Gustin, 1998; Booth, 2003).

The active interest of the scientific community in the continuous research of safer operating conditions is evident from the great number of efforts made in assessing and characterizing nitrating reactive systems (Andreozzi et al., 1992; Cantillo et al 2014; Lunghi et al., 2002; Klais et al., 2009; Kowalczyk et al., 1997; Maestri et al., 2009; Andreozzi et al., 2006; Chen et al., 2012; Zaldivar et al., 1993; Maestri et al., 2006; di Miceli Raimondi et al., 2015; Di Somma et al., 2012; Chen et al., 1998; Chen et al., 1996; Zaldivar et al., 1992; Wiss et al., 1995).

1.3. Innovative reactors for chemical synthesis: an overview on microreactors

On the basis of the previous considerations, it is clear that a high-quality-output and safe production of nitrated products must meet the following fundamental requirements: an efficient thermal power dissipation and a well-designed mixing between the immiscible organic and acidic liquid phases in order to realize a stringent and punctual control of the operating conditions. Therefore, the scale-up from a lab scale to a pilot plant, and from a pilot plant to a full-scale reactor is of crucial importance in designing the process. In this regard, it is clear why sectoral studies focused their attention on new inherently safer reactor configurations. Specifically, a particular attention was paid to microreactor systems. Microreactor technology is particularly suitable for highly priced materials production, such as pharmaceuticals or innovative materials (Roberge et al. 2005; Roberge et al., 2008; Wong-Hawkes et al., 2006). The interest for microreactors is proved by the exceptional increasing number of publications of the last 30 years (Fig. 1.7).

The broad definition of "microreactors" refers to a big number of different devices with a typical size ranging from a few tens of microns to a few millimeters. Microreactors are also distinguished by manufacturing materials, techniques and micro-mixing devices. Most adopted materials are metals and metallic alloys, glass and ceramic, polymers and silicon (McMullen et al., 2010; Knapkiewicz, 2013). This makes it very difficult to have a global and united vision of the topic. The available studies often refer to "miniaturized devices" produced by photo-lithographic techniques with characteristic size of tens of microns (Watts et al., 2005; Knapkiewicz, 2013).

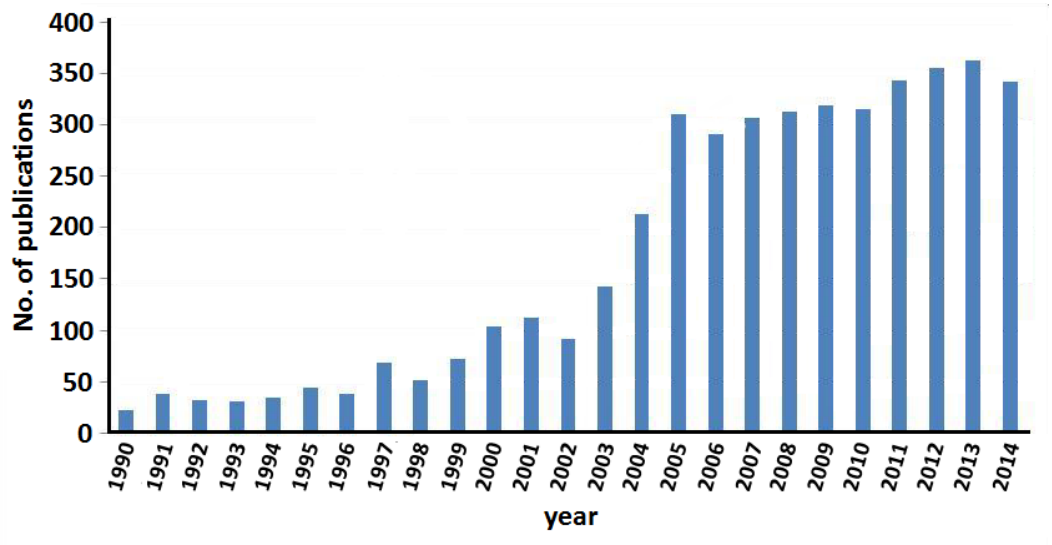

Fig. 1.7. No. of publications on microreactors between 1990 and 2014.

Despite the unquestionable importance of these studies for lab-scale optimization techniques and for the understanding of micrometric phenomena, these devices have only little relevance for industrial applications because of the limited amounts of obtainable products, high costs, and complexity of their manufacturing. On the other hand, microreactors present absolutely exceptional performances in the enhancement of transport phenomena. Small internal diameters make radial diffusion and dispersion very effective in inter-phase mixing. The surface/volume ratio can be several orders of magnitude higher than in the bulk of a traditional batch reactor. In the case that diffusion and dispersion are not effective in allowing favorable reaction conditions, micro-mixing devices assume a crucial importance, as shown in different review papers (Cherlo et al., 2009; Kockmann et al., 2009; Suh et al., 2010). An incredible variety of micro-mixing devices is also reported in the literature. In this case too, the challenge is to combine efficient performances, minimizing the manufacturing complexity.

The ratio between the external surface and internal volume in microreactors is also exceptionally high, allowing an enhanced thermal exchange and a punctual temperature control also in the case of exothermal reactive fluid dynamics. Ultimately, even though a laminar flow is the typical flow regime in microreactors, micro-dimensional scales allow a thermal and material exchange absolutely atypical for traditional macroscopic reactors operating under the same fluid dynamic conditions. It is worth to mention that such an efficient heat exchange is achievable not only under strictly defined micrometric conditions ($\leq$ 100 μm), but also with millimetric devices (Kulkarni et al., 2009; Kockmann et al., 2009). Therefore, millimetric devices are a very interesting industrial technology for highly priced materials synthesis, since they combine the advantages of micrometric scale devices with significant productivity and flexibility. It should be remembered that millimetric scales are also economically attractive for the reduced complexity of their manufacturing process. The typical productivity of a single device is of Kgs of product per day (Zhang et al., 2004).

Microreactors also represent an attractive alternative to the problem of the scale-up of traditional reactors, seeing that it could be replaced by an easier “numbering-up”, once the process is optimized for the single micro-productive unit (Roberge et al., 2009; Nemethne-Sovago et al., 2014).

Lastly, it is important to emphasize the importance of simulative techniques in the understanding of transport phenomena in microreactors (Cherlo et al., 2009), considering that small dimensional scale do not easily allow a feasible adoption of micro-sensors to monitor the operating variables evolution along the channels. Nevertheless, several efforts have been

made to experimentally measure temperature, pressure and concentration profile along micro-channels in order to validate simulations (Cherlo et al., 2009; Knapkiewicz, 2013; McMullen et al., 2010).

2. State of art

2.1. Nitrobenzaldehydes

2.1.1. Nitrobenzaldehydes production and uses

In this work, the production and process intensification of the two isomers 2- and 3-nitrobenzaldehyde will be investigated. The structural formulas of the ortho- and meta-substituted isomers are presented in Fig. 2.1.

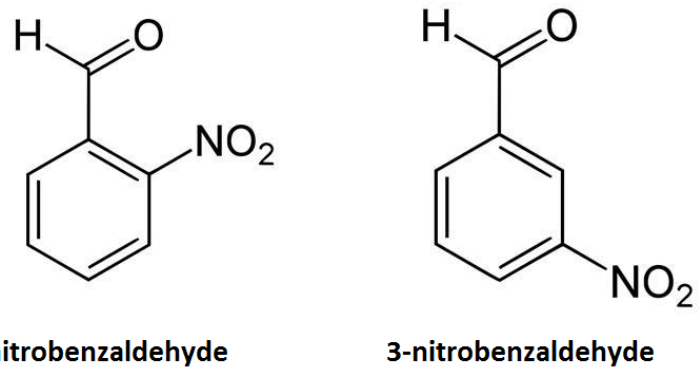

Fig. 2.1. Structural formulas of o- and m- nitrobenzaldehydes.

Nitrobenzaldehydes have several industrial applications (Venkatesan et al., 2010; Yan et al., 2011).

3-nitrobenzaldehyde is used for the production of pharmaceuticals, plastic additives, fragrances, flavorings, dyes and sector-specific products for galvanometry and X-ray contrast media (Kulkarni et al., 2009). The possibility of synthesizing important intermediates for Nicardipine and Pranidipine production in high purity has been recently highlighted (Neelakandan et al., 2014). Important products traditionally synthesized starting from m-nitrobenzaldehyde are 3-hydroxybenzaldehyde, 3-nitrobenzoic acid, and rosoxacin, an antigonorrheal agent (Bruhne, 2003).

2-nitrobenzaldehyde is involved in pharmaceutical drug and dyes industry, and is also used as a photo-removable protecting group for several functional groups as well as in the synthesis

of new innovative non-linear optical materials (Wang et al., 1988; Kulkarni et al., 2009; Sebej et al., 2009; Abubshait et al., 2011; Chigorina, 2014; Maddirala et al., 2016). Important industrial intermediates prepared starting from o-nitrobenzaldehyde are 2-aminobenzaldehyde, 4-4'-dichloroindingo, and 2H-indazole derivatives (Bruhne, 2003). Both isomers are also involved in the preparation of benzodiazepines and other cardiovascular drugs (Kulkarni et al., 2009).

3-nitrobenzaldehyde is traditionally obtained from nitration of benzaldehyde in mixed acid at 5 - 10 °C (Bruhne, 2003). More recently, the process is reported to be carried out between -5 °C and 15 °C with the slow drop-wise addition of the organic substrate, i.e. benzaldehyde, to the nitrating mixture in a fed-batch reactor; sometimes, the reverse configuration is adopted with the addition of mixed acid to benzaldehyde (Kulkarni et al., 2009). The reactor configuration and the adopted low temperature are indicative of the hazard of thermal runaway. Under these inevitable conditions, the complete conversion takes up to 6 hours. The ortho-substituted isomer is the unfavoured reaction product (Davey et al., 1950; Kulkarni, 2014) with yields up to 20% (Bruhne, 2013). For these reasons, together with the traditional nitration/oxidation of cinnamic acid, several alternative processes have been proposed among which the oxidation of 2-nitrostyrene (Gosteli, 1977; Hagedorn et al., 1978), 2-nitrobenzyl bromide (Ertel, 1978; Bernhardt et al., 1979), and the hydrolysis/oxidation of 2-nitrobenzyl bromide by nitric acid (Sauer et al., 1976). Oxidation of 2-nitrotoluene and the synthesis from alfa-halo-nitrotoluene have also been proposed and patented (Sainz-Diaz, 2002; Ertel, 1991). However, for some of the abovementioned processes safety issues related to the instability of the involved intermediates and explosions have been documented (Cardillo et al., 1982).

2.1.2. Dependence of isomers yield on mixed acid composition

For all the above reasons, an attempt of understanding the relationship between the ortho- and meta- isomers obtainable yields and the operative conditions for the nitration of benzaldehyde by mixed acid was found in the literature (Sainz-Diaz et al., 1999; Di Somma et al., 2014b). The previous investigations highlighted that no relevant formation of the para-substituted isomer was detected and it was present at trace level under all the adopted conditions. Di Somma et al. (2014b) carried out 12 experimental runs in homogeneous phase in the neighborhood of the standard mixed acid composition with nitric acid and sulfuric acid weight percentage varying in the ranges 14-29 % and 57-63 %, respectively. The results of the kinetic runs show a normalized initial slope of benzaldehyde concentration profile ranging

from $4.05 \cdot 10^{-5}$ to $2.12 \cdot 10^{-1}$ $L \cdot mol^{-1} \cdot min^{-1}$, more than 5-thousand-fold increment in the initial concentration, demonstrating that the kinetics are dramatically dependent on the nitrating mixture composition. Moreover, 2-nitrobenzaldehyde yield was qualitatively related to the acidity of the mixture through the definition of a proper function, namely H_R acidity function. A better description of this function will be reported in Section 2.3. In the neighbourhood of the standard mixed acid composition, it can be calculated from nitric and sulfuric acid concentration as (Di Somma et al., 2012)

$$-H_R = (0.56 \cdot [H_2SO_4]_0 + 0.52 \cdot [HNO_3]_0)\left(0.33 + \frac{49.0}{T}\right) \qquad \text{eq. 2.1}$$

where $[H_2SO_4]_0$ and $[HNO_3]_0$, are the initial concentrations of sulfuric and nitric acid in $mol \cdot L^{-1}$, and T is the absolute temperature in K. The measured 2-nitrobenzaldehyde yield increased from 18 to 27 %, decreasing the value of the H_R from -3.4 to -5.4. The preliminary results are in accordance with the previous observation by Sainz-Diaz (2002) who noticed an increase in the selectivity to 2-nitrobenzaldehyde when increasing the concentration of nitric acid in the mixture. A first attempt to predict the reactivity in dependence of the mixed acid composition was carried out on the basis of classic nitration mechanisms (Di Somma et al., 2014; Di Somma et al 2012) but the results were not consistent with it.

The results were qualitatively explained by Sainz-Diaz (2002) with a different mechanism of formation of 2-nitrobenzaldehyde starting from the coordination of nitronium ion on the aldehydic group of benzaldehyde (Fig 2.2).

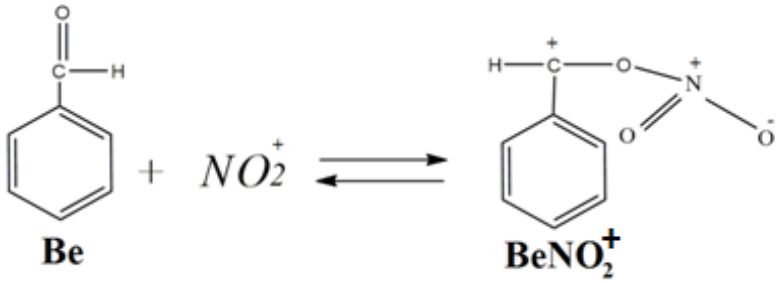

Fig. 2.2. Coordination of nitronium ion on the aldehydic group of benzaldehyde.

The coordinated species $BeNO_2^+$, once formed, can be attacked by a second nitronium ion and internally rearrange to form the coordinated form of 2-nitrobenzaldehyde (Fig. 2.3). The coordinated form of 2-nitrobenzaldehyde, once the acidic media is diluted, gives rise to the uncoordinated form of 2-nitrobenzaldehyde. This mechanism strongly depends on nitronium ion concentration. This is in agreement with the observed higher yield of the ortho-substituted isomer at lower H_R values, since the concentration of nitronium ion is higher for both higher nitric and sulfuric acid in mixed acid in accordance to the equilibrium reaction r.1.2.

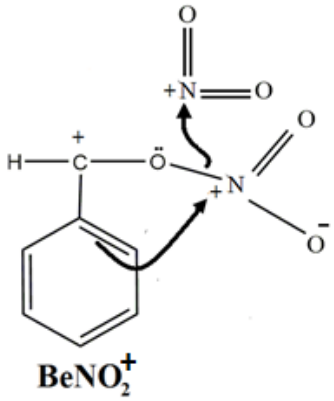

Fig. 2.3. Internal rearrangement of the coordinated form of benzaldehyde to give 2-nitrobenzaldehyde.

The reported studies suggest a complex kinetic scheme, dramatically influenced by the temperature and the reacting system composition. However, no detailed studies are present about the kinetic modeling of the system and the dependence of kinetic parameters on the adopted operating conditions.

2.1.3. Safety considerations on benzaldehyde nitration

The reported considerations about the significant changes in the reactivity, depending on the acidic media composition and temperature, pose a serious safety problem for benzaldehyde nitration processes. The possibility of a thermal runaway scenario can be deduced by simple thermal estimation. According to Di Somma et al. (2014b), a ΔH = -1185 $J \cdot g^{-1}$ can be estimated for benzaldehyde nitration by group contribution method (Medard, 1989). Assuming a mean specific heat equal to 2 $J \cdot g^{-1} \cdot K^{-1}$ (Grewer et al., 2015) and a ratio between

the aromatic substrate and the nitrating mixture mass of 0.5, an adiabatic temperature rise of 197 K can be estimated, which corresponds to a maximum adiabatic temperature of about 500 K, under which dinitration reactions surely start (Olah et al., 1989). Moreover, the formation of more thermally unstable intermediates cannot be ruled out (Di Somma et al., 2014b; Cho et al., 2005), because of the excess of nitric acid with respect to the organic substrate.

2.2. Traditional and alternative benzaldehyde synthesis

In this work, the possibility of synthesizing nitrobenzaldehydes starting from benzyl alcohol instead of benzaldehyde was investigated. As shown in the next Chapters, nitrobenzaldehydes are easily obtainable from benzyl alcohol since this is rapidly oxidized to benzaldehyde and successively nitrated to nitrobenzaldehydes in the same reaction media. In this Section, an overview of the traditional processes to obtain benzaldehyde and a comparison with the oxidation of benzyl alcohol are given.

2.2.1. Traditional processes for benzaldehyde production

Benzaldehyde is the organic substrate used in the previously described nitration process. The traditional industrial routes to synthesize benzaldehyde are (i) the catalytic oxidation of toluene and (ii) the hydrolysis of dichloro-methyl-benzene (Bruhne, 2003). Both processes present different shortcomings (Joshi et al., 2005). A scheme of toluene partial oxidation plant is presented in Fig. 2.4. The oxidation is realized in gas or liquid phase with molecular oxygen. In the first case, toluene vapor and air are fed to a fluidized-bed reactor through a catalyst at a temperature of 250 – 650 °C depending on the specific process. Lower temperatures are adopted in liquid phase toluene oxidation (80 – 250 °C) whereas higher pressure is necessary to keep the reacting mixture liquid. The main drawbacks are associated with the required expensive catalysts, high mean temperature (136 – 160 °C) and pressure (2 – 70 atm). The adopted catalysts are oxides of the V and VI group elements. Lots of oxidation by-products, such as benzoic and acetic acids, maleic, citraconic, and phtalic anhydrides, anthraquinone, cresol, together with carbon monoxide and dioxide are also produced (Kroschwitz et al., 1992; Susana et al., 2001; Joshi et al., 2005; Bruhne, 2003), so that a stringent control of the operating conditions is necessary to keep a low conversion rate and a short residence time with a consequent recycle of unconverted toluene.

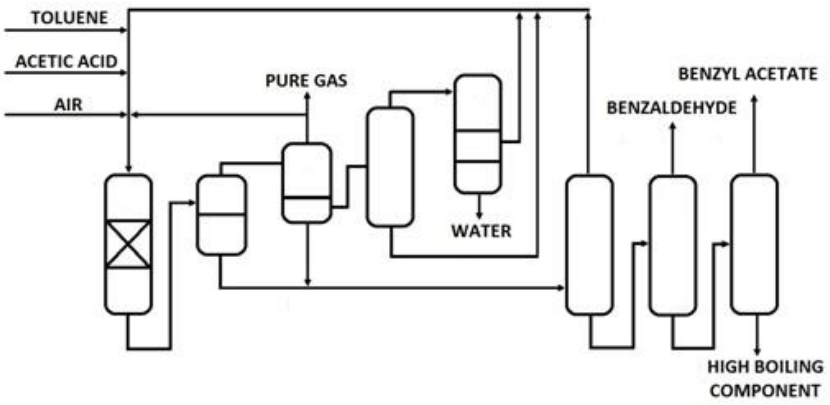

Fig. 2.4. A general scheme of toluene oxidation by oxygen (adapted from Di Somma et al., 2017).

Hydrolysis of dichloro-methyl-benzene is among the oldest processes to obtain benzaldehyde. It can be carried out in alkaline or acidic media. A scheme of benzaldehyde production through this process is shown in Fig. 2.5. In this case, the main problem is associated with the impossibility to obtain chlorine free benzaldehyde. Even though chlorine content can be reduced, the presence of impurities can be of crucial importance in the safety assessment of the following nitration processes.

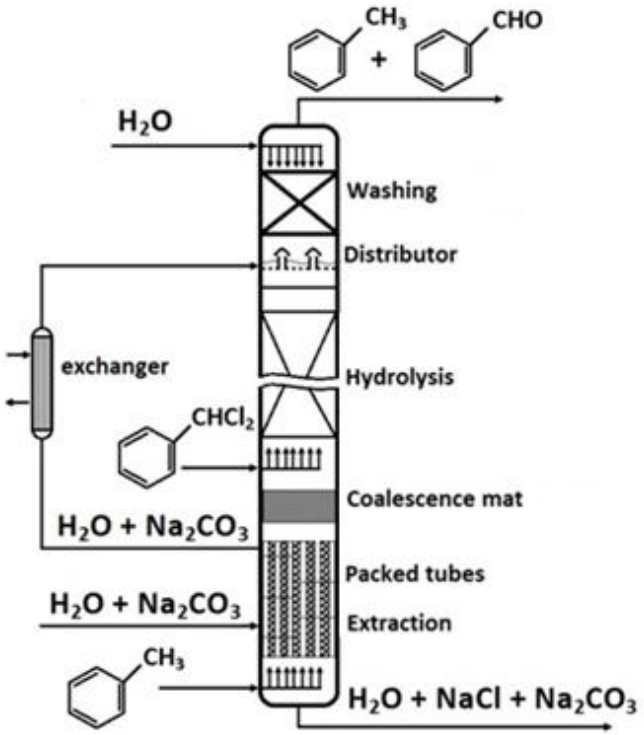

Fig. 2.5. Scheme of dichloro-methyl-benzene hydrolysis (adapted from Di Somma et al., 2017 and Bruhne, 2013).

2.2.2. Benzaldehyde synthesis by benzyl alcohol oxidation

In the light of the previously reported disadvantages associated with the traditional routes for benzaldehyde production, the direct synthesis of benzaldehyde from benzyl alcohol has been considered as an interesting alternative. For this reason, several studies have been carried out to obtain benzaldehyde from benzyl alcohol through inorganic catalysts (Li et al., 1989; Huang et al., 1982; Santaniello et al., 1983; Lee et al., 1976; Morimoto et al., 1988; Dakka et al., 1988; Sato et al., 1997; Liu et al., 1993; Semmelhack et al., 1984; Chouhary et al., 2003). However, the above proposed methods suffer from two main drawbacks: conversion degrees lower than the traditional processes and high costs of the investigated inorganic catalysts (Joshi et al., 2005).

Direct oxidation without solid heterogeneous catalysts is thus a very attractive scenario. The literature of the last 50 years proposed aqueous nitric acid or aqueous mixed acid as a very efficient oxidizing agent for benzyl alcohol with unitary conversion and selectivity and no detection of nitro-substituted alcohol derivatives (Ogata et al., 1966; Ross et al., 1986;

Strazzolini et al., 2003). Even though several studies were published, the knowledge of the reactive system is still fragmentary. Most Authors observed an induction period, after which the benzyl alcohol oxidation takes place (Ogata et al., 1966; Ross et al., 1986; Strazzolini et al., 2003; Joshi et al., 2005). Some of them attribute the presence of the induction period to the formation of a catalytic amount of nitrous acid, since the reaction starts without any delay after the addition of low quantities of nitrous acid or sodium nitrite to the nitrating mixture according to the proposed general mechanism

$$H^+ + NaNO_2 \rightarrow HNO_2 + Na^+ \qquad \text{r. 2.1}$$

$$\Phi CH_2OH + HNO_2 \rightleftarrows \Phi CH_2ONO + H_2O \qquad \text{r. 2.2}$$

$$\Phi CH_2ONO \rightarrow \Phi CHO + HNO \qquad \text{r. 2.3}$$

$$HNO + HNO_3 \rightarrow 2HNO_2 \qquad \text{r. 2.4}$$

$$2HNO \rightarrow N_2O + H_2O \qquad \text{r. 2.5}$$

However, it must be highlighted that in some cases no induction periods were observed (Gasparrini et al., 1988). In addition, most previously published works suffer from different limitations such as the limited investigated range of nitric acid concentration and the use of organic solvents (Aellig et al., 2011; Ogata et al., 1966; Gasparrini et al., 1988; Strazzolini et al., 2003; Ross et al., 1986). Moreover, no unitary vision about the reaction mechanism exists, since both ionic and radical mechanisms have been proposed.

The most detailed radical mechanism was proposed by Ogata et al. (1966) to explain their experimental observation on benzyl alcohol oxidation in diluted nitric acid and it is based on the evidence of the presence of NO_2 radicals in mixed acids (Squadrito et al., 1998). Their observations can be summarized as follows: (i) an induction period was observed and its duration is reduced by a catalytic amount of nitrous acid; (ii) the reaction follows a first-order kinetic with benzyl alcohol and nitric acid concentration; and (iii) the oxidation is faster when the acidity of the solution was increased with perchloric acid. The proposed mechanism was

$$HNO_3 + HNO_2 \rightleftarrows 2NO_2^{\bullet} + H_2O \qquad \text{r. 2.6}$$

$$\Phi CH_2OH + NO_2^{\bullet} \rightleftarrows \Phi CH^{\bullet}OH + HNO_2 \qquad \text{r. 2.7}$$

$$\Phi CH^{\bullet}OH + NO_2^{\bullet} \rightleftarrows \Phi CH(OH)ONO \qquad \text{r. 2.8}$$

$$\Phi CH(OH)ONO + H_2O \xrightarrow{H^+} \Phi CH(OH)_2 + HNO_2 \qquad \text{r. 2.9}$$

$$\Phi CH(OH)_2 \rightleftarrows \Phi CHO + H_2O \qquad \text{r. 2.10}$$

In the same work, the decomposition of benzyl nitrate is ruled out since it is not in accordance with the experimental results. This point was successively proved, since benzyl nitrate, added to mixed acid, was not quantitatively converted to benzaldehyde (Aellig et al., 2011; Aellig et al., 2012).

On the other hand, an ionic detailed mechanism was proposed by Ross et al., (1986) based on the formation of benzyl nitrite through reaction r. 2.11, and its decomposition to benzaldehyde in its unprotonated (r. 2.3) and protonated (r. 2.12) form.

$$\Phi CH_2OH + HNO_2 \rightleftarrows \Phi CH_2ONO + H_2O \qquad \text{r. 2.11}$$

$$\Phi CH_2ONO \rightarrow \Phi CHO + HNO \qquad \text{r. 2.3}$$

$$\Phi CH_2OHNO^+ \rightarrow \Phi CHOH^+ + HNO \qquad \text{r. 2.12}$$

The most recent investigation (Aellig et al., 2011) evaluated the role of oxygen in nitric acid decomposition to nitrous acid and the oxidation of nitroxyl, namely HNO, to nitrous acid. Despite this investigation is based on the results collected by means of an oxygen bubbling reactor, the proposed scheme, Fig. 2.6, summarizes the role of nitric acid reduction in the oxidation mechanism

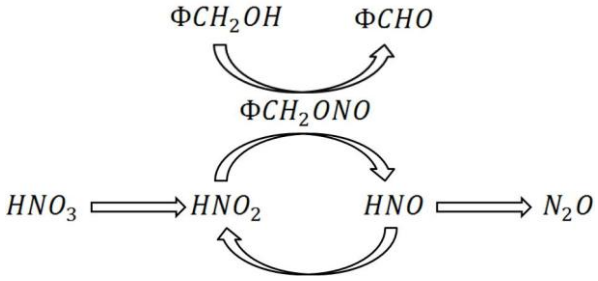

Fig. 2.6. Scheme of the oxidation mechanism proposed by Aellig et al., 2011.

Despite fragmentary information, all the reported investigations are united in identify benzyl nitrite as a key-intermediate. It is considered to be in equilibrium with benzyl alcohol (r. 2.2) and it decomposes irreversibly to benzaldehyde (r. 2.3) (Aellig et al., 2011; Ogata et al., 1966; Gasparrini et al., 1988; Strazzolini et al., 2003; Ross et al., 1986; Aellig et al., 2012; Nishiguchi et al., 1990).

A brief summary of the main conclusions reported in the literature is shown in Table 2.1.

Ref	Oxidizing agent	Mechanism	Solvent	Induction Period	Nitrite addition	Nitric acid ($mol \cdot L^{-1}$)
Ogata et al., 1966	Dilute nitric acid	Radical	Aqueous Dioxane 40%	> 8 hr (with pure nitric acid at 90°C)	Sodium nitrite	0.0496 – 0.134
Ross et al., 1986	Nitrous and nitric acid in aqueous sulfuric acid (50-75%)	Ionic	Absent	up to 4.7 hr (reduced by the adding of nitrous acid)	sodium nitrite	up to $6.67 \cdot 10^{-3}$
Gasparrini et al., 1988	Dilute nitric acid	Not proposed	Absent	Not observed	No addition	3.4
Strazzolini et al., 2003	Concentrated nitric acid	Radical	DCM	Variable induction times observed.	No addition	7.5
Joshi et al., 2005	Dilute nitric acid	Radical	Absent	2% conversion after 4hr in absence of sodium nitrite ($[HNO_3]$=1.6 M, 70°C)	Sodium nitrite	1.59 – 4.77
Aellig et al., 2011, 2012	O_2 + HNO_3	Ionic	1,4-dioxane	Observed	Sodium nitrite	$1.25 \cdot 10^{-1}$

Table. 2.1. Summary of the literature survey on benzyl alcohol oxidation by nitric acid.

2.3. Kinetic modeling in mixed acids

The development of a detailed kinetic model, capable of predicting the behavior of an oxidation/nitration reactive system in mixed acid, is not a trivial issue. Concentrated aqueous mixed acid is a strongly non-ideal solution. Several equilibrium reactions are involved in mixed acid to generate a variety of ionic species. Moreover, the presence of organics makes the system even more complex because of the coordination of organics with ionic species and protonation reactions. Proof of this is the fact that different simplified approaches have been proposed in the literature and a great variety of semi-empirical relations have been used to model deviations from ideality. In this Section an overview of the main problems connected with the kinetic modeling in mixed acid is given together with the main proposed theories

2.3.1. Nitronium ion concentration modeling and the H_R function

As presented in Chapter 1, nitronium ion is the real nitrating agent in nitration of aromatics in mixed acid. Therefore, the prediction of NO_2^+concentration is of crucial importance in the development of adequate kinetic models. As previously stated, the formation of nitronium ion in mixed acid can be associated to the general equilibrium

$$HNO_3 + H_2SO_4 \rightleftarrows NO_2^+ + HSO_4^- + H_2O \qquad \text{r. 2.13}$$

whereas other Authors (Zaldivar et al., 1995; Di Somma et al., 2012), in the presence of significant amount of water, proposed the following modified equilibrium

$$HNO_3 \cdot H_2O + H_2SO_4 \rightleftarrows NO_2^+ + HSO_4^- + 2H_2O \qquad \text{r. 2.14}$$

In this case the equilibrium relation can be written as follows

$$K = exp\left(-\frac{\Delta H}{RT}\right) exp\left(\frac{\Delta S}{R}\right) = [NO_2^+]\gamma_{NO_2^+} \frac{[H_2O]\gamma_{H_2O}}{[HNO_3]\gamma_{HNO_3}} \frac{a_{HSO_4^-} a_{H_2O}}{a_{H_2SO_4}} \qquad \text{eq. 2.2}$$

The acidity function, i.e. H_R, in mixed acid has been defined as (Zaldivar et al., 1995; Di Somma et al., 2012)

$$-H_R = log \frac{a_{H_2SO_4}}{a_{HSO_4^-} a_{H_2O}} \qquad \text{eq. 2.3}$$

It is reported that H_R values can be related to the initial nitric and sulfuric acid concentrations and absolute temperature T through the semi-empirical relation (Zaldivar et al., 1992; Di Somma et al., 2012)

$$-H_R = (a[HNO_3] + b[H_2SO_4])\left(c + \frac{d}{T}\right) \qquad \text{eq. 2.4}$$

Most authors tends to assume that $[NO_2^+] \approx a_{NO_2^+}$ in equation 2.2. This is in agreement with the fact that nitronium ion in the mixtures adopted in the above mentioned investigations is present at trace levels. However, it could be more opportune to assume that, for small deviation from the standard mixed acid composition (or a different arbitrary composition), $\gamma_{NO_2^+}$ variations can be neglected and incorporated in the constant entropic contribute of eq. 2.2. This reason, together with the adoption of r. 2.13 instead of r. 2.14 can probably explain the conflicting values of a, b, c, and d in eq. 2.4 reported by different authors. With the assumptions described above, the nitronium ion concentration can be calculated by

$$[NO_2^+] = exp\left(\frac{\Delta H}{RT}\right) exp\left(\frac{\Delta S^*}{R}\right) \frac{\gamma_{HNO_3}}{\gamma_{H_2O}} \frac{[HNO_3]}{[H_2O]} 10^{-H_R} \qquad \text{eq. 2.5}$$

Despite equation 2.5 has been widely adopted it is not capable of describing nitronium ion concentration for all the possible ternary mixture of sulfuric acid, nitric acid, and water. Even so, the normally used nitrating mixtures have concentration of nitric acid, sulfuric acid and water varying in relatively small ranges. Eq. 2.5 has been prevalently used to predict very low NO_2^+ concentrations, for which no experimental measurements are available since $[NO_2^+]$ is lower than the limit of detection and quantification by Raman analysis. In fact, in spite of its low concentration, nitrations occur also in mixtures with no evidence of nitronium ion by Raman analysis, suggesting that the reactions can start even for $[NO_2^+]$ lower than 40 mmol·L^{-1}[1]. The most extended available Raman experimental data on nitronium ion concentrations can be found in Albright et al. (1996) and Edwards et al. (1994). However, all the reported experimental concentrations are higher than 40 mmol·L^{-1} and were measured for highly acidic media, for which reaction kinetics are too fast to safely carry out nitrations. On the basis of the available experimental data on nitronium ion concentrations, an attempt to model the equilibrium concentrations of the ionic species was made (Albright et al., 1996). This proposed model was based on the following equilibria together with reaction r. 2.13

$$H_2SO_4 \rightleftarrows H^+ + HSO_4^- \qquad \text{r. 2.15}$$

$$HNO_3 \rightleftarrows H^+ + NO_3^- \qquad \text{r. 2.16}$$

Unfortunately, the model is based on the unrealistic hypothesis of ideal mixture without taking into account the contribution of the activity coefficients of the single species. Under this assumption, the values of the three equilibrium constant for reactions 2.13, 2.15, and 2.16 were evaluated minimizing the mean square deviation between the experimental and calculated NO_2^+ concentrations. Although the experimental nitronium concentrations were predicted with some accuracy, the model fails for nitric acid molar percentage lower than 0.5%, is inaccurate for low nitric acid molar percentage (<5%), (Albright et al., 1996) and is completely inadequate to describe the above-mentioned low concentration range of nitronium ion for water concentration higher than 50% mol/mol, i.e., for example, standard mixed acid composition. In fact, in all these cases, the predicted value is significantly higher than the limit of quantification by Raman whereas there is no experimental evidence of Raman peaks associated with NO_2^+ (Edwards et al., 1995). Moreover, optimization was carried out on a single species (NO_2^+) whereas other six species (H_2O, HNO_3, H_2SO_4, H_3O^+, NO_3^-, and HSO_4^-) were only numerically predicted without any further experimental verification.

2.3.2. The H_0 Hammett function

The Hammett acidity function H_0 was first proposed in 1932 (Hammett et al., 1932), only a few years after the publication of the Bronsted acidity theory, to describe the protonation of weak organic bases in strong acids and to explain some previous observations on the different protonating strength in strongly acidic media (Pagni, 2009). Considering a concentrated solution of a strong acid HA in a solvent, the protonation equilibrium of an added weak base B can be expressed as

$$B + H^+ \rightleftarrows BH^+ \qquad \text{r. 2.17}$$

$$\frac{1}{K} = \frac{[BH^+]}{[B]} \frac{\gamma_{BH^+}}{\gamma_B a_{H^+}} \qquad \text{eq. 2.6}$$

where K is the ionization constant of BH^+, γ_i the activity coefficients and a_{H^+} the activity of H^+. The Hammett acidity function is then defined as (Hammett et al., 1932)

$$H_0 = -log\left(a_{H^+} \frac{\gamma_B}{\gamma_{BH^+}}\right) = pK - log\frac{[BH^+]}{[B]} \qquad \text{eq. 2.7}$$

It is worth noting that the H_0 definition can be considered as an extension of the pH scale in concentrated aqueous acid solutions. In fact, for a highly diluted solution

$$H_0 = -log\left(a_{H^+}\frac{\gamma_B}{\gamma_{BH^+}}\right) \approx -log[H^+] = pH \qquad \text{eq. 2.8}$$

The general procedure to quantify H_0 consists in adding a weak base with a known pK value into a solution with a known strong acid concentration. The relative concentrations of BH^+ and B are then measured, usually by UV-Vis spectrophotometry, and H_0 is calculated by eq. 2.7. When the ratio between $[BH^+]$ and $[B]$ is too high, a weaker base is chosen. Adopting this procedure, the H_0 of neat sulfuric acid in water was calculated to be -12 (Pagni, 2009). This value was chosen as a dividing line between strongly acidic (H_0 > -12) and superacidic media (H_0< -12). It must be stressed that, as a generalization of the pH scale, such a value in pure sulfuric acid would correspond to an inconsistent value of H^+ concentration. In this regard, H_0 must be considered as a quantification of the protonating strength; some authors suggested that such a high protonating strength is in accordance with the presence of $H_3SO_4^+$ in neat sulfuric acid, which is a much stronger acid than H_2SO_4.

The Hammett acidity function was successfully used to explain the changes in the reaction rate of organics in concentrated acid (Hammett et al., 1934; Taft, 1952; Thomazeau et al., 2003; Gu et al., 2005).

In spite of its undisputed importance, the Hammett acidity function suffer from some limitations. In fact, as a measure of the strength of an acid, it is required that its definition is independent on the particular and arbitrary weak base chosen as a reference. To overcome this problem, it is generally assumed that the ratio between $\gamma_B$and γ_{BH^+} is close to 1, since the concentration of weak base is deliberately kept at low levels (Pagni, 2009). Under this assumption, the Hammett acidity function would be an indirect measure of the activity of H^+. Even though this could be verified for some organic weak bases in certain ranges, it must be considered that, under all the possible conditions, the infinite dilution behaviour cannot be deemed equivalent to the ideal behaviour. Commonly used indicators are nitroanilines. Moreover, in this case, the different indicators adopted for different acidity ranges could influence the H_0 determination. For these reasons, bases of the same structural type are usually used, for which a similar value of the activity coefficients can be expected.

Finally, even though the Hammett acidity function has been successfully adopted to describe some nitration kinetics in mixed acid, e.g. pyridine N-oxide nitration (Johnson et al., 1967),

there are no detailed studies on the changes in the H_0 values when considering a mixture of strong acids such as nitric and sulfuric acid. However, for diluted nitric acid in concentrated sulfuric acid, the experience has shown that no substantial changes must be considered since the former is much less strong that the latter. Despite Hammett's insightful intuition, his acidity function was demonstrated to be inadequate in describing the protonation of some classes of weak bases, e.g. tertiary aromatic amines, pyrroles, indoles, ketones, aldehydes, carboxylic acids, *etc.* so that new special acidity functions have been defined for some of these other compounds (Arnett et al., 1970)

2.3.3. The M_C activity function

The M_C activity function was first proposed by Marziano et al. (1973). The new function was proposed to overcome the problems associated to the definition of the Hammet acidity function and its dependence, in some cases, on the particular weak base adopted as an indicator. According to Marziano et al. (1973), considering a concentrated solution of an acid HA in a solvent in the presence of an arbitrary number z of weak bases B_i, the following equilibrium reactions occurs

$$HA \rightleftarrows A^- + H^+ \qquad \text{r. 2.18}$$

$$B_1 + H^+ \rightleftarrows B_1H^+ \qquad \text{r. 2.19}$$

...

$$B_i + H^+ \rightleftarrows B_iH^+ \qquad \text{r. 2.20}$$

...

$$B_z + H^+ \rightleftarrows B_zH^+ \qquad \text{r. 2.21}$$

The experimental campaign, based on UV-Vis spectrophotometric measurements similar to those previously described for the H_0 acidity function, demonstrated that a linear relationship can be found between the logarithms of the ratios between the activity coefficients involved in equilibrium relations for r. 2.18 – r. 2.21 as follows

$$log\left(\frac{\gamma_{H^+}\gamma_{A^-}}{\gamma_{HA}}\right) = h_1 log\left(\frac{\gamma_{H^+}\gamma_{B_1}}{\gamma_{B_1H^+}}\right) = \left(\prod_{j=1}^{i} h_j\right) log\left(\frac{\gamma_{H^+}\gamma_{B_i}}{\gamma_{B_iH^+}}\right) \qquad \text{eq. 2.8}$$

Where h_i is the proportionality constant between the i-th constant and the previous one. The M_C activity function of the acid was thus described as (Sampoli et al., 1985a)

$$M_C = -\log\left(\frac{\gamma_{H^+}\gamma_{A^-}}{\gamma_{HA}}\right) \qquad \text{eq. 2.9}$$

As a consequence, a linear relation can be defined between the M_C function of the acid and of the i-th weak base B_i

$$M_C^{B_i} = n_i M_C \qquad \text{eq. 2.10}$$

Once the set of equilibrium relations is chosen, i.e. r. 2.18 – r. 2.21, the thermodynamic equilibrium constants can be expressed by

$$K_{HA} = \frac{[A^-][H^+]}{[AH]} 10^{-M_C} \qquad \text{eq. 2.11}$$

$$K_{B_1} = \frac{[B_1H^+]}{[B_1][H^+]} 10^{n_1 M_C} \qquad \text{eq. 2.12}$$

...

$$K_{B_i} = \frac{[B_iH^+]}{[B_i][H^+]} 10^{n_i M_C} \qquad \text{eq. 2.13}$$

...

$$K_{B_z} = \frac{[B_zH^+]}{[B_z][H^+]} 10^{n_z M_C} \qquad \text{eq. 2.14}$$

The values of M_C have been published as a polynomial function of the initial sulfuric acid concentration (Zaldivar et al., 1995), although different Authors often use different polynomial expressions depending of the sulfuric acid concentration range of interest. Since its first publication, the M_C acidity function theory was adopted and verified for a wide range of weak bases and different acids including sulfuric, nitric, methanesulfonic (Marziano et al., 1986), perchloric, and trifluoromathanesulfonic (Marziano et al., 1991a) acids.

The M_C function was successfully used to describe nitration kinetics of different organics in mixed acid. An important extension was demonstrated in 1985 (Sampoli et al., 1985b)

adopting the M_C function to model the nitric acid dissociation in sulfuric acid ranging from 1 to 98 wt %. To this merit, the relation

$$M_C^{HNO_3} = -log\left(\frac{\gamma_{H^+}\gamma_{NO_3^-}}{\gamma_{HNO_3}}\right) = nM_C^{H_2SO_4} \qquad \text{eq. 2.15}$$

was verified in the whole sulfuric acid range. Despite the fact that the relation was verified only using nitric acid concentration ranging from 10^{-4} to 10^{-1} mol·L^{-1} (Deno et al., 1961), eq. 2.15 was successfully used to model benzene, toluene and chlorobenzene nitrations which occur for higher nitric acid concentrations (Zaldivar et al., 1995), and, more recently, to investigate the nitration of 2-ethylhexanol in microreactors (Li et al., 2017). Less complex kinetic models, based on the M_C function, were also used to model benzene, fluorobenzene, chlorobenzene, bromobenzene, iodobenzene, (Traverso et al., 1977; Marziano et al., 1980; Marziano et al., 1999) and sulphonic acids nitration (Marziano et al., 1991b).

An important extension of the M_C function was also proposed to model the nitronium ion formation in mixed acid (Sampoli et al., 1985b). According to this theory for the equilibrium

$$HNO_3 + H^+ \rightleftarrows NO_2^+ + H_2O \qquad \text{r. 2.22}$$

an analogous M_C function can be defined for this equilibrium as follows

$$M_C^{NO_2^+} = -log\left(\frac{\gamma_{H^+}\gamma_{HNO_3}}{\gamma_{NO_2^+}}\right) \qquad \text{eq. 2.16}$$

Therefore, the equilibrium relation for r. 2.22 is

$$K_{NO_2^+} = \frac{[NO_2^+]a_{H_2O}}{[HNO_3][H^+]}10^{n_{NO_2^+}M_C} \qquad \text{eq. 2.17}$$

where M_C is the activity coefficient function of sulfuric acid. The linear relation between $log\left([NO_2^+]a_{H_2O}/[HNO_3][H^+]\right)$ and M_C was demonstrated for sulfuric acid wt. % higher than 80 % for nitric acid at trace levels. From the slope and the intercept of the linear equation, it is possible to extrapolate $K_{NO_2^+}$ and $n_{NO_2^+}$ values. Later on, the obtained results have been

sporadically used to describe nitration kinetics (Zaldivar et al., 1995; Li et al., 2017), although some discrepancies can be found in the adopted values of the constants and in the definition of the $M_C^{NO_2^+}$, that, in some cases, includes the activity coefficient of water in eq. 2.16.

2.4. Nitrations in microreactors

In the previous Chapter the main features of microreactors were presented. They can be summarized as follows

- great flexibility and manufacturing variety
- enhanced heat and mass transfer
- punctual control of temperature
- inherent safety in hazardous reaction control under harsh conditions
- relatively low productivity

For all the above-mentioned reasons, microreactor technology naturally suits the nitration processes management requirements, especially for highly priced and low-throughput materials production or niche technology applications. Therefore, several examples of application of the microreactor technology to the synthesis of nitrated products can be found.

2.4.1. Synthesis intensification in microreactors

In a recent review article (Kulkarni, 2014), the main issues related to the management of nitration processes in miniaturized devices are analyzed and the main investigated reactions are presented. As reported, despite the fact that microreactor technology was first adopted in academia and research institutions, its importance was soon acknowledged by the industry both as a useful tool for pilot plant investigations and as a productive unit for specific applications.

It has been estimated that, for typical residence times from 5 s to 15 min, a satisfying temperature control is possible for microreactors with diameters ranging from 1.6 to 13 mm; in fact, most nitrations reported in the literature are carried out in such dimensioned reactor configurations. Under those conditions, the typical advantages connected with a micro-scale reactor are also combined with higher productivities. A typical lab-scale experimental setup

consists of preheating channels connected to separated pumps, to feed the organic substrates and the nitrating mixtures to a mixing device. The mixing device is thus connected to the single or multiple channel reactor immersed in a thermostatic bath. At the output of the channels reactive samples are collected, quenched and analyzed. Innovative microreactors have embedded mixers and heat exchangers, to reduce the number of devices and the experimental complexity and to achieve a higher compactness.

The reported investigations highlighted the possibility to intensify processes in order to get higher conversions, selectivities and/or yields with shorter reaction times.

As an example, toluene nitration resulted in a higher ortho and meta isomers yields when adopting a mixture of acetic anhydride and nitric acid instead of mixed acid in microreactors; the adoption of micro-devices made it possible to safely carry out toluene nitrations in inherently unsafe acetic anhydride mixtures. As a model reaction, toluene nitration has been widely investigated in microreactors (Burns et al., 2002; Antes et al., 2003; Halder et al., 2007). In spite of the importance of those investigations in the understanding of the process, microreactors are not suitable in the industry for bulk productions reaction such as toluene nitration. Another impressive example of intensification of a bulk production reaction in microreactors is the naphthalene nitration; in batch mode, the process requires a cooling system operating between -50 and -20 °C; in a microreactor the same reaction was carried out in 3 s at 30 °C (Kulkarni, 2014). For the highly priced materials production, some reported process intensifications are the nitration of pyridine-N-oxide and nitropyridine for which yield increases from 72 to 78 % and from 52 to 97 % were obtained, respectively (Panke et al., 2003). In most cases, the increased yields and selectivities can be attributed to the stringent temperature control that allows to avoid the trigger of secondary undesired reactions such as in the case of nitration of salicylic acid (Kulkarni et al., 2008) and 3-methyl-4-nitropyrazole (Ducry et al., 2005); higher 5-nitrosalicylic acid yields were obtained in microreactors compared to batch reactors while the complete absence of di-nitrated products was reported for the nitration of the latter in miniaturized devices.

The effective temperature control is deeply related to the flow conditions, the exchange area and the residence time. A higher flow rate is associated with enhanced thermal exchange; however, when carrying out immiscible liquids phase reactions, the enhanced mass transfer between the organic and the aqueous acidic phase can increase the rate of conversion and, consequently, the heat generation, causing a rise in the local temperature and the trigger of secondary reaction. Control of residence time and flow rate is thus a key issue in reaction intensification.

Finally, it is worth highlighting that for liquid-liquid immiscible phase reactions, almost 80% of the reported reactions, the mass transfer can significantly affect the reaction rate so that most Authors cannot obtain kinetic parameters from microfluidic investigations and only overall data and apparent kinetic constants are often reported. To this merit, the adoption of highly diluted conditions, under which a homogeneous liquid phase is possible, or the combination with batch reactions can be a useful procedure for the parametric and process optimization (Kulkarni, 2014).

2.4.2. Benzaldehyde nitration in microreactors

As previously mentioned, different safety issues as well as selectivity problems must be addressed in benzaldehyde nitration. As a result, this reaction can be considered of interest in microfluidic applications especially if one considers its applications to high-added value products processing.

In fact, a preliminary investigation on benzaldehyde nitration in mixed acid in a micro-channel reactor showed interesting qualitative results (Kulkarni et al., 2009). The experiments were carried out both in batch and continuous mode at temperature, HNO_3 to benzaldehyde molar ratio and HNO_3 to H_2SO_4 molar ratio varying in the ranges 5 – 25 °C, 1.18 – 3.5, and 0.3 – 0.6, respectively. Under these conditions, the reactive system is always in an immiscible liquid-liquid heterogeneous phase. For this reason, the mixing between the organic phase and the reactive aqueous acidic phase is of crucial importance to efficiently carry out the reaction. The continuous flow experiments were thus carried out in a 6 m long Hastelloy tube with an internal diameter of 1.38 mm connected to a spilt and recombine caterpillar micromixer. Preliminary experimental runs demonstrated that a simple T-junction mixer was inadequate. The results were compared with those obtained in a glass jacketed glass reactor of 50 mL. The results showed that at a fixed HNO_3 to H_2SO_4 concentration ratio the ortho- to meta- isomer ratio decreased with increasing residence time and HNO_3 to benzaldehyde concentration ratio. As a general result, an increase in nitric acid concentration and temperature generally resulted in a decrease of the molar ratio between 3-nitrobenzaldehyde and 2-nitrobenzaldehyde. As expected, at higher temperature, the residence time to achieve a complete conversion is lower changing from 15 min to 30 s at an inlet fixed composition of nitric acid to sulfuric acid and a nitric acid to benzaldehyde mole ratio of 0.6:1 and 3.5:1, respectively. In the investigated ranges, no solid products formation was observed.

Similar experiments, carried out in a mixture of sulfuric acid, nitric acid and acetic anhydride led to a homogeneous liquid phase but resulted in an over-oxidation of the organic substrate with the formation of solid benzoic acid and the consequent clogging of the reactor.

3. Aims of the thesis

The main purpose of this thesis is to investigate the possibility to safely produce the two isomers ortho- and meta-nitrobenzaldehyde using benzaldehyde and/or benzyl alcohol as a row material and aqueous mixtures of nitric and sulfuric acid, namely mixed acid, as an oxidizing/nitrating agent according to the general scheme presented in Fig. 3.1.

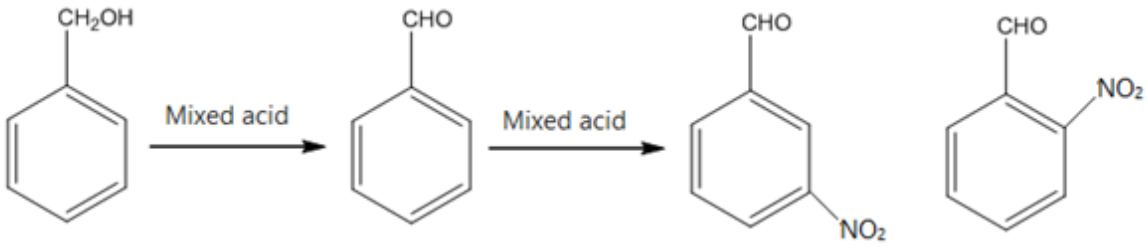

Fig. 3.1. General scheme of the oxidation of benzyl alcohol and the consecutive benzaldehyde nitration in mixed acid.

In this regard, the first goal was the kinetic characterization of the reacting system in order to describe and predict the behavior of the systems also under operative conditions different from the normally adopted ones in the industry, in order to maximize the two isomers yields. For a deeper understanding of the kinetic process, the ionic speciation in mixed acid was better investigated and characterized.

Moreover, the work aims to an evaluation of traditional batch reactors and innovative microfluidic devices performances in the process management to highlight strengths and weaknesses of each of the reactor configurations.

4. Materials and Methods

4.1. Chemicals

All the chemicals adopted in the experimental campaign were purchased from Sigma-Aldrich and used as received.

The used analytical grade reagents were: benzyl alcohol ≥ 99.0 %; benzaldehyde ≥ 99.0 %; 2-nitrobenzaldehyde 98 %; 3-nitrobenzaldehyde 99 %; 4-nitrobenzaldehyde ≥ 99.0 %; benzoic acid ≥ 99.5 %; 2-nitrobenzoic acid 95 %; 3-nitrobenzoic acid 99.0 %; 4-nitrobenzoic acid ≥ 98.0 %; sodium nitrite ≥ 99.0 %.

Red fuming nitric acid ≥ 99.5 %, sulfuric acid 99.9999 %, and bidistilled water were used to prepare oxidizing and nitrating acid mixtures.

Bidistilled water and technical ethylene glycol with corrosion inhibitor were used as cooling/heating fluids depending on the adopted experimental device.

HPLC analysis was carried out using acetonitrile ≥ 99.9 %, methanol ≥ 99.9 %, phosphoric acid 85 wt. % in water.

1,1-diphenyl-2-picrylhydrazyl ≥ 99.0 % was used as a radical trapper and 5,5-dimethyl-1-pyrroline N-oxide ≥ 97 %, namely DMPO, was used for EPR analyses.

Urea 99 % was used as a chemical quencher.

4.2. Batch experiments under homogeneous conditions: reactor and procedures

Batch experimental runs were carried out in a jacketed magnetically stirred glass reactor (30 mL), refrigerated using a Julabo F32 circulator. Water was used as cooling fluid. The reactor was equipped with a thermocouple and a sampling device. A scheme of the used batch reactor is provided in Fig. 4.1. The reactor and the glassware were repeatedly washed with chromic acid mixture and bidistilled water to prevent any contamination. Proper amount of nitric acid, sulfuric acid and bidistilled water were separately weighed and added drop-wise under continuous cooling and stirring. The mixture was always prepared adding the reagents in the following order: water, sulfuric acid, and nitric acid. Once the mixture was prepared, it was heated to the desired temperature. Each experimental run was started adding a proper amount

of the liquid organic substrate at once. In the case of solid substrates, experiments were started when those were completely dissolved. Liquid samples volumes (100 μL) were collected at different reaction times and rapidly quenched by diluting (1:100) with a solution of urea in acetonitrile ($6.66 \cdot 10^{-2}$ mol·L^{-1}) before HPLC analysis. Urea is reported to rapidly react with nitric acid and was added as a chemical quenching agent.

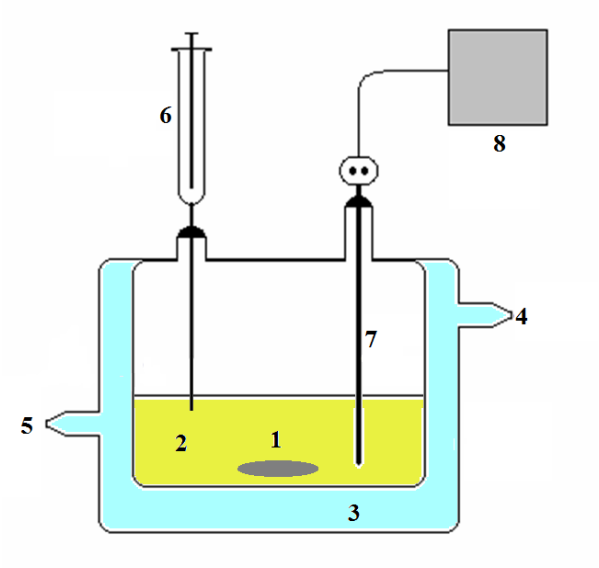

Fig. 4.1. Scheme of the batch reactor. 1. Magnetic stirrer; 2. Reacting Mixture; 3. Jacket; 4. Cooling fluid inlet; 5. Cooling fluid outlet; 6. Sampling; 7. Thermocouple; 8. Temperature acquisition and control.

Homogeneous oxidation experiments of benzyl alcohol were carried out at varying temperature, nitric acid concentration and sulfuric acid concentration in the ranges 10 – 30 °C, 2.0 – 8.5 mol·L^{-1}, and 0 – 1.81 mol·L^{-1}, respectively.

Homogeneous nitration experiments of benzaldehyde were carried out at varying temperature, nitric acid concentration and sulfuric acid concentration in the ranges 10 – 50 °C, 2.41 – 6.72 mol·L^{-1}, and 8.9 – 10.0 mol·L^{-1}, respectively.

4.3. Batch experiments under heterogeneous conditions: reactor and procedures

At organics concentrations higher than their solubility in the acidic mixture a heterogeneous liquid-liquid reacting system was observed. To safely carry out reactions in isothermal mode, small amounts of organic substrate and nitrating mixture (total volume 1 mL) were stirred in a

test tube (10 mL) at a fixed impeller speed varying between 800 and 1200 rpm. The test tube was being immersed in a magnetically stirred thermostatic bath during the experiments. The reaction was quenched by dilution adding 9 mL of cold acetonitrile in the test tube since it is impossible to separately sample from the aqueous and the organic phase. The resulting homogeneous solution was further diluted (1:100) before HPLC analyses. The procedure was repeated for each experimental reaction time.

4.4. Continuous experiments: microreactor and procedures

Microreactor experiments were carried out adopting two different microreactor configurations: a bath-immersed tubular reactor and an integrated microreactor with embedded static mixer and heat exchanger.

In the first case, the experimental setup consisted of two syringe pumps (Harvard Apparatus) connected to a cross mixer with pre-heating channels of 1 mm internal diameter. The cross mixer was connected to the microreactor channel (2 mm internal diameter). The preheating channels, cross mixer, and tubular reactor were immersed in a thermostatic water bath. A scheme of the reactor is provided in Fig. 4.2. Tubular microreactor of different lengths were used depending on the experimental conditions. In this reactor configuration, the nitrating mixture was prepared as described in the previous Section and successively transferred to the syringes. The liquid organic substrate was fed separately. Reaction time was changed varying the reactor length and the flow rates. Samples were collected at the outlet of the reactor and rapidly quenched and analyzed.

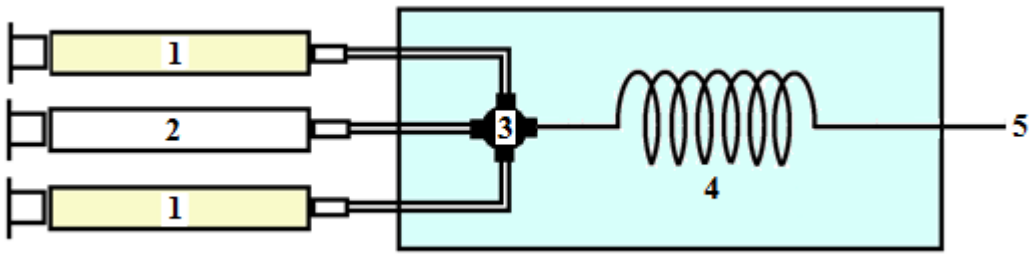

Fig. 4.2. Scheme of the immersed microreactor. 1. Nitrating mixture; 2. Organic substrate; 3. Cross mixer; 4. Tubular microreactor; 5. Sampling point.

The second adopted microreactor configuration is a commercially available integrated borosilicate microreactor with static embedded mixer and heat exchanger (Little Things

Factory XXL-ST-04). A scheme of the reactor is provided in Fig. 4.3. It consists of a borosilicate plate with separate circuits for the reagents and the cooling fluid. Two pre-heating/cooling channels (1 mL) are provided to separately feed the organics and the nitrating mixture. Pre-heated reagents are ducted into the main channel which is internally shaped to continuously mix the organics and mixed acid along the whole length. Three sampling ports are present along the reactor length to collect samples at different reaction times. Details about the volumes of the reactor sections are shown in Fig. 4.3. Mixed acid was fed by means of a peristaltic pump (V-3 pump, Vapor tec Ltd.), whereas a syringe pump (PhD Ultra Harvard Apparatus) was used to feed the organics. In this case, ethylene glycol was used as a cooling fluid to prevent borosilicate cracking due to thermal expansion and/or accidental water freezing. For each experimental run, the borosilicate plate was heated/cooled at the desired temperature. Acids were separately mixed, preheated at the desired temperature and fed to the pump. Residence time was changed varying both the flow rate and the volume in the ranges 0.45 – 9.99 $mL \cdot min^{-1}$ and 1.5 – 4.5 mL, respectively. The volume was changed sampling at different reactor lengths (sampling points in Fig. 4.3). The collected samples were quenched before analyses as previously described.

Continuous flow experiments were carried out at varying temperature, nitric acid concentration and sulfuric acid concentration up to 68 °C, 8.3 $mol \cdot L^{-1}$, and 10.7 $mol \cdot L^{-1}$, respectively.

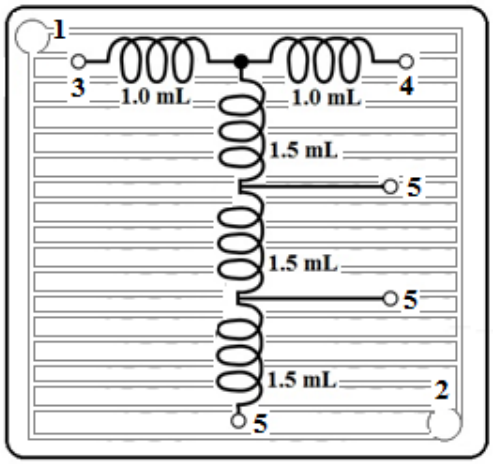

Fig. 4.3. Scheme of the integrated commercial microreactor. 1. Coolant inlet; 2. Coolant outlet; 3. Mixed acid inlet; 4. Organic inlet; 5. Sampling points.

4.5. Analytical methods

HPLC analysis was performed using an Agilent 1100 model, equipped with an UV DAD detector and a Phenomenex Synergi 4 μm polar RP/80A column, thermostated at 30 °C. The mobile phase, flowing at 1.0 $mL \cdot min^{-1}$ was constituted of eluent (A) (buffer solution: methanol 5 v/v % and phosphoric acid 0.4 v/v % in water) and eluent (B) (acetonitrile). The gradient was as follows: 15 % B for 8 min, increased to 25% B in 10 min, and successively decreased to 15 % B in 5 min. Signals were acquired at 210, 230, 250, and 265 nm. All the substances were calibrated using analytical standards and showed a good linearity in the considered ranges of concentration with R^2 values always higher than 0.989.

Electron paramagnetic resonance analysis (EPR) was performed adding a proper amount of an aqueous DMPO radical trapper solution to each sample before dilution.

Raman spectra were acquired using a Raman microscope (Horiba XploRA) equipped with a 20X objective (Olympus UPlanFL). The laser source was a frequency doubled Nd:YAG laser (λ= 532 nm, 12 mW maximum laser power at the sample). The calibration of the system was performed against the Stokes Raman signal of pure silicon at 520 cm^{-1}. A 100 μm pinhole was used for confocal photons collection. Spectra were obtained with a laser beam power of 100%, and an accumulation-exposure time of 3 cycles of 10 s each. Liquid acid mixtures were prepared as described in Section 4.2., cooled down to room temperature and collected in a quartz closed cuvette for spectrophotometry, that was successively placed under the objective. The calibration procedure for bisulphate ions concentration was carried out at 426 $cm^{-1}$and 1048 cm^{-1}, using sulfuric acid concentrated solutions for which a full conversion to bisulphate is reported (Robertson et al., 1964). Nitrate ions intensity peaks were calibrated at 1048 cm^{-1} using different sodium nitrate solutions and the results were verified with different nitric acid samples with known dissociation degree to nitrate (Davis et al., 1964). For ternary mixture of sulfuric acid and nitric acid in water, bisulphate ion concentration was measured at 426 cm^{-1}, and the results were used to estimate nitrate concentration at 1048 cm^{-1} through a deconvolution procedure.

5. Results I: Speciation of ternary HNO_3-H_2SO_4-H_2O mixtures

5.1. Introduction

As mentioned in the previous Chapters, ternary mixtures of nitric acid, sulfuric acid and water, i.e. mixed acid, are the most widely employed nitrating agent in the industry and research, and the most effective mixtures for benzaldehyde nitration. In this Chapter, the results of an experimental campaign for a simplified description of nitric acid and sulfuric acid speciation in ternary aqueous mixtures is presented. The aim of the present investigation is to verify and justify the assumptions found in the literature and show their limitations in the modeling of reacting systems.

The modeling of the equilibrium concentration of undissociated acids and ionic species deriving from their dissociation is of crucial importance in investigating oxidation and nitration kinetics and several semi-empirical or simplified approaches can be found in the literature (Albright et al., 1996; Zaldivar et al., 1995; Minogue et al., 2003; Chen et al., 2016a; Wang et al., 2017). Most investigations agree on the fact that the main ionic species deriving from the acids dissociation are the nitrate ion NO_3^-, the nitronium ion NO_2^+ and H^+, together with bisulfate HSO_4^- and sulfate SO_4^{2-} ions, even though the incidence of the latter is very little significant with respect to HSO_4^- for relatively diluted aqueous mixtures and negligible for highly acidic media. The presence of other species deriving from the protonation of strong acids, i.e. $H_2NO_3^+$ and $H_3SO_4^+$, are assumed by some Authors (Hoggett et al., 1971; Minkwitz, 2002). Despite this, the former rapidly decomposes to nitronium ion and water, whereas the latter is assumed to be present only for almost neat sulfuric acid (Hoggett et al., 1971; Galabov et al., 2016; Minkwitz, 2002).

As a result, for the normally adopted nitrating mixture the following equilibria are considered to be sufficient in describing the acids speciation

$$HNO_3 + H_2SO_4 \leftrightarrow NO_2^+ + HSO_4^- + H_2O \qquad \text{r. 5.1}$$

$$HNO_3 \leftrightarrow H^+ + NO_3^- \qquad \text{r. 5.2}$$

$$H_2SO_4 \leftrightarrow H^+ + HSO_4^- \qquad \text{r. 5.3}$$

Equilibrium 5.1 is by far the most important in the modeling of nitration processes, since the aromatic electrophilic substitution reaction rate is directly related to the nitronium ion concentration. The most extended available Raman experimental data on nitronium ion concentrations are presented by Albright et al. (1996) and Edwards et al. (1994) together with a simplified approach to their modeling, presented in Chapter 2.

Despite that, it must be noted that most kinetic investigations are carried out in mixtures in which the concentration of nitronium ion is lower than the limit of quantification (and often the limit of detection) by Raman analysis (Edwards et al., 1995). In fact, under those less acidic conditions, nitration rates are slower and easy to follow. Too high nitronium ion concentrations often give rise to very fast or instantaneous reactions and precise reaction rate evaluations are not possible. Finally, most Authors often choose to carry out slow nitration for safety reasons and to keep constant temperature up to the complete conversion within the limits of the commercially available cooling systems (Chen et al., 2016b; Di Somma et al., 2014a; Di Somma et al., 2012; Li et al., 2017; Russo et al., 2017a; Di Somma et al., 2017, Russo et al, 2017b).

Lastly, the commercially available software for the non-ideal systems equilibrium composition calculation, i.e. ASPEN, are based on very complex models (Pitzer, eNRTL, etc.), but, to the present, there is a serious lack of data about the parameters of the models for the nitronium ion concentration evaluation.

Similar difficulties have to be faced in the modeling and prediction of the dissociation of nitric acid in sulfuric acid and *viceversa*. The only extensive available data were published for binary nitric acid / water and sulfuric acid / water systems (Davis et al., 1964; Redlich et al., 1968; Robertson et al., 1964; Tomikawa et al., 1998; Fraenkel, 2015).

5.2. Nitronium ion concentration prediction

For the prediction of nitronium ion concentrations by r. 5.1, in all the possible aqueous ternary mixtures of nitric and sulfuric acids, no thorough and complete equilibrium models exist. It must be remarked that, from the available nitronium ion concentration measurements and from the literature indications, it is clear that NO_2^+ is present at trace level and is not detectable in mixtures with a water molar fraction higher than 0.5 and its concentration rapidly increases of several orders of magnitude in more acidic media (Edwards et al., 1995).

Nitric acid is fully ionized to nitronium ion for sulfuric acid concentrations higher than 95 wt. % (Hoggett et al., 1971). On the basis of the literature findings (Albright et al., 1996; Edwards et al., 1994) and the results of the present thesis work, three main regions can be individuated in a ternary diagram. The light green region in Fig. 5.1 represents all the mixtures in which nitronium ion is detectable by Raman. As a result, no experimental measurements exist out of this region. For this reason, the dividing line between the green and the pale blue region is identified as the 0% dissociation line of nitric acid to nitronium ion (Edwards et al., 1994). In spite of this, nitrations of organic substrates are reported to occur beyond this line, in the pale blue region of Fig. 5. 1, in the present investigation as well as in previous works (Zaldivar et al., 1995; Di Somma et al., 2014b; Andreozzi et al., 2006). To this merit, even though NO_2^+ is not detectable by Raman in this region, it is still present and effective in the nitration of aromatics. Finally, the purple region of Fig. 5.1. contains all the mixtures for which no nitration of organic substrate occurs, or it is so slow that is not suitable for laboratory accurate kinetic study and industrial applications.

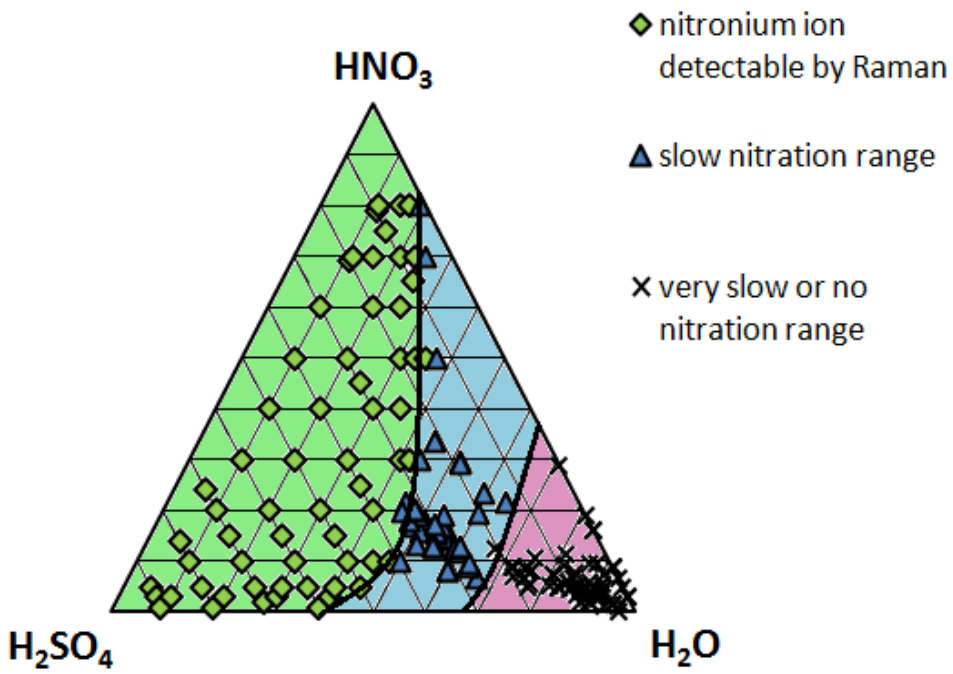

Fig. 5.1. Investigated experimental conditions in the literature and this thesis for nitronium ion determination.

The only reported attempt to model the experimental data of the green region of Fig. 5.1 was proposed by Albright et al. (1996). As outlined in Chapter 2, the proposed model is inadequate, since it is based on the assumption of ideal behavior of the equilibrium species in

a wide range of highly acidic experimental conditions. The previous presented semi-empirical approach of the H_R acidity function was adopted for nitration kinetics in the pale blue region.
In Chapter 2, the M_C function was presented. In the same Section, it was shown that the relation

$$M_C^{NO_2^+} = -log\left(\frac{\gamma_{H^+}\gamma_{HNO_3}}{\gamma_{NO_2^+}}\right) = nM_C^{H_2SO_4} \qquad \text{eq. 5.1}$$

taking into account the non-ideal behavior of reaction r. 5.1, was verified for nitric acid concentrations up to 0.1 mol·L^{-1} and successfully used for modeling nitrations occurring in the pale blue region of Fig. 5.1, although some changes in the value of the constants and the definition of $M_C^{NO_2^+}$ were introduced. In Zaldivar et al., 1995, for example, the activity coefficient of water is also included in the denominator of eq. 5.1. However, any attempt to reproduce the experimental data by Albright et al. (1996) in the high acidic region by means of the previously proposed $M_C^{NO_2^+}$ function gave disappointing results. This is completely reasonable if one considers that the validity of the M_C function, as defined by 5.1, has been proved only in the range 80 – 100 % wt. of sulfuric acid for nitric acid at trace levels (Sampoli et al., 1985). Moreover it must be highlighted that the definition of $M_C^{NO_2^+}$ is significantly different from that of M_C for the protonation of a generic base, which was extensively studied and proved in a wide range of sulfuric acid concentration, because of the different nature of the species considered in the reported ratio (eq. 5.1).
The experimental nitronium ion concentrations by Albright et al. (1996) are shown in Fig. 5.2 as plotted by Edwards et al. (1994). It can be noted that, at a fixed molar percentage of HNO_3 the molar concentration of NO_2^+ *vs*. the molar percentage of H_2SO_4 (S%) follows a sigmoidal profile for all the adopted conditions.

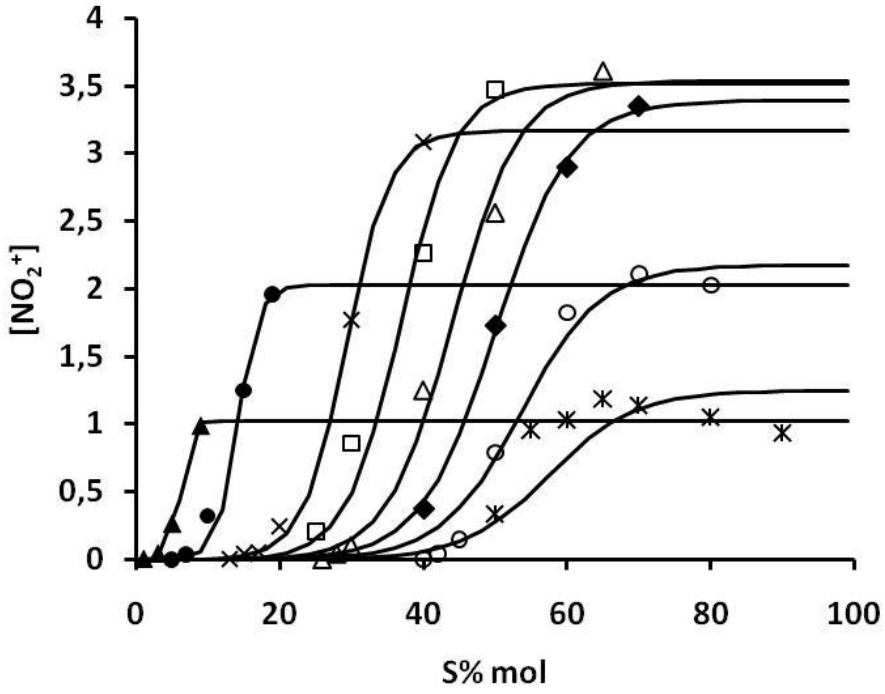

Fig. 5.2. [NO_2^+] molar concentration vs H_2SO_4molar percentage (S%) at varying nitric acid molar percentage (N%). (ж) 5 N%; (○) 10 N%; (♦) 20 N%; (△) 30 N%; (□) 40 N%; (X) 50 N%; (●) 70%; (▲) 80%. Experimetal data from Albright et al., (1996) and Edwards et al. (1994).

In this region, a semi-empirical approach can thus be applied. The following expression was used to fit the experimental data

$$[NO_2^+] = \frac{a}{1 + b \cdot \exp(-c \cdot S\%)} \qquad \text{eq. 5.2}$$

where $S\%$ is the sulfuric acid molar percentage and $[NO_2^+]$ the concentration of nitronium ion in mol·L^{-1}. The values of the constant parameters a, b, and c were optimized in order to minimize the mean square deviation between the experimental and calculated data, and their values were plotted *vs.* the nitric acid molar percentage $N\%$ in the mixture. The results are shown in Fig. 5.3. The values of the parameters can be expressed by the following polynomial expressions.

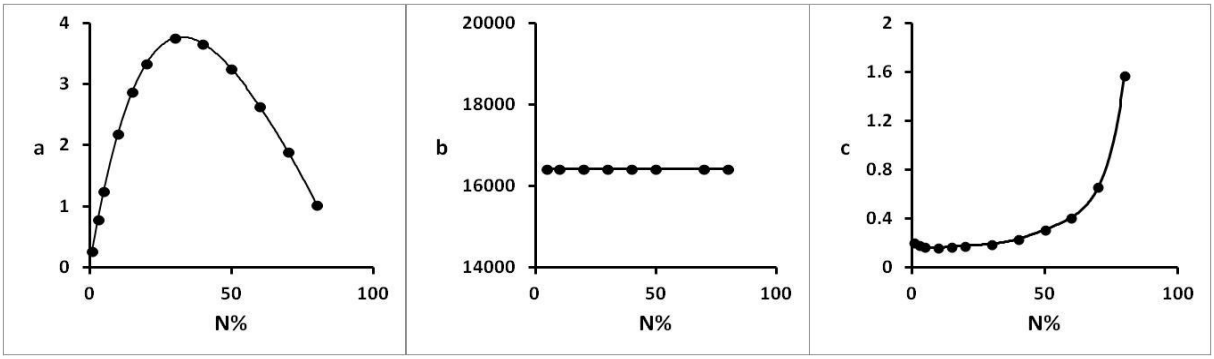

Fig. 5.3. Dependence of the parameters of equation 5.2 on the nitric acid molar percentage $N\%$.

$$a = -2.409 \cdot 10^{-7}(N\%)^4 + 6.392 \cdot 10^{-5}(N\%)^3 - 6.942 \cdot 10^{-3}(N\%)^2 + 2.823 \cdot 10^{-1}(N\%) \quad \text{eq. 5.3}$$

$$b = 16426 \quad \text{eq. 5.4}$$

$$c = 1.891 \cdot 10^{-10}(N\%)^6 - 3.934 \cdot 10^{-8}(N\%)^5 + 3.169 \cdot 10^{-6}(N\%)^4 - 1.226 \cdot 10^{-4}(N\%)^3 + 2.395 \cdot 10^{-3}(N\%)^2 - 2.085 \cdot 10^{-2}(N\%) + 2.2686 \cdot 10^{-1} \quad \text{eq. 5.5}$$

where a is expressed in mol·L^{-1}, and b and c are adimensional parameters.

Eq. 5.2 is inaccurate in calculating nitronium ion concentrations in the pale blue and purple regions of Fig. 5.1, since it overestimated their values. In these cases, even though a small absolute error is present, it is relatively significant for very low nitronium ion concentrations and can be dramatically important in kinetics investigations carried out under these conditions.

For nitrations occurring in the neighbourhood of standard mixed acid composition, i.e. 20 % wt. HNO_3 and 60 % wt. H_2SO_4, represented by the blue triangles in Fig. 5.1. with a nitric acid molar fraction lower than about 0.2, the H_R function-based models have been reported (Di Somma et al., 2012; Zaldivar et al., 1992). As previously mentioned, according to this semi-empirical approach the nitronium ion concentration can be estimated as

$$[NO_2^+] = exp\left(\frac{\Delta H}{RT}\right) exp\left(\frac{\Delta S^*}{R}\right) \frac{\gamma_{HNO_3}}{\gamma_{H_2O}} \frac{[HNO_3]}{[H_2O]} 10^{-H_R} \quad \text{eq. 5.5}$$

where γ_{HNO_3} and γ_{H_2O} can be evaluated as shown in Khudhairy et al. (1989). The values of ΔH and ΔS^* were recalculated on the basis of those reported by Di Somma et al. (2014a), but removing the simplifying assumption of independence of the activity coefficients on temperature. Their values are 50.94 kJ·mol^{-1} and 39.63 J·mol^{-1}·K^{-1}, respectively. H_R values can be calculated according to eq. 2.1. Even though eq. 5.5 has already been used for NO_2^+ concentration estimation, there are no experimental measurements available to prove its validity. In this Chapter, an indirect experimental method for its evaluation is proposed. According to the general reaction mechanism of nitration, under the adopted conditions, the nitration reaction rate of an aromatic substrate Ar is

$$r = k_{int}[NO_2^+][Ar] \qquad \text{eq. 5.6}$$

where k_{int} is the intrinsic kinetic constant of the reaction between nitronium ion and the aromatic substrate. Nitration of benzaldehyde was chosen as a reference reaction. Considering two experimental runs carried out at the same temperature but in different nitrating mixtures, the initial reaction rate for t = 0 can be derived from the initial slope of the concentration profile *vs.* the time. It can be expressed as

$$r_1^0 = k_{int}[NO_2^+]_1^0[Ar]_1^0 \qquad \text{eq. 5.7}$$

$$r_2^0 = k_{int}[NO_2^+]_2^0[Ar]_2^0 \qquad \text{eq. 5.8}$$

where the subscripts 1 and 2 refer to two different experimental runs. From equations 5.7 and 5.8 the following expression can be derived

$$[NO_2^+]_2^0 = \frac{r_2^0}{r_1^0}\frac{[Ar]_1^0}{[Ar]_2^0}[NO_2^+]_1^0 \qquad \text{eq. 5.9}$$

that makes it possible to calculate the concentration of nitronium ion in an unknown mixture 2, once the $[NO_2^+]_1^0$ concentration is known. Equation 5.9 can be adopted to estimate nitronium ion steady-state concentrations in all the possible ternary mixtures, once the initial reaction rate is measured. The method was validated verifying the validity of equation 5.9 for three different nitrating mixture for which experimental data are available (Albright et al.,

1996). The three nitration experiments were run at 20 °C with experimental nitronium ion concentration of 0.149, 0.086, and 0.041 mol·L^{-1}. Benzaldehyde profiles *vs.* time are shown in Fig. 5.4.

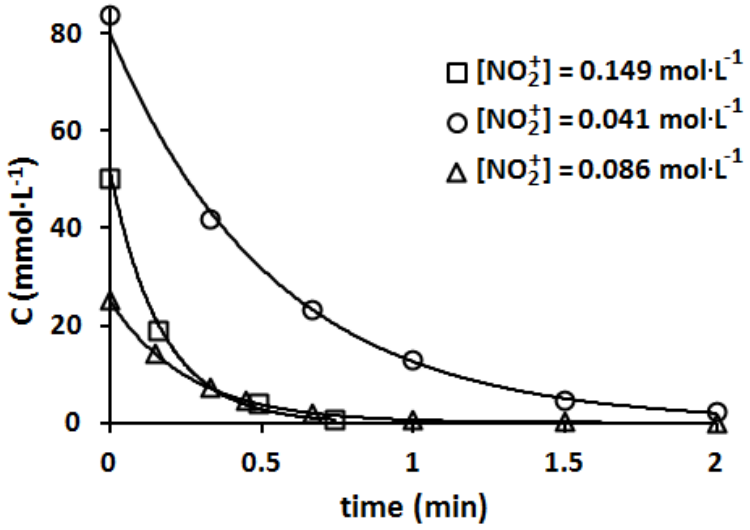

Fig. 5.4. Benzaldehyde profiles *vs.* time for three different experimental runs. Lines are for convenience of the eye.

The concentration of nitronium ion for each run was estimated by eq. 5.9 considering one at time the other two as a reference and the estimated values were always close to the experimental ones with a maximum 7% error.

Once validated, the method was used to estimate the nitronium ion concentration in mixtures with an unknown concentration of nitronium ion in the concentration range represented by the blue triangles in Fig. 5.1. The results were compared with the values estimated by using equation 5.5. The initial nitric acid and sulfuric acid concentrations for the analyzed mixtures are summarized in Table 5.1.

In Fig. 5.5, the results of the described indirect measurements are directly compared with the prediction of the model proposed by Albright et al. (1996), the predictions of equation 5.2, i.e. the sigmoidal model, and the estimations given by eq. 5.5. The calculated and experimental nitronium ion concentrations have been arbitrarily plotted *vs.* the molar concentration of nitric acid. The above-mentioned overestimation of the proposed models for highly acidic mixtures (green region of Fig. 5.1) is shown in Fig 5.5a. The expanded scale in Fig. 5.5b shows the

good agreement between the indirectly measured NO_2^+ concentrations and the H_R function-based calculations in this range of concentrations.

$[HNO_3]_0$(mol·L^{-1})	$[H_2SO_4]_0$(mol·L^{-1})
2.41	9.49
3.04	9.40
3.87	9.16
4.93	10.03
5.25	9.35
4.70	9.86
5.03	9.23
5.21	8.80
4.55	9.25
5.26	8.96
5.61	9.41
4.07	9.22
3.31	9.08
5.93	8.45
4.85	9.35
4.86	9.37
5.29	9.14

Table 5.1. Adopted experimental condition to estimate nitronium ion concentration in the neighbourhood of the standard mixed acid.

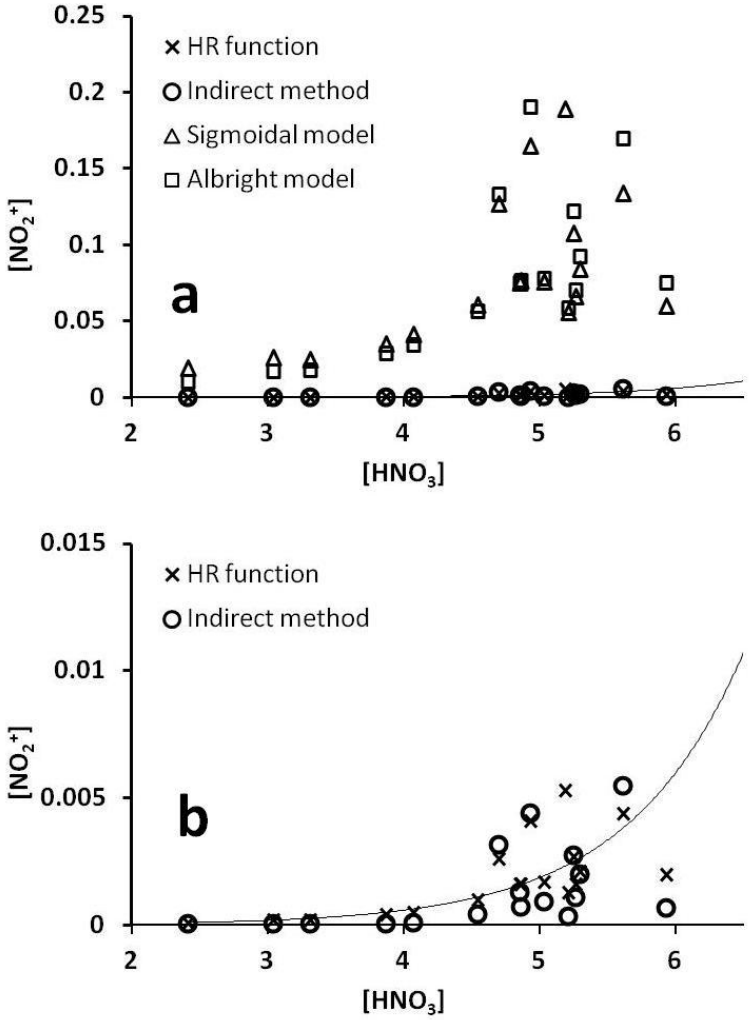

Fig. 5.5. a) comparison between NO_2^+ concentrations calculated using the model by Albright et al. (1996) and the proposed sigmoidal model, and the lower concentrations calculated by indirect measurement and the H_R function. b) Comparison between the NO_2^+ concentrations calculated using indirect measurement and the H_R function (zoom in).

5.3. Raman dissociation measurements of sulfuric acid to bisulphate and nitric acid to nitrate

As mentioned in the introductive Section 5.1, no available data on nitric acid dissociation to nitrate and sulfuric acid to bisulphate in concentrated acidic mixtures are available in the literature. Most Authors (Sampoli et al., 1985; Zaldivar et al., 1995; Li et al., 2017) considered, as an implicit simplifying assumption, that there was no influence of nitric acid on

sulfuric acid dissociation, being the former (reported pK_a ranging from -3 to -9, (Mosier et al., 2002; Kawamoto et al., 2007; Shin et al., 2013; Allinger et al., 1972)) a much stronger acid than the latter, pK_a = -1.4 (Perrin, 1982). This assumption is surely true and verified for low nitric acid concentrations (Deno et al., 1961). However, no direct measurement can support this hypothesis for higher nitric acid concentrations, which are normally adopted in nitrating mixtures. A first experimental evidence is provided in the following. In Fig. 5.6, Raman peaks of three different aqueous mixtures of sulfuric acid are compared with those of ternary mixtures with the same sulfuric acid concentration but in the presence of significant amounts of nitric acid. The shown Raman peaks at 426 cm^{-1}, are reported to be due to the ν_2 band of HSO_4^- (Tomikawa et al., 1998, Walrafen et al., 2002). No peaks are present for aqueous nitric acid at the same wavelength (not shown).

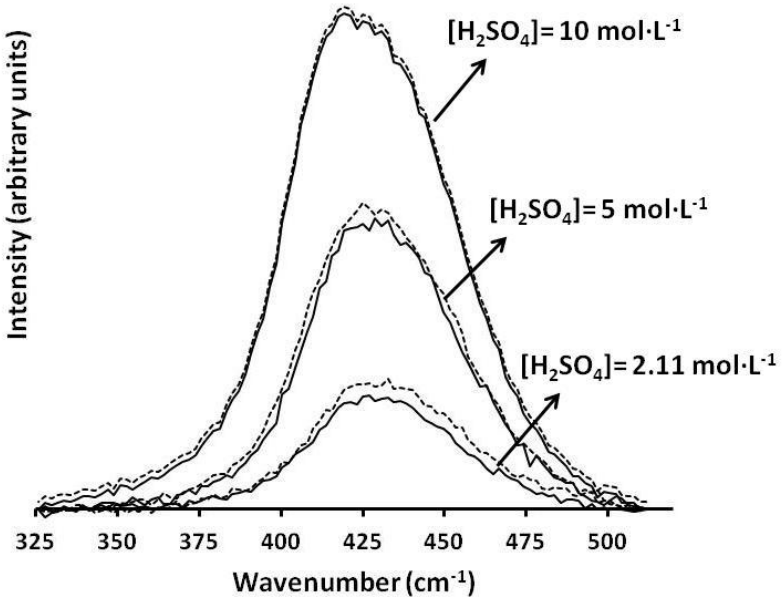

Fig. 5.6. Comparison of the bisulphate Raman peak at varying sulfuric acid concentration without nitric acid (continuous line) and with added nitric acid (dashed lines). The added nitric acid concentrations are 1, 3, and 5 mol·L^{-1} for sulfuric acid concentrations of 2.11, 5 and 10 mol·L^{-1}, respectively.

As evident from Fig. 5.6., no substantial changes in the peak shape, position and intensity are recorded, especially for higher acids concentrations, proving that the sulfuric acid dissociation is not affected by nitric acid even for comparable concentrations.

To better investigate the acids speciation, other 31 ternary mixtures with nitric acid, sulfuric acid, and water initial concentrations varying in the ranges 1.14 – 10.93 mol·L^{-1}, 1.75 – 15.9 mol·L^{-1} and 5.69 – 44.7 mol·L^{-1}, respectively, were submitted to Raman analysis. An example of Raman spectra of a concentrated ternary aqueous mixture of nitric and sulfuric acid is shown in Fig. 5.7.

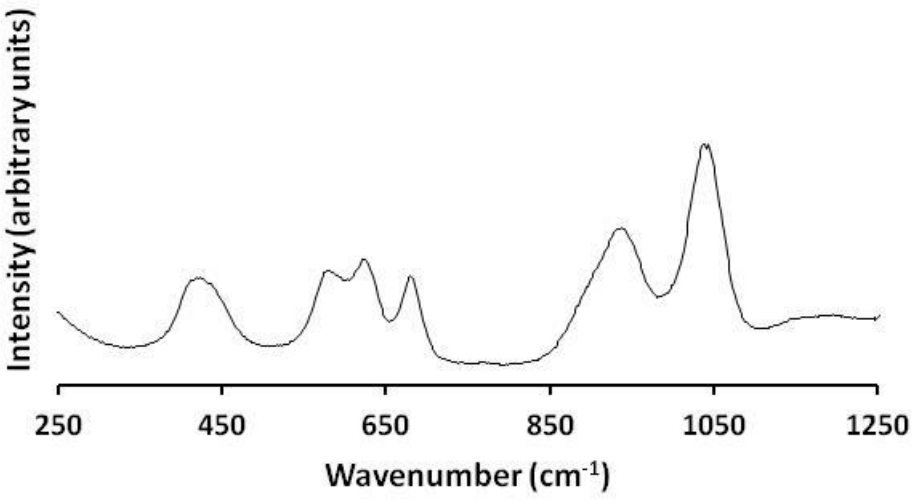

Fig. 5.7. Raman spectra of a ternary mixture of nitric acid, sulfuric acid, and water. $[HNO_3]_0$ = 8.72 mol·L^{-1}; $[H_2SO_4]_0$ = 7.56 mol·L^{-1}.

Bisulphate ion concentrations were estimated by the peak intensity at 426 cm^{-1}. The calibration procedure was carried out through several binary aqueous sulfuric acid mixtures with a sulfuric concentration lower than 11 mol·L^{-1}, for which a unitary dissociation degree is reported (Robertson at al., 1964; Tomikawa et al., 1998; Fraenkel, 2015). Once the bisulphate ion concentration was estimated, the nitrate concentration was calculated using a deconvolution procedure at 1048 cm^{-1}. The nitrate ion concentration was predicted with good accuracy for binary aqueous solutions of nitric acid with known dissociation degrees, once a calibration line was obtained using aqueous sodium nitrate solutions. Further details are provided in Chapter 4. Nitronium ion concentration was estimated as shown in Section 5.2. The results of the Raman analyses for the investigated mixtures are shown in Table 5.2. H_2SO_4 and HNO_3 concentrations were calculated as the difference between their initial

analytical concentration and the concentrations of the ionic species deriving from their dissociation.

$[HNO_3]_0$	$[H_2SO_4]_0$	$[H_2O]_0$	$[H_2SO_4]$	$[HSO_4^-]$	$[HNO_3]$	$[NO_3^-]$	$[NO_2^+]$
2.77	12.45	12.45	0.95	11.50	2.52	0.10	0.15
8.72	7.56	12.79	0.06	7.50	8.19	0.53	0.00
6.02	10.84	7.23	0.84	10.00	5.92	0.10	0.00
1.14	15.94	5.69	1.46	14.49	0.00	0.00	1.14
4.53	13.59	4.53	1.47	12.12	1.20	0.42	2.91
6.96	11.60	4.64	0.91	10.69	3.98	0.42	2.56
9.51	9.51	4.76	0.06	9.45	7.13	0.12	2.27
10.93	6.83	9.56	0.16	6.67	10.21	0.51	0.21
2.41	9.49	23.28	0.09	9.40	2.14	0.27	0.01
4.93	10.03	14.52	0.28	9.75	4.52	0.41	0.01
5.81	9.52	13.72	0.48	9.04	5.37	0.44	0.02
5.03	9.23	16.84	0.23	9.00	4.65	0.38	0.00
5.61	9.41	14.61	1.53	8.94	5.18	0.43	0.02
6.17	9.54	13.06	0.56	8.98	5.74	0.44	0.03
2.92	2.78	42.11	0.36	2.42	1.61	1.31	0.00
6.59	6.76	20.34	0.12	6.64	6.23	0.36	0.00
3.18	8.80	22.74	0.15	8.64	2.86	0.31	0.00
0.92	1.75	50.39	0.26	1.49	0.56	0.37	0.00
3.25	6.27	30.47	0.29	5.98	2.79	0.46	0.00
1.93	10.39	21.11	0.00	10.39	1.60	0.32	0.00
2.64	7.04	29.49	0.15	6.89	2.27	0.37	0.00
2.63	7.86	9.26	0.11	7.75	1.94	0.69	0.02
10.02	6.42	13.35	0.59	5.84	9.66	0.36	0.02
9.28	5.94	16.30	0.90	5.68	8.98	0.29	0.01
2.00	2.11	44.70	0.06	2.05	1.11	0.89	0.00
3.00	5.00	33.85	0.11	4.89	2.30	0.70	0.00
4.61	1.30	41.36	0.02	1.28	2.50	2.10	0.00
4.64	1.92	39.58	0.00	1.92	2.73	1.92	0.00
4.73	3.28	35.69	0.01	3.27	3.34	1.39	0.00
3.13	1.94	43.01	0.23	1.71	1.49	1.64	0.00
6.24	3.22	32.31	0.04	3.19	4.92	1.32	0.00

Table 5.2. Experimental equilibrium concentrations by Raman analyses.

As presented in Table 5.2, H_2SO_4 dissociation degree resulted to be always higher than 90% for sulfuric acid initial concentrations up to 11 mol·L^{-1}, with a mean dissociation degree of about 95%. This is in agreement with literature data about binary $H_2SO_4 - H_2O$ mixtures (Robertson et al., 1964; Tomikawa et al., 1998; Fraenkel, 2015) for which the dissociation is almost complete. Nitric acid dissociation degrees are almost always lower than 10% in highly

acidic mixtures whereas a maximum ionisation degree of 52% was calculated for less acidic mixtures. The reported general considerations are in accordance with the previously published observations (Sampoli et al., 1985; Zaldivar et al., 1995). Contrary to what was observed for sulfuric acid, nitric acid dissociation is significantly influenced by the presence of sulfuric acid and the registered ionization of nitric acid to nitrate is always lower than in pure water. As a general consideration at higher H_2SO_4 concentration, the dissociation of nitric acid to nitrate ion is inhibited. Moreover, nitric acid dissociation is inhibited by the presence of nitric acid itself, since it is known that its dissociation degree decreases for higher concentrations even in binary nitric acid/water mixtures. The previous considerations are well described by Zaldivar et al. (1995) in the diagram reported in Fig. 5.7. As shown, the nitric acid dissociation degree to nitrate in sulfuric acid decreases when increasing the initial concentration of sulfuric acid in the mixture. However, the diagram in Fig. 5.7. is obtained for nitric acid at trace levels, i.e. 10^{-4} mol·L^{-1}. The reported curve is reasonably parametric with nitric acid concentration. In this sense, the experimental measurements reported in this work can be considered as an extension of the results presented by Deno et al. (1961) for higher nitric acid compositions.

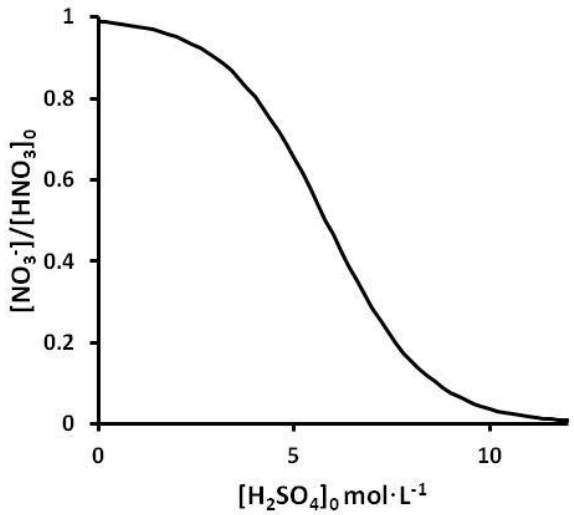

Fig. 5.7. Dissociation degree of nitric acid to nitrate *vs.* initial sulfuric acid concentration; data from Deno et al. (1990); Zaldivar et al. (1995).

5.4. Equilibrium simplified model

On the basis of the previous investigations and the data presented in this Chapter, a simplified model was proposed to predict the equilibrium species concentrations, based on the following reactions

$$H_2SO_4 \rightarrow HSO_4^- + H^+ \qquad \text{r. 5.4}$$

$$HNO_3 \rightleftarrows NO_3^- + H^+ \qquad \text{r. 5.2}$$

Incongruous information is reported for sulfuric acid pK_a ranging from -3 to -9 (Allinger et al., 1972; Mosier et al., 2002; Kawamoto et al., 2007; Shin et al., 2013). This is probably due to the difficulties in calculating such a high value for the dissociation constant that can vary in a wide range, when small errors in the equilibrium concentrations determination are made. In addition, there are several difficulties in evaluating with high accuracy the activity coefficient variation of ionic and neutral species in a strongly non-ideal solution for the full range of concentrations. In fact, the proposed thermodynamic models (Song et al., 2009; Bollas et al., 2008; Chen et al., 2004; Wang et al., 2017) are often based on very complicated equations and the identification of the model parameters is still an important subject of study. Therefore, simplified approaches have been proposed in the literature (Marziano et al., 1973; Zaldivar et al., 1995). However, for all practical purposes, at sulfuric acid concentrations up to about 11 $mol \cdot L^{-1}$ a full dissociation can be assumed without committing a too significant error. For the nitric acid dissociation in the presence of sulfuric acid the following equilibrium relation was considered

$$\frac{K_N}{55.56} = \frac{[NO_3^-][H^+]}{[HNO_3] \cdot a_{H_2O}} 10^{-n_N M_C} \qquad \text{eq. 5.10}$$

It is worth noting that the equation was slightly modified to take into account the definition of pK_N for high diluted acid solutions. In this case the reported value of 55.56 is the molar concentration of pure water that is usually included in the equilibrium constant value for highly diluted mixtures. In this case, it was chosen to express the equilibrium relation taking into account the variations of the water activity a_{H_2O}. For highly diluted systems eq. 5.10 is reduced to eq. 5.11, and pK_N is then defined and calculated.

$$K_N = \frac{[NO_3^-][H^+]}{[HNO_3]} \qquad \text{eq. 5.11}$$

According to the M_C function theory, the values of M_C were calculated by the following polynomial expression, eq. 5.12, obtained interpolating data from Marziano et al. (1981)

$$M_C = -2.0359 \cdot 10^{-4} \cdot [H_2SO_4]_0^4 + 8.2033 \cdot 10^{-3} \cdot [H_2SO_4]_0^3 - 1.2824 \cdot 10^{-1} \cdot [H_2SO_4]_0^2 + 5.6384 \cdot 10^{-2} \cdot [H_2SO_4]_0 - 2.3932 \cdot 10^{-1} \qquad \text{eq. 5.12}$$

where $[H_2SO_4]_0$ is expressed in mol·L^{-1}. Contrary to what was reported for the estimation of nitronium ion using the M_C function theory in Chapter 2, the validity of eq. 5.10 was verified in the whole range of sulfuric acid concentration and gave consistent results. In fact, the M_C definition is strictly applicable for r. 5.2, and improperly extended in eq. 5.1.

On the basis of the mentioned assumption, the model relied on the following mass balances

$$[HNO_3]_0 = [HNO_3] + [NO_3^-] + [NO_2^+] \qquad \text{eq. 5.13}$$

$$[H^+] + [NO_2^+] = [NO_3^-] + [HSO_4^-] \qquad \text{eq. 5.14}$$

$$\frac{K_N}{55.56} = \frac{[NO_3^-][H^+]}{[HNO_3] \cdot a_{H_2O}} 10^{-n_N M_C} \qquad \text{eq. 5.10}$$

$$[HSO_4^-] \approx [H_2SO_4]_0 \qquad \text{eq. 5.15}$$

$$[H_2SO_4] \approx 0 \qquad \text{eq. 5.16}$$

where eq. 5.13 and 5.14 are the nitrogen and charge balance, respectively. In both equations the nitronium ion concentration $[NO_2^+]$ was estimated as described in Section 5.2 depending on the initial conditions. The set of equations was solved by means of the software Matlab in order to find the values of K_N and n_N to minimize the mean square deviation between the calculated concentrations of the species and the experimental data reported in Table 5.2.

The best estimated values were K_N = 25.5± 0.87 mol·L^{-1} and n_N = 0.37± 0.03. It is worth noting that the K_N estimated value corresponds to pK_N= -1.4, very close to the one reported in the literature (Perrin, 1982). The results, in terms of the experimental (symbols) and calculated (continuous lines) concentrations of the species in all the considered mixtures, are reported in Fig. 5.8.

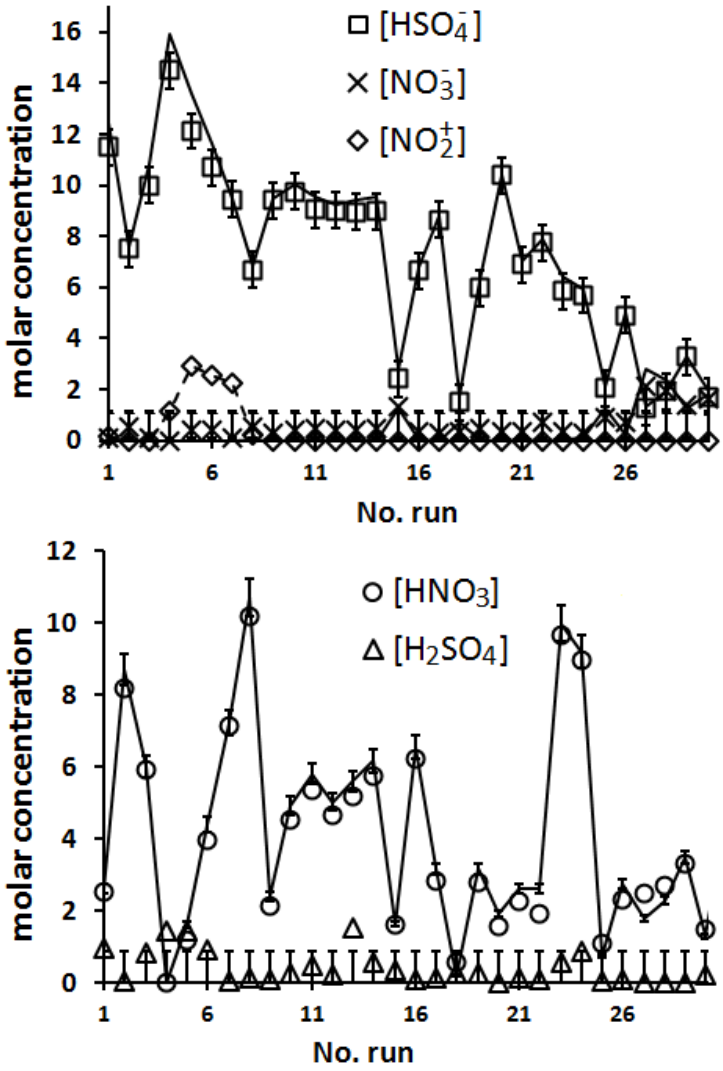

Fig. 5.8. Experimental (symbols) and calculated (continuous lines) concentrations for ionic and neutral species at the equilibrium.

As shown, the model is capable of predicting with good accuracy the speciation of nitric and sulfuric acid in ternary concentrated mixtures with sulfuric acid concentrations up to 11 $mol \cdot L^{-1}$.

In conclusion, according to the above results and considerations, nitronium ion concentration can be calculated using either the H_R function (low acidity range) or the sigmoidal empirical model (high acidity range), depending on the initial concentrations of nitric and sulfuric acid. Under the normally adopted conditions for nitrations, i.e. in the neighborhood of standard mixed acid composition, nitric acid decomposition to nitrate is negligible. On the other hand, for more diluted systems, which are normally used to oxidize organic compounds, the dissociation of sulfuric acid is unaffected by the presence of nitric acid, and the contribution

of nitric acid dissociation to the acidity of the media can be calculated according to the above-developed simplified model.

6. Results II: Preliminary investigations on nitrobenzaldehydes synthesis from benzyl alcohol

6.1. Feasibility of tandem oxidation-nitration of benzyl alcohol in mixed acid

Preliminary experimental runs were carried out in order to confirm literature indications and verify preliminary hypothesis about the reacting system.

The results of three different isothermal runs, carried out adding low concentrations of benzyl alcohol to three different nitrating mixtures, are shown in Fig. 6.1. A 25 % wt. aqueous mixture of nitric acid was used in Fig. 6.1a; recorded concentration profiles confirmed the indications found in the literature, since benzyl alcohol was quantitatively converted to benzaldehyde with unitary yield and selectivity. The reaction time was considerably decreased in the kinetic run of Fig. 6.1b, for which an amount of 10 % wt. of sulfuric acid was added. Lastly, concentrated mixed acid, i.e. 21.9 % wt. HNO_3, 58 % wt. H_2SO_4, and 20.1 % wt. H_2O, were adopted in Fig. 6.1c. The results of this last run confirmed the initial hypothesis on the possibility to obtain nitrobenzaldehydes from benzyl alcohol in mixed acid. As shown, benzyl alcohol is almost instantaneously converted to benzaldehyde so that only traces of benzyl alcohol can be detected in the first sample assumed as the zero-time reaction sample. No traces of nitrated derivatives of benzyl alcohol were detected. Moreover, the pseudo-first order kinetics of both nitration and oxidation reactions were confirmed. Instantaneously formed benzaldehyde was successively nitrated in the same reaction media with a higher occurrence of 3-nitrobenzaldehyde.

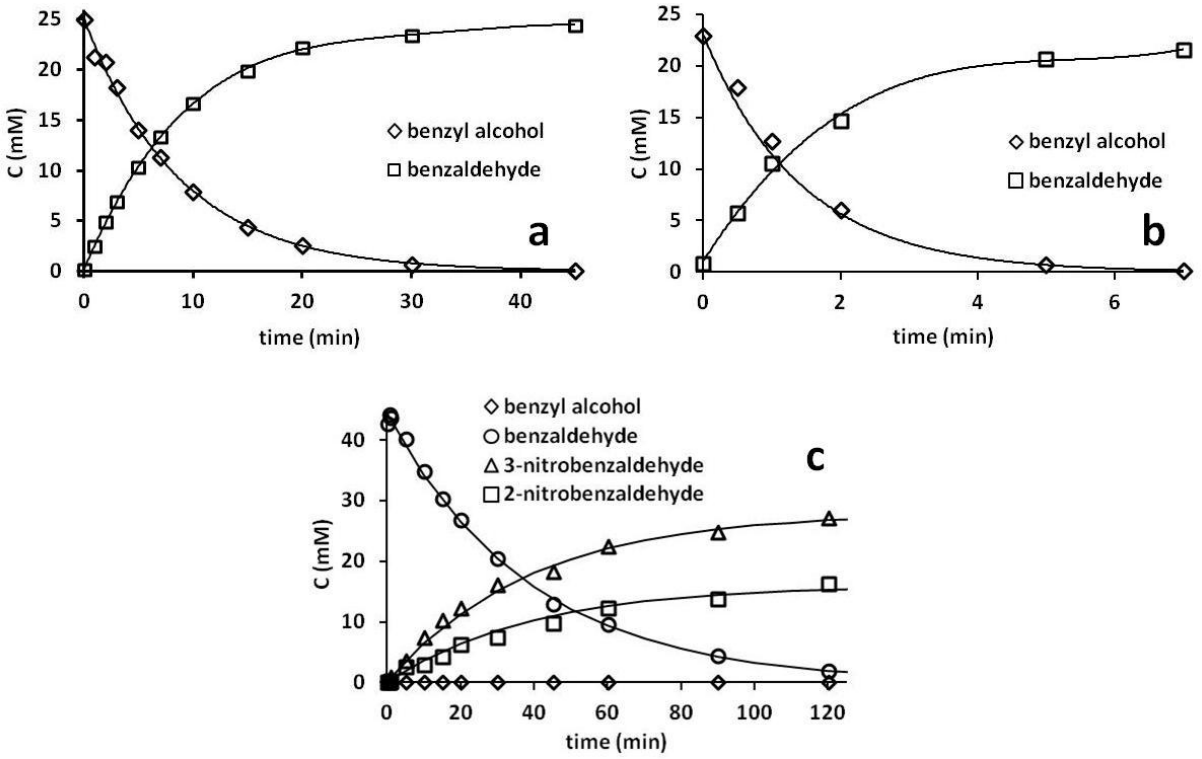

Fig. 6.1. Preliminary kinetic runs on benzyl alcohol in different mixtures. a) 25 % wt. HNO_3, 75 % wt. H_2O, T = 30 °C. b) 25 % wt. HNO_3, 10 % wt. H_2SO_4, 65 % wt. H_2O, T = 30 °C. c) 21.9 % wt. HNO_3, 58 % wt. H_2SO_4, 20.1 % wt. H_2O, T = 20 °C. Lines are for the convenience of the eye.

Contrary to what was reported in the literature (Ogata et al., 1966; Ross et al., 1986; Strazzolini et al., 2003), the oxidation of benzyl alcohol in aqueous nitric acid and mixed acid occurs even without the addition of nitrite. The addition of sodium nitrite did not affect the reaction rate up to 8700 ppm, in agreement with the suggested catalytic role that it could explicate in the reaction mechanism. As an example, in Fig. 6.2., the normalized concentration profiles of benzaldehyde in a 25 % wt. aqueous mixture were reported for different amounts of added sodium nitrite. Similar results were obtained in the presence of sulfuric acid.

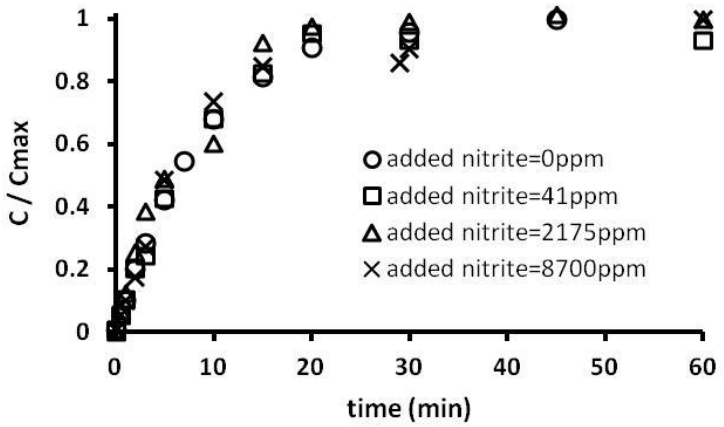

Fig. 6.2. Normalized concentration profiles of benzaldehyde during benzyl alcohol oxidation at varying sodium nitrite concentrations. 25 % wt. HNO_3, 75 % wt. H_2O, T = 30 °C.

Finally, an experimental run was carried out under the same operating conditions of Fig. 6.1c starting from benzaldehyde instead of benzyl alcohol. The comparison between the results is shown in Fig. 6.3.

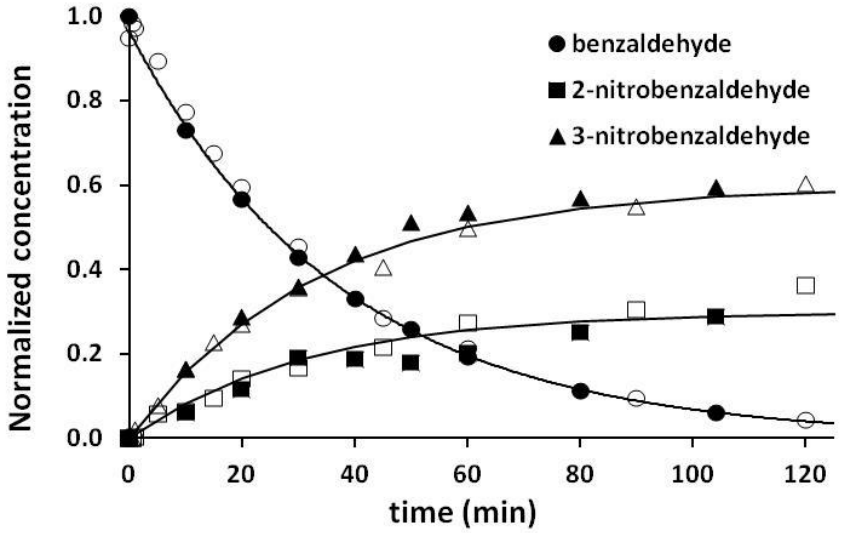

Fig. 6.3. A comparison of two experimental runs starting from benzaldehyde (full symbols) or benzyl alcohol (empty symbols). 21.9 % wt. HNO_3, 58 % wt. H_2SO_4, 20.1 % wt. H_2O, T = 20 °C. Lines are for the convenience of the eye.

Concentration profiles are coincident, suggesting that the nitration process is not affected by the starting material, since the oxidation rate of benzyl alcohol is much higher than the nitration rate of benzaldehyde. As a result, the whole process can be seen as a tandem two-steps reaction with very different time scales.

6.2. Safety considerations

In spite of the possibility of obtaining nitrobenzaldehydes from benzyl alcohol, realizing tandem oxidation-nitration in the same mixture, some safety considerations are needed. In fact, in order to carry out the two reactive steps in the same mixture, highly acidic media must be adopted. Under these conditions, the oxidation reaction was proved to be very fast so that a great thermal energy is generated in a very short time. In addition, the consequent, but slower, heat release due to the nitration reactions must be taken into account, too. The experiments presented in Fig. 6.3 were carried out at low organic concentrations and long reaction times to operate under isothermal conditions. An increase in concentrations of either the acids or the reactants will consequently impose more stringent requirements for heat removal. Following the approach presented in Section 1.2.1, an estimation of the adiabatic temperature rise for the tandem process can be easily provided. By group contribution method (Medard, 1989), a heat of reaction of 1100 $J \cdot g^{-1}$ and 1185 $J \cdot g^{-1}$ were estimated for benzyl alcohol oxidation and benzaldehyde nitration, respectively. Assuming a mean specific heat of 2 $J \cdot g^{-1} \cdot K^{-1}$ the adiabatic temperature rise can be calculated by

$$\Delta T_{ad} = \frac{\Delta H_{ox} + \Delta H_{nit}}{c_p} \frac{m_{Ar}}{m_{Ar} + m_{mix}} \approx 380\ K \qquad \text{eq. 6.1}$$

where m_{Ar} and m_{mix} are the masses of the aromatic substrate and mixed acid, respectively, and a ratio between the substrate and mixed acid of 0.5 was chosen, since it is a common choice in industrial applications (Olah et al., 1989). Even for lower ratios, such a high adiabatic temperature rise value indicates a high probability of thermal explosions occurrence. To clarify this aspect, a temperature profile was recorded during tandem oxidation reaction carried out in batch mode under isoperibolic conditions, i.e. at constant temperature of the cooling fluid, water, in this case. The experiment was carried out in standard mixed acid with

a m_{Ar}/m_{mix} ratio of 0.4. The cooling system temperature was constantly 23 °C. The substrate was added to the mixture at once and the total mixture mass was about 12 g.

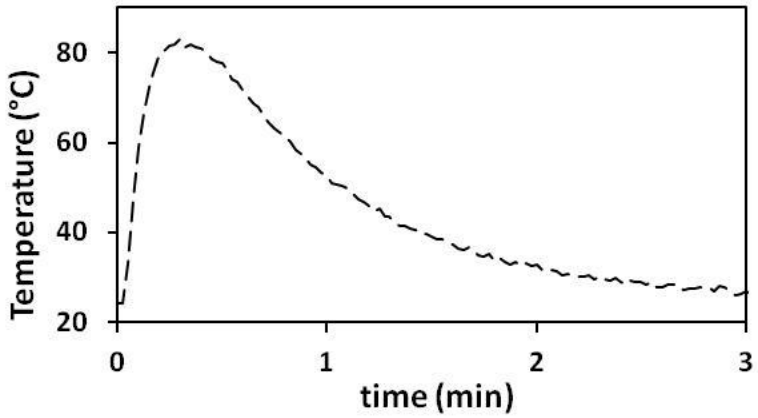

Fig. 6.4. Temperature rise in isoperibolic mode. Organic/mixed acid ratio = 0.5; cooling system T = 23 °C. Standard mixed acid composition.

Despite the low amount of reacting mixture, the temperature rise was dramatically high, and temperature increased from 23 °C to 83°C almost instantaneously. For the adopted lab-scale batch reactor, the product $U \cdot A$ was estimated to be 5.1 $J \cdot s^{-1} \cdot K^{-1}$, where U is the global exchange coefficient and A the exchange surface. Moreover, it must be considered that the thermal inertia of the reactor is estimated to be 2.07, more than double that of an industrial scale batch reactor. Thermal inertia Φ is defined as

$$\Phi = 1 + \frac{M \cdot C}{m \cdot c_p} \qquad \text{eq. 6.2}$$

where M and C are the mass and the mean specific heat of the reactor materials and m and c_p the mass and mean specific heat of the reacting mixture in the reactor. Φ is used to take into account the contribution of reactors walls heating to experimentally measured temperature increments. In an industrial scale reactor, the thermal energy involved in the reactors walls heating is negligible compared to that necessary to heat the reacting mixture and the thermal inertia is about 1. At higher values of thermal inertia, the experimentally measured temperature rise is less conservative, so that, for an industrial reactor with the same cooling efficiency of the one used in Fig. 6.4., the temperature rise would be double. As a result, even

though tandem oxidation-nitration process starting from benzyl alcohol seems an attractive option, serious safety concern must be considered.

7. Results III: Benzyl alcohol oxidation kinetics

7.1. Introduction

Tandem oxidation-nitration of benzyl alcohol was shown to be attractive, even though several safety issues must be considered (Chapter 6). Hence, a detailed kinetic model needs to be developed in order to predict the reactivity of the species involved in the process at varying process conditions. In the previous Chapter, preliminary experimental runs showed the feasibility of nitrobenzaldehydes synthesis using benzyl alcohol as a row material. However, the same experiments showed that, under the experimental conditions usually adopted to nitrate aromatic substrates, benzyl alcohol oxidation kinetics are too fast to be easily followed. To this merit, it is possible to investigate the two reaction steps separately, since oxidation of benzyl alcohol usually occurs under less acidic conditions, under which no or very slow nitration was observed. In this Chapter, on the basis of the experimental evidence, a detailed kinetic model is developed to better characterize the oxidation reaction highlighted in Fig. 7.1.

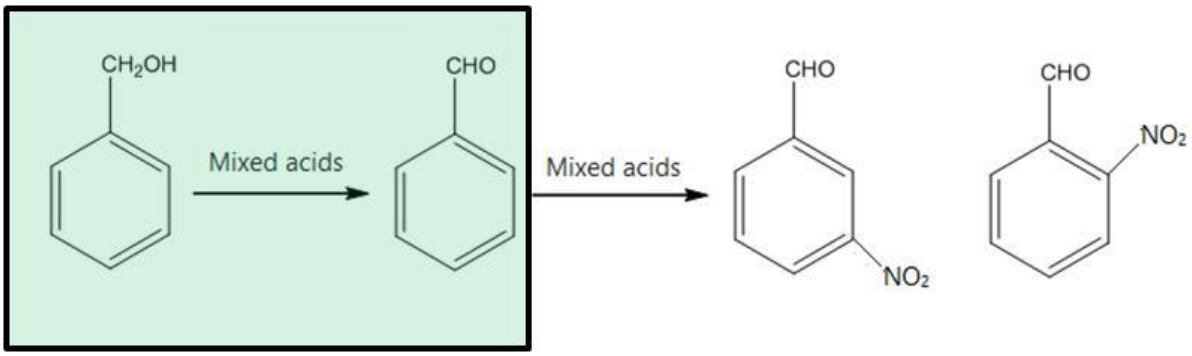

Fig. 7.1. Oxidation of benzyl alcohol in tandem oxidation-nitration process.

7.2. Reaction mechanism discrimination

Despite conflicting indications in the literature (Section 2.2.2), the most recent papers suggest an ionic mechanism, highlighting the role of benzyl nitrite (Fig. 7.2) as a key intermediate (Aellig et al., 2011; Aellig et al., 2012).

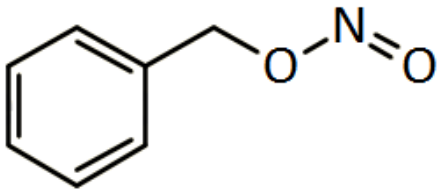

Fig. 7.2. Benzyl nitrite structural formula.

Different experimental investigations were carried out to clarify these aspects. The results of three experimental runs carried out in mixed acid at varying concentrations of added 1,1-diphenyl-2-picrylhydrazyl (DPPH), a well known radical scavenger (Chandrasekar et al., 2006) are presented in Fig. 7.3. The addition of DPPH did not significantly affect the reaction rate, suggesting the absence of radical intermediates involved in the process. Similar results, even though in the presence of a solid catalyst, were obtained by Aellig et al. (2011), using 2,4,5-tri-tert-butylphenol as a radical scavenger.

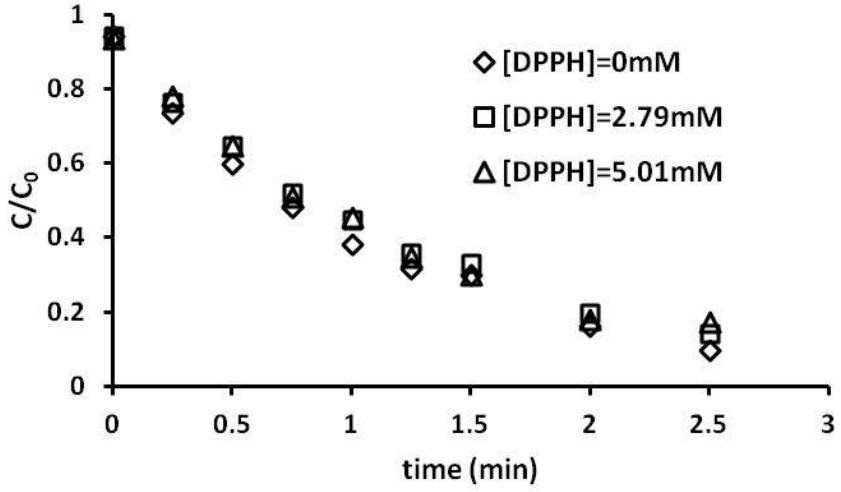

Fig. 7.3. Normalized concentration profiles of benzyl alcohol in mixed acid (24 % wt. HNO_3, 15 % wt. H_2SO_4, 61 % wt. H_2O) at varying DPPH concentration. T = 30 °C. C_0 = 20mM.

To confirm the experimental results, EPR spectra of reactive samples, collected 30 and 90 s after the addition of the organic substrate, were compared to those of the acid mixture collected before the addition of the organic substrate, Fig. 7.4. The only detected radical species was $NO_2^{\bullet}$, whereas there was no evidence of C-centered or O-centered radicals.

Moreover, the three recorded spectra were coincident suggesting the absence of radical reaction involving the organic substrate.

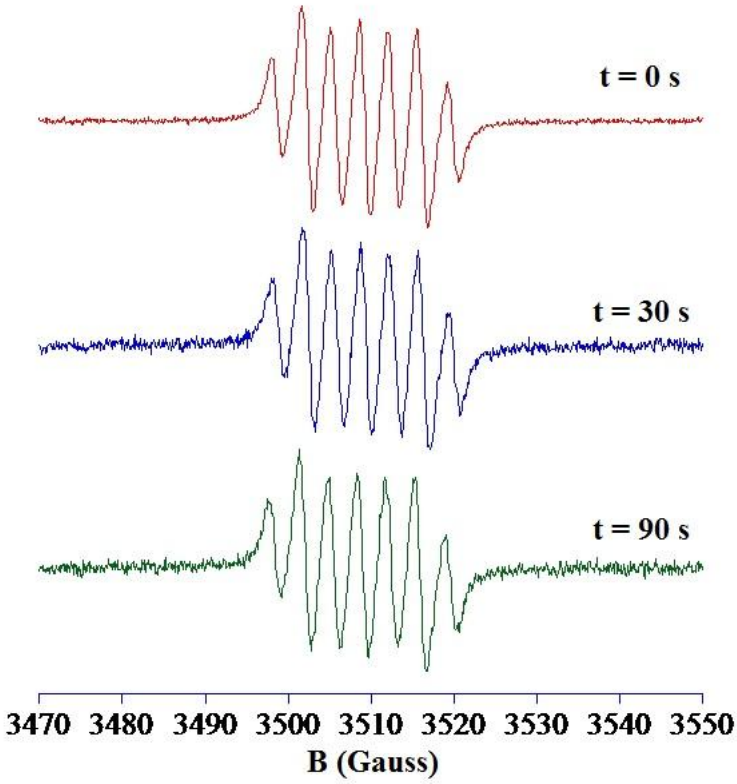

Fig. 7.4. EPR spectra of reacting mixture samples at different reaction times.

Similar results were obtained for experiments conducted in aqueous concentrated nitric acid, in the absence of sulfuric acid.

7.3. Results and Discussion

Several experimental runs were carried out at varying temperature, nitric acid concentration and sulfuric acid concentration in the ranges 10 – 30 °C, 2.0 – 8.5 mol·L^{-1}, and 0 – 1.81 mol·L^{-1}, respectively. At higher acidic conditions, oxidation kinetics were too fast to be accurately followed. In order to estimate kinetic parameters without the interference of mass transfer between phases, benzyl alcohol concentrations were chosen lower than its solubility in the acid solutions. The results, in terms of benzyl alcohol concentration profiles, of experimental runs carried out in aqueous nitric acid at different nitric acid concentrations are presented in Fig. 7.5. Benzaldehyde profiles were omitted for the sake of clarity.

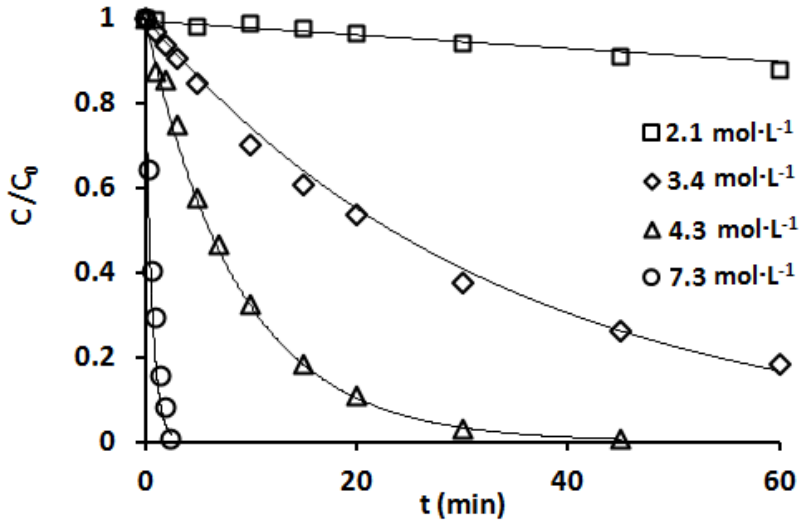

Fig. 7.5. Normalized concentration profile of benzyl alcohol in aqueous nitric acid at varying nitric acid concentrations. T = 30 °C. The lines are for convenience of the eye.

As shown, in aqueous nitric acid, benzyl alcohol was converted to benzaldehyde with unitary selectivity and the reaction was faster when the nitric acid concentration was increased. Specifically, at fixed reaction times the conversion was a sigmoidal function of the nitric acid concentration as presented in Fig. 7.6

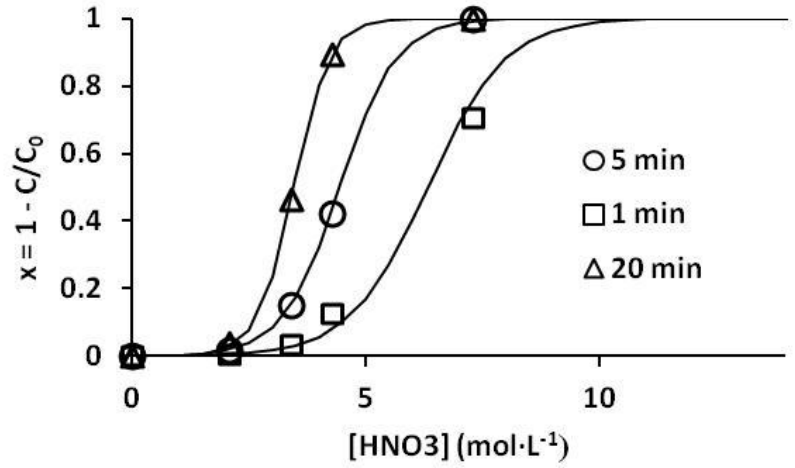

Fig. 7.6. Conversion of benzyl alcohol as a function of nitric acid concentration at different reaction times. T = 30 °C.

Similar results were obtained at fixed nitric acid concentration, when adding different amounts of sulfuric acid, as shown in Fig. 7.7.

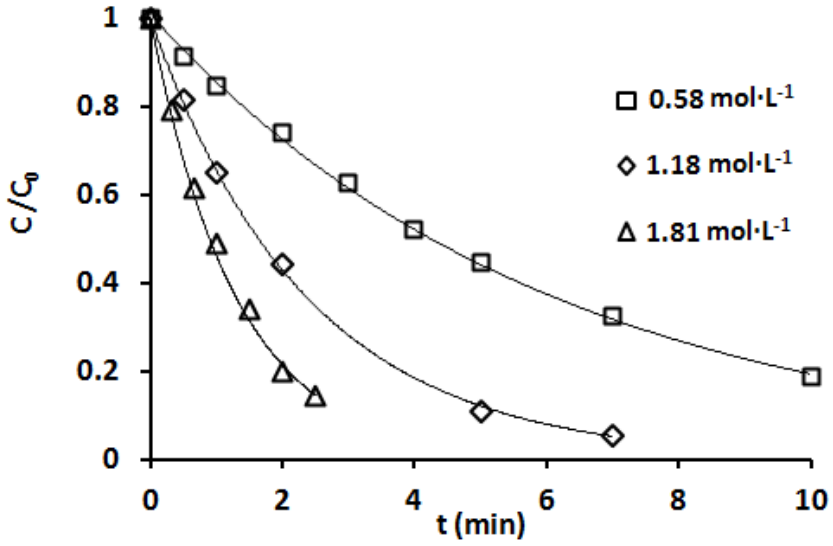

Fig. 7.7. Normalized concentration profile of benzyl alcohol in mixed acid at varying sulfuric acid concentrations. T = 30 °C. [HNO_3] = 4.45 mol·L^{-1}. The lines are for convenience of the eye.

As reported, the reaction was faster at higher sulfuric acid concentrations. Differently from the case of aqueous nitric acid, conversion has a linear dependence on sulfuric acid concentration below the limit of unitary conversion, as shown in Fig. 7.8.

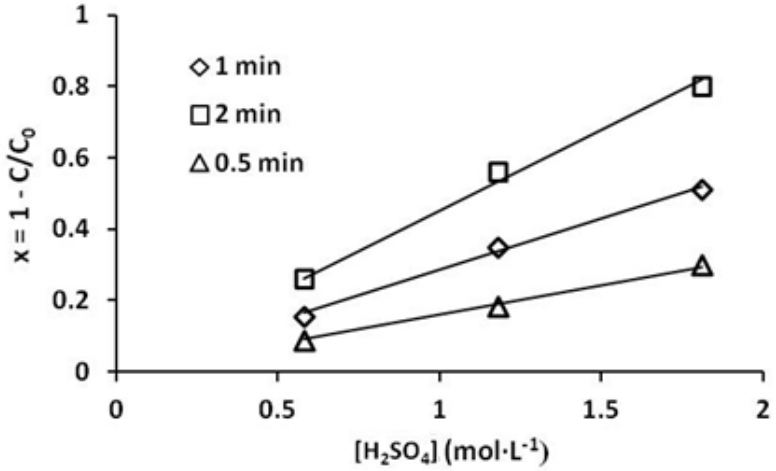

Fig. 7.8. Conversion of benzyl alcohol as a function of sulfuric acid concentration at different reaction times. T = 30 °C.

The concentration dependence of benzyl alcohol conversion presented in Fig. 7.6 and 7.8 suggest that the reaction rate is directly related to the acid dissociation and, consequently, to the H^+ concentrations in the mixture. In this regard, the found linear and sigmoidal dependences are in complete agreement with the qualitative results presented in Chapter 5 on the acids dissociation. In fact, at the investigated concentrations, nitric acid dissociation follows a sigmoidal profile with its initial concentration (Davis et al., 1964; Redlich et al., 1968), whereas sulfuric acid can be considered completely dissociated. Lastly, from the comparison between Fig. 7.5 and 7.7, it is clear that the addition of small amounts of sulfuric acid in the mixture is capable of significantly increasing the oxidation reaction rate in comparison to the case of aqueous nitric acid.

Finally, the effect of the temperature was investigated in Fig. 7.9.

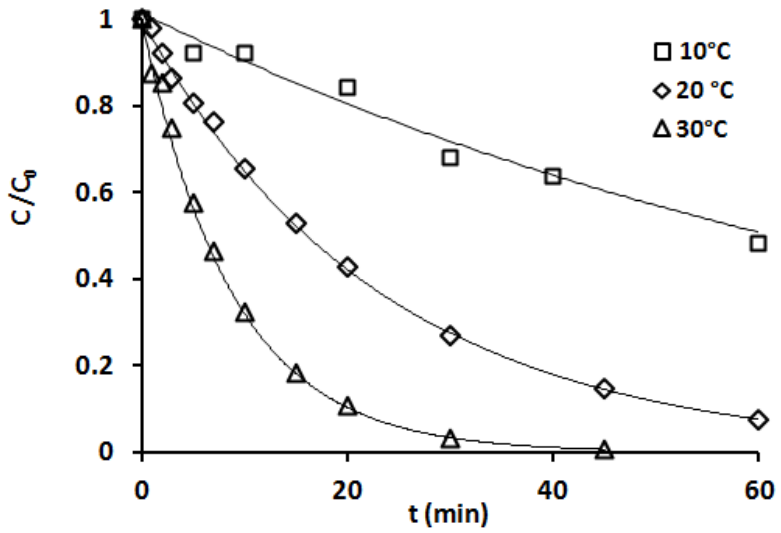

Fig. 7.9. Normalized concentration profile of benzyl alcohol in aqueous nitric acid at varying temperatures. [HNO_3] = 4.33 mol·L^{-1}. The lines are for convenience of the eye.

In this case, an increase in temperature resulted in a higher reaction rate, since the Arrhenius-like dependence of the kinetic constant on temperature. The assumption was confirmed by the results in Fig. 7.10, where the logarithms of the pseudo first-order kinetic constants k' of Fig. 7.9 were plotted against the reciprocal of absolute temperature T according to

$$ln\, k' = ln\, k'_0 - \frac{E_a}{RT} \qquad \text{eq. 7.1}$$

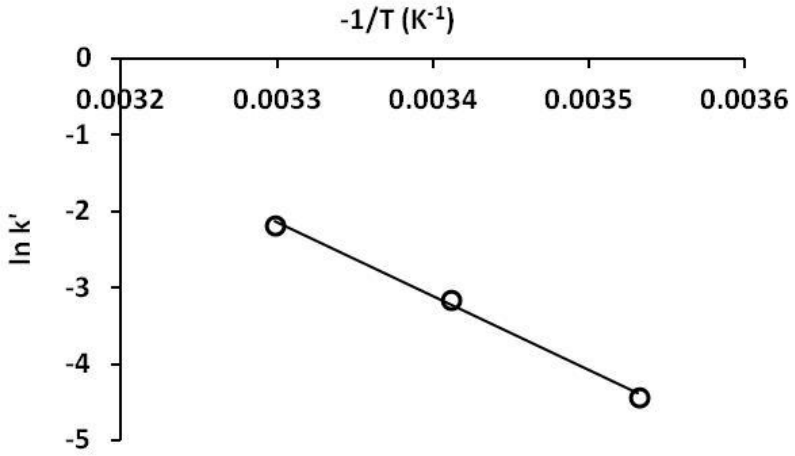

Fig. 7.10. Pseudo first-kinetic constant dependence on temperature. [HNO_3] = 4.33 mol·L^{-1}.

Contrary to what reported in the literature, no induction periods were observed under all the investigated conditions, also in the absence of added nitrite. It is possible to conclude that a catalytic amount of nitrite is always present in mixed acids because of the occurrence of the following equilibrium of decomposition of nitric acid to nitrous acid

$$HNO_3 \rightleftarrows HNO_2 + 0.5O_2 \qquad K_1 \qquad \text{r. 7.1}$$

7.4. Kinetic model

On the basis of the literature indications (Section 2.2.2) and the experimental evidence, the following reaction scheme can be proposed

$$HNO_3 \rightleftarrows HNO_2 + 0.5O_2 \qquad K_1 \qquad \text{r. 7.1}$$

$$HNO_3 \cdot H_2O + H_2SO_4 \rightleftarrows HSO_4^- + NO_2^+ + 2H_2O \qquad K \qquad \text{r. 7.2}$$

$$\emptyset CH_2OH + HNO_2 + H^+ \rightleftarrows H_2O + \emptyset CH_2ONOH^+ \qquad K_3 \qquad \text{r. 7.3}$$

$$\emptyset CH_2OH_2^+ \rightleftarrows \emptyset CH_2OH + H^+ \qquad K_4 \qquad \text{r. 7.4}$$

$$H_2SO_4 \rightarrow H^+ + HSO_4^- \qquad \text{r. 7.5}$$

$$HNO_3 \rightleftarrows H^+ + NO_3^- \qquad K_N \qquad \text{r. 7.6}$$

$$\emptyset CH_2ONOH^+ \overset{k_1}{\rightarrow} \emptyset CHO + HNO + H^+ \qquad k_1 \qquad \text{r. 7.7}$$

where the dependence on temperature of each equilibrium constant K_i is

$$K_i = exp\left(-\frac{\Delta H_i - T\Delta S_i}{RT}\right) \qquad \text{eq. 7.2}$$

and the reaction rate r_1 for reaction r. 7.7 is

$$r_1 = k_1[\emptyset CH_2ONOH^+] = k_1^0 exp\left(-\frac{E_{a1}}{RT}\right)[\emptyset CH_2ONOH^+] \qquad \text{eq. 7.3}$$

Equilibrium r. 7.1 is the above-mentioned decomposition of nitric acid to nitrous acid. Thermodynamic parameters for this equilibrium are easily calculated using the enthalpy and entropy of formation of the involved species; the calculated ΔH_1 and ΔS_1 values are 53.97 KJ·mol^{-1}·K^{-1} and -1.97·10^{-1} KJ·mol^{-1}, respectively. Formed nitrous acid, in acidic environment, attacks benzyl alcohol to give rise to the protonated form of benzyl nitrite (r. 7.3). The decomposition of protonated benzyl nitrite is the rate determining step for the formation of benzaldehyde (r. 7.7), Fig. 7.11.

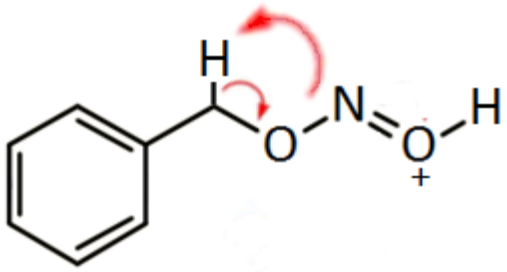

Fig. 7.11. Protonated benzyl nitrite decomposition.

Equilibrium reaction r. 7.4 takes into account benzyl alcohol protonation. For the sake of completeness, the equilibrium of nitronium ion formation r. 7.2, was also included in the model. However, under the adopted conditions, no nitrations occur and the equilibrium is fully shifted to the left; as a result, no significant changes occurred in the development of the kinetic model when this equilibrium was discarded.

On the basis of the proposed mechanism the following material balances can be considered

$$K_1 = \frac{[HNO_2][O_2]_{liq}^{0.5}}{[HNO_3]} \cdot \frac{1}{\gamma_{HNO_3}} \qquad \text{eq. 7.4}$$

$$[NO_2^+] = exp\left(\frac{\Delta H}{RT}\right) exp\left(\frac{\Delta S^*}{R}\right) \frac{\gamma_{HNO_3}}{\gamma_{H_2O}} \frac{[HNO_3]}{[H_2O]} 10^{-H_R} \qquad \text{eq. 7.5}$$

$$[HNO_3]_0 = [HNO_3] + [HNO_2] + [HNO] + [NO_2^+] + [NO_3^-] + [\emptyset CH_2ONOH^+] \qquad \text{eq. 7.6}$$

$$[H_2SO_4]_0 \approx [HSO_4^-] \qquad \text{eq. 7.7}$$

$$[H_2SO_4] \approx 0 \qquad \text{eq. 7.8}$$

$$\frac{K_N}{55.56} = \frac{[H^+][NO_3^-]}{[HNO_3][H_2O]} \cdot \frac{1}{\gamma_{H_2O}} \cdot 10^{-M_C^{HNO_3}} \qquad \text{eq. 7.9}$$

$$K_3 = \frac{[\emptyset CH_2ONOH^+][H_2O]}{[H^+][HNO_2][\emptyset CH_2OH]} \cdot \gamma_{H_2O} \cdot 10^{n_3 \cdot M_C^{HNO_3}} \qquad \text{eq. 7.10}$$

$$\frac{K_4}{55.56} = \frac{[H^+][\emptyset CH_2OH]}{[\emptyset CH_2OH_2^+][H_2O]} \cdot \frac{1}{\gamma_{H_2O}} \cdot 10^{-n_4 \cdot M_C^{HNO_3}} \qquad \text{eq. 7.11}$$

$$[H^+] + [NO_2^+] + [\emptyset CH_2ONOH^+] + [\emptyset CH_2OH_2^+] = [NO_3^-] + [HSO_4^-] \qquad \text{eq. 7.12}$$

$$[\emptyset_{TOT}] = [\emptyset CH_2OH] + [\emptyset CH_2OH_2^+] + [\emptyset CH_2ONOH^+] \qquad \text{eq. 7.13}$$

$$\frac{d[\emptyset_{TOT}]}{dt} = -r_1 \qquad \text{eq. 7.14}$$

$$\frac{d[\emptyset CHO]}{dt} = r_1 \qquad \text{eq. 7.15}$$

$$\frac{d[HNO]}{dt} = r_1 \qquad \text{eq. 7.16}$$

In the following the main assumption of the model will be discussed. Equation 7.5 is the equilibrium relation to estimated nitronium ion concentration. It has been already pointed out

the negligibility of this equilibrium for the adopted conditions, nevertheless it was included in the model; a detailed discussion about its validity and limits was presented in Chapter 5. Equations 7.7 and 7.8 take into account the complete dissociation of sulfuric acid under the adopted relatively high diluted solutions whereas equation 7.9 is the equilibrium relation for nitric acid dissociation. In order to take into account the definition of pK_N for highly diluted acid solutions, the molar concentration of pure water (55.56 mol·L^{-1}), together with the water activity $\gamma_{H_2O}[H_2O]$, were included in the equation, as previously explained in Chapter 5. The M_C function definition was used to estimate the activity coefficients contribution of the other species. In this case, they were related to the acidity function of nitric acid itself, instead of that of the sulfuric acid, since most of the experiments were carried out in the absence of sulfuric acid. Strictly speaking, in the presence of sulfuric acid the following relation should be considered in equations 7.9 – 7.11

$$M_C^{HNO_3} = n_N \cdot M_C^{H_2SO_4} \qquad \text{eq. 7.17}$$

However, in the considered range of sulfuric acid concentration, the influence of sulfuric acid on nitric acid dissociation can be neglected with an estimated maximum error of 4 %, that is lower than the maximum error associated to HPLC analysis. For this reason, the models developed either taking into account or deliberately ignoring eq. 7.17 for runs in the presence of sulfuric acid, did not significantly affect the results of the parametric estimation. With respect to this, it must be remembered that, according to literature data (Fig. 5.7) and simulations carried out with the model developed in Chapter 5, nitric acid dissociation to nitrate in sulfuric acid follows a sigmoidal profile. As shown in Fig. 7.12, at a maximum adopted sulfuric acid of 1.81 mol·L^{-1}, the almost constant straight section of the sigmoidal profile is intercepted and a small error is committed when calculating nitric acid dissociation in the absence of sulfuric acid instead of that in the presence of a small amount of sulfuric acid (brick red line in Fig. 7.12). $M_C^{HNO_3}$ can be calculated according to

$$M_C^{HNO_3} = 1.4691 \cdot 10^{-6}[HNO_3]_0^5 + 5.6793 \cdot 10^{-5}[HNO_3]_0^4 - 9.8857 \cdot 10^{-4}[HNO_3]_0^3 + 5.5605 \cdot 10^{-3}[HNO_3]_0^2 - 9.7124 \cdot 10^{-2}[HNO_3]_0 \qquad \text{eq. 7.18}$$

Eq. 7.18 was deduced interpolating the data by Redlich et al., (1968) on nitric acid dissociation in the investigated range.

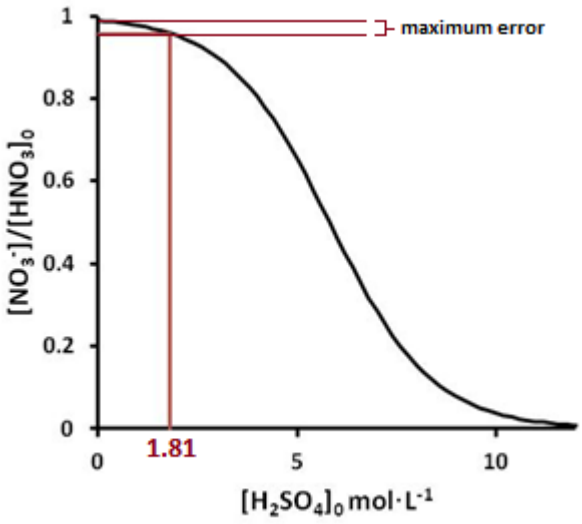

Fig. 7.12. Difference between the nitric acid dissociation values calculated in the absence and the presence of sulfuric acid for a maximum concentration of 1.81 mol·L^{-1}.

Equations 7.6 and 7.13 are the total nitrogen and charge balances, respectively.

Equations 7.14 and 7.15 represent the differential balances for the benzyl alcohol and benzaldehyde consume and formation. It must be stressed that for eq. 7.14 a total mass balance for all the species in equilibrium with benzyl alcohol is necessary. In fact, the dilution quenching of the collected reactive samples shifts equilibria 7.3 and 7.4 to benzyl alcohol so that the benzyl alcohol concentration measured by HPLC analysis of diluted sample represents the sum of all the concentrations of the species included in eq. 7.13. Moreover, according to the pseudo-component theory for the generic reaction scheme

$$A \rightleftarrows B \rightleftarrows C \overset{k}{\rightarrow} D \qquad \text{r. 7.8}$$

in which the conversion of C to D is the rate determining step the following differential equation can be considered

$$\frac{d[C_{TOT}]}{dt} = \frac{d[A+B+C]}{dt} = -k[C] \qquad \text{eq. 7.19}$$

where C_{TOT} is a pseudocomponent. In fact, as soon as $[C]$ is decreased because of the occurrence of the irreversible reaction, equilibria are rapidly shifted to keep $[C]$ at the equilibrium value, so that only an overall consume rate can be evaluated.

Oxygen concentration in aqueous nitric acid and mixed acid was estimated according to Tromans (1998) empirical model for the estimation of oxygen solubility in electrolytic solutions. According to this theory, oxygen solubility can be expressed by equations 7.20 and 7.21 in the presence and the absence of sulfuric acid, respectively.

$$[O_2]_{liq} = P_{O_2} \cdot k(T) \cdot f_{H_2SO_4} (f_{HNO_3})^{0.8} \quad \text{eq. 7.20}$$

$$[O_2]_{liq} = P_{O_2} \cdot k(T) \cdot f_{HNO_3} \quad \text{eq. 7.21}$$

where P_{O_2} is the oxygen partial pressure in the reactor freeboard (0.21 atm) and $k(T)$ is a known function of temperature (Tromans, 1998)

$$k(T) = exp\left(\frac{0.046T^2 + 203.35\ln(T/298) - (299.378 + 0.092T)(T - 298) - 20591}{8.314T}\right) \quad \text{eq. 7.22}$$

$f_{H_2SO_4}$ and f_{HNO_3} are two factors that can be expressed as a function of the molality of H_2SO_4 and HNO_3, respectively.

$$f_{H_2SO_4} = (1 + 0.09 m_{H_2SO_4}^{1.4})^{-1.5} \quad \text{eq. 7.23}$$

$$f_{HNO_3} = (1 + 0.16 m_{HNO_3}^{0.95})^{-0.7} \quad \text{eq. 7.24}$$

where $m_{H_2SO_4}$ and m_{HNO_3} are the molal concentrations of the acids. The semi-empirical approach was successfully adopted to predict experimental concentrations of oxygen and it takes into account also the activity coefficient variations of oxygen in the mixtures, since the parameters of the model were calculated only on the basis of the experimental measurements.

For the modeled experimental runs, it was assumed that the concentration of oxygen was constant with time and equal to the solubility value. This assumption can be considered valid because of the strong agitation of the mixture that enhance the oxygen transfer between the solution and the freeboard and because there is no significant gaseous product formation to change the gaseous phase composition in the freeboard. Moreover, the freeboard volume is more than double the volume of the liquid reacting mixture. γ_{HNO_3} and γ_{H_2O} were calculated

according to Khudhairy et al. (1989). In the absence of other indications, γ_{HNO_2} was considered unitary since HNO_2 is present at trace levels because of the value of K_1. However, a sensitivity study conducted on the results of the mathematical model showed that the model is not significantly affected for γ_{HNO_2}varying in the range 0.1 – 10. This is completely justified considering that combining equations 7.3, 7.4, 7.10, and 7.14, without discarding the nitrous acid activity coefficient, the following expression can be derived

$$\frac{d[\emptyset_{TOT}]}{dt} = -k_1 K_1 K_3 \frac{\gamma_{HNO_3}}{a_{H_2O}} 10^{-n_3 \cdot M_C^{HNO_3}} \frac{[H^+][HNO_3]}{[O_2]_{liq}^{0.5}} [\emptyset CH_2OH] \qquad \text{eq. 7.25}$$

in which the γ_{HNO_2} activity coefficient has no influence. Moreover, once the acidic media composition was fixed, for low organic concentrations, the acid consume could be considered negligible during each experimental run and equation 7.25 can be written as

$$\frac{d[\emptyset_{TOT}]}{dt} = -k'[\emptyset CH_2OH] \qquad \text{eq. 7.26}$$

which is in agreement with the observed pseudo first-order kinetics.
Finally, it must be considered that formed HNO during the experimental run can undergo the following reactions

$$HNO + HNO_3 \rightarrow 2HNO_2 \qquad \text{r. 7.9}$$

$$HNO \rightarrow 0.5N_2O + 0.5H_2O \qquad \text{r. 7.10}$$

However, when these reactions were included in the modeling, they did not affect the results. In fact, under the adopted conditions, this is easily related to the presence of HNO at trace levels, so that its decomposition is completely negligible in all the nitric acid consume evaluations. Experimental titration of acidic mixture before and after the addition of benzyl alcohol confirmed the hypothesis of negligible acid consume (data not shown). Moreover, literature indications (Ogata et al., 1966) suggested that, even for higher amount of benzyl alcohol, one mole of nitric acid is consumed for each mole of produced benzaldehyde; as a result, the reaction rate of r. 7.10 is likely to be much higher than 7.9. Lastly, even if a small amount of HNO reacts with HNO_3 to generate nitrous acid, the accumulation of this species

can be ruled out since it would be rapidly converted to nitric acid through equilibrium r.1, that is strongly shifted to the left under all the possible experimental conditions.

Equations 7.4 – 7.16 were simultaneously solved by using Matlab software, in order to find the best estimated values of the parameters to minimize the mean square deviation between the experimental and calculated concentrations. The objective function was defined as follows

$$\sum_{g=1}^{h}\sum_{i=1}^{l}\sum_{m=1}^{n}\left(y_{g,i,m}-c_{g,i,m}\right)^2 \qquad \text{eq. 7.27}$$

were y and c are the calculated and experimental concentrations and h, l, and n respectively represents the number of experimental data recorded in each experiment, the number of the measured reacting species, and the number of experiments used in the optimization procedure. The estimated values of the parameters were summarized in Table. 7.1. together with their 97% intervals of confidence. In Fig. from 7.13 to 7.19 the comparison between experimental and calculated data, for some of the experimental runs used in the optimization procedure, are presented. Moreover, as an additional model verification, in Fig. 7.20 and 7.21 it is shown the comparison between experimental and calculated data for two experimental runs that were not included in the optimization procedure, for which the continuous lines represent the simulated predicted concentration profiles.

Equilibrium constants	
$\boldsymbol{\Delta S_i}$**(J·mol^{-1})**	$\boldsymbol{\Delta H_i}$**(J·mol^{-1}·K^{-1})**
$\Delta S_3 = (6.803 \pm 0.0201) \cdot 10$	$\Delta H_3 = (15.803 \pm 0.079) \cdot 10^3$
$\Delta S_4 = 41.798 \pm 0.042$	$\Delta H_4 = (-8.406 \pm 0.042) \cdot 10^3$
Reaction	
$\boldsymbol{k_1^0}$**(min^{-1})**	$\boldsymbol{E_{a1}}$**(J·mol^{-1})**
$(2.344 \pm 0.035) \cdot 10^{12}$	$(4.406 \pm 0.067) \cdot 10^3$
Acidity function parameters	
$n_3 = (1.135 \pm 0.270) \cdot 10^{-1}$	$n_4 = (1.112 \pm 0.265) \cdot 10^{-1}$

Table 7.1. Estimated model parameters.

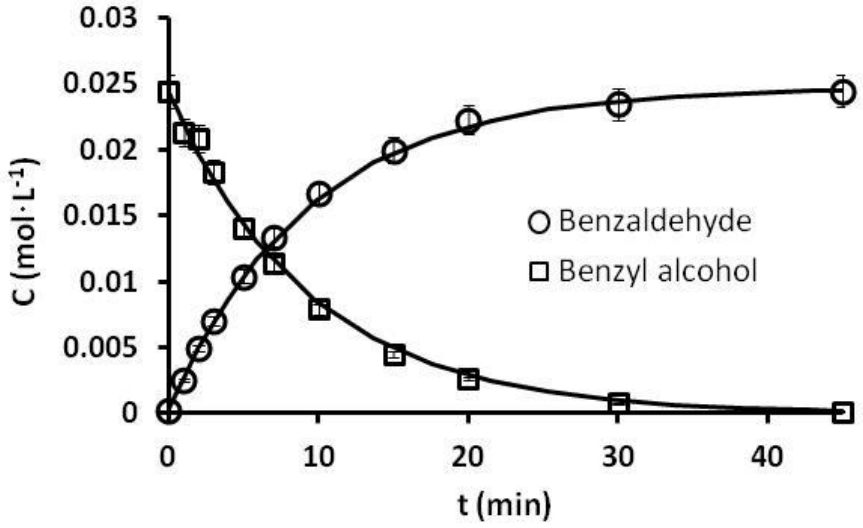

Fig. 7.13. Concentration profiles. Experimental (symbols) and calculated (continuous lines) data. [HNO_3] = 4.34 mol·L^{-1}; T = 30 °C.

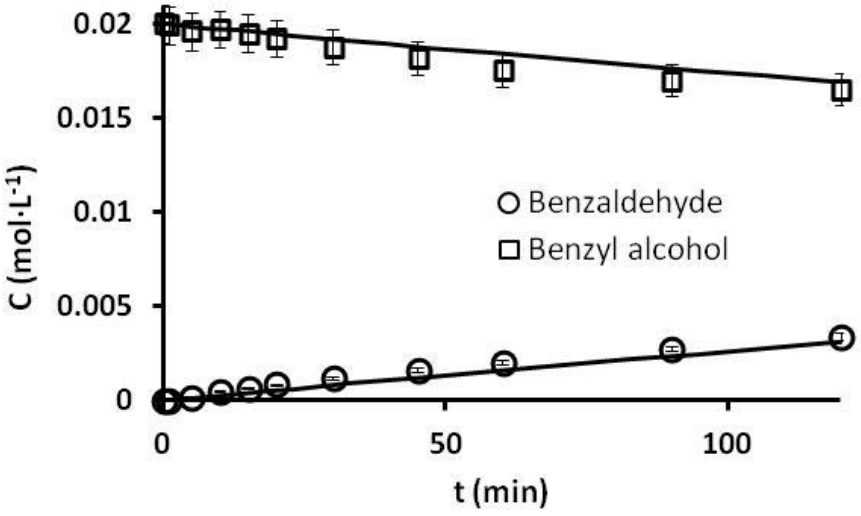

Fig. 7.14. Concentration profiles. Experimental (symbols) and calculated (continuous lines) data. [HNO_3] = 2.10 mol·L^{-1}; T = 30 °C.

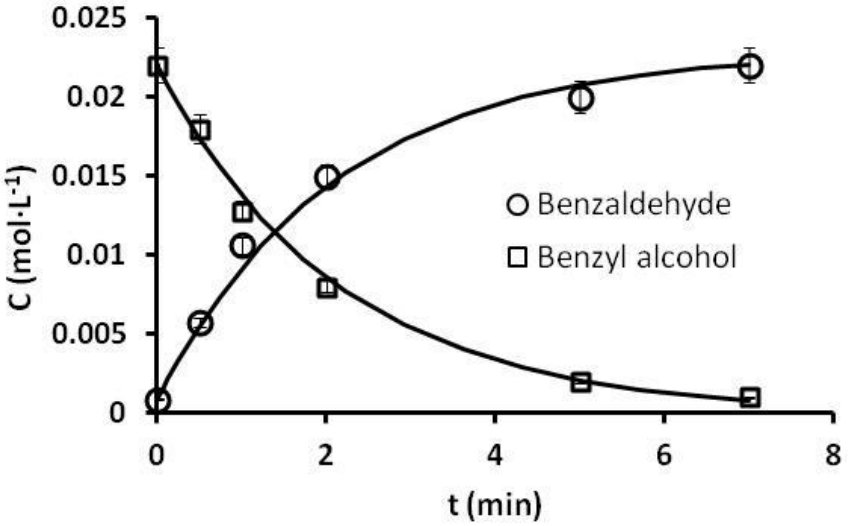

Fig. 7.15. Concentration profiles. Experimental (symbols) and calculated (continuous lines) data. [HNO_3] = 4.57 mol·L^{-1}; [H_2SO_4] = 1.18 mol·L^{-1}; T = 30 °C.

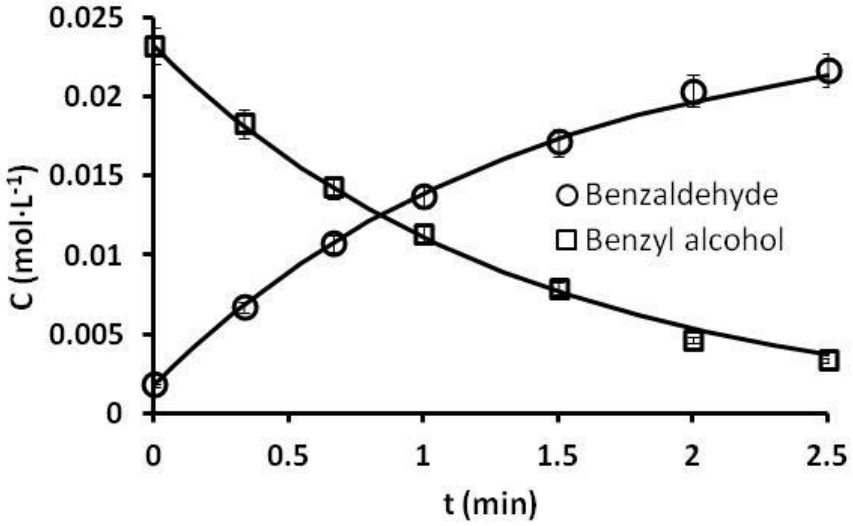

Fig. 7.16. Concentration profiles. Experimental (symbols) and calculated (continuous lines) data. [HNO_3] = 4.47 mol·L^{-1}; [H_2SO_4] = 1.81 mol·L^{-1}; T = 30 °C.

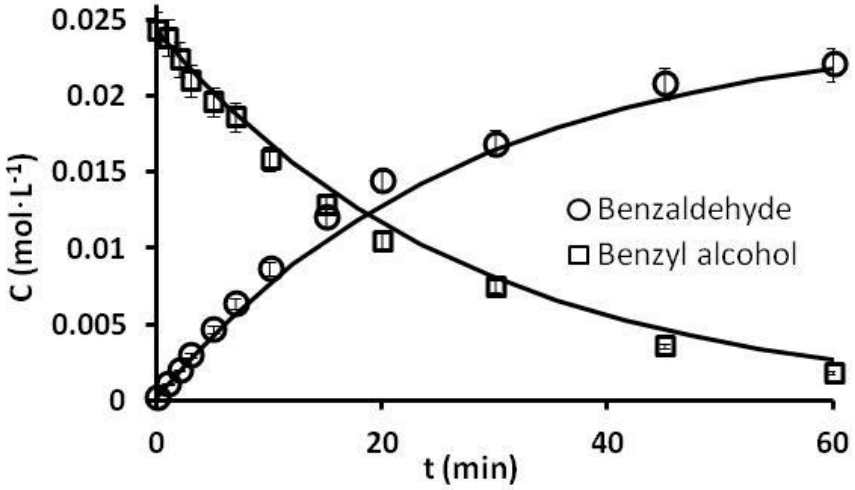

Fig. 7.17. Concentration profiles. Experimental (symbols) and calculated (continuous lines) data. [HNO_3] = 4.34 mol·L^{-1}; T = 20 °C.

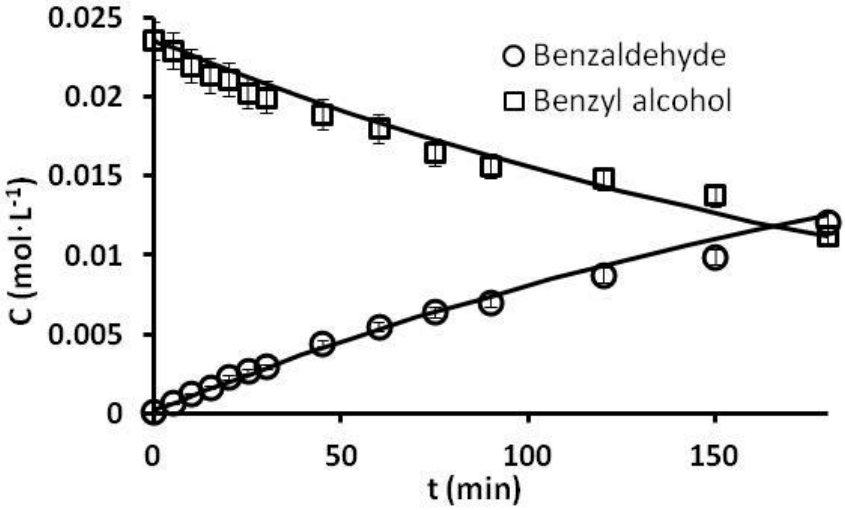

Fig. 7.18. Concentration profiles. Experimental (symbols) and calculated (continuous lines) data. [HNO_3] = 3.45 mol·L^{-1}; T = 12 °C.

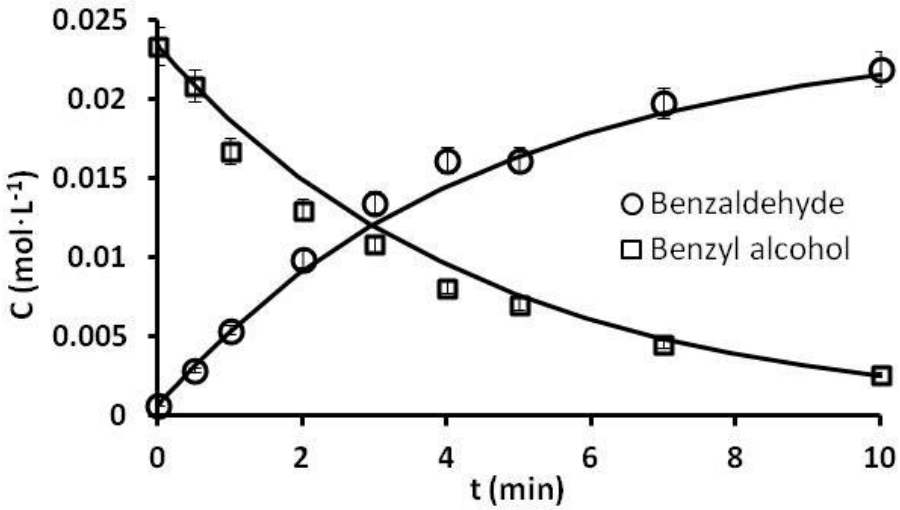

Fig. 7.19. Concentration profiles. Experimental (symbols) and calculated (continuous lines) data. [HNO_3] = 4.45 mol·L^{-1}; [H_2SO_4] = 0.57 mol·L^{-1}; T = 30 °C.

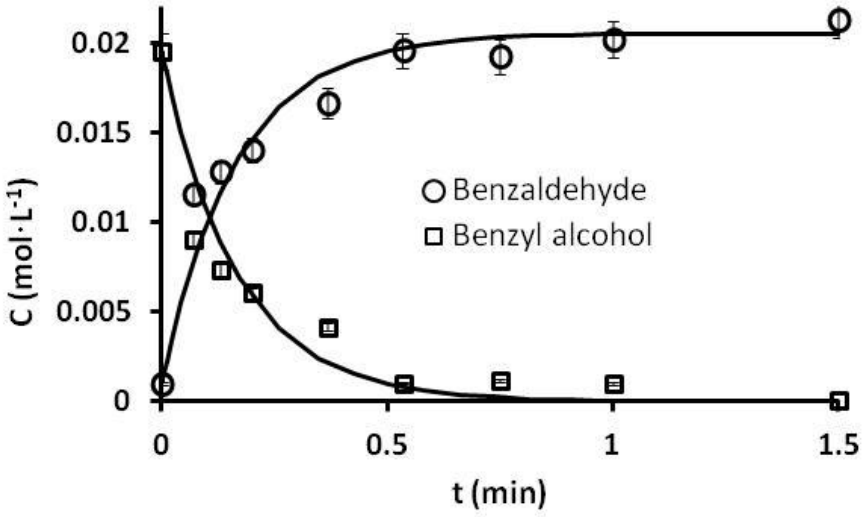

Fig. 7.20. Simulated concentration profiles. Experimental (symbols) and calculated (continuous lines) data. [HNO_3] = 8.44 mol·L^{-1}; T = 30 °C.

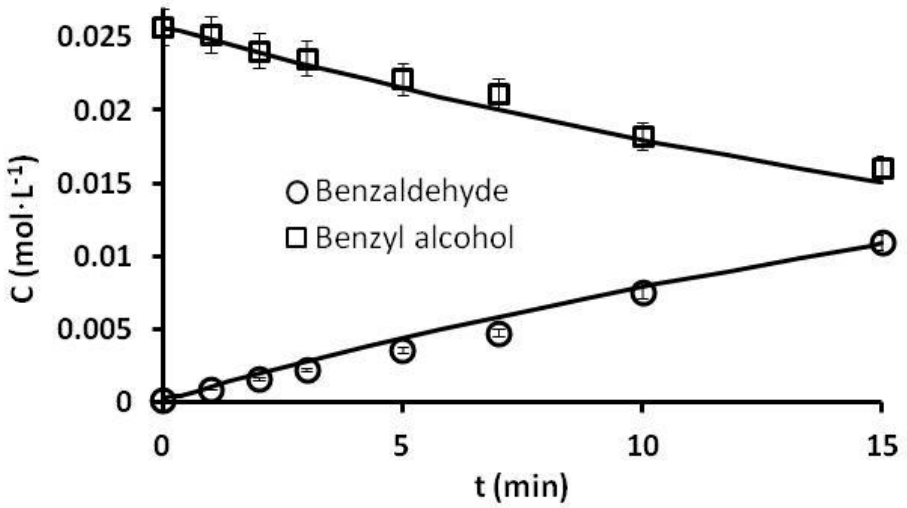

Fig. 7.21. Simulated concentration profiles. Experimental (symbols) and calculated (continuous lines) data. [HNO_3] = 3.58 mol·L^{-1}; [H_2SO_4] = 1.16 mol·L^{-1}; T = 16 °C.

As shown, the model is capable of predicting experimental data with high accuracy.

The kinetic parameters in Table 7.1 were estimated at varying temperature, nitric acid concentration and sulfuric acid concentration in the ranges 10 – 30 °C, 2.0 – 8.5 mol·L^{-1}, and 0 – 1.81 mol·L^{-1}, respectively, which are their validity ranges. Moreover, as shown in Chapter 9, they are capable of predicting fast conversion of benzyl alcohol to benzaldehyde at nitric acid and sulfuric acid concentrations up to 8.3 mol·L^{-1} and 10.7 mol·L^{-1}, respectively.

8. Results IV: Benzaldehyde nitration kinetics

8.1. Introduction

In this Chapter, the results of an extensive experimental campaign, carried out to characterize the second step of proposed tandem oxidation-nitration process, are presented. The results were analyzed and a kinetic model was proposed to predict reaction rates and selectivities to the main reaction products: 2- and 3- nitrobenzaldehydes. The simplified reaction scheme under investigation is highlighted in Fig. 8.1. Similarly to the case of benzyl alcohol oxidation, benzaldehyde nitration kinetics have a great importance in the development of a safe process, also regardless its coupling with oxidation reaction in the proposed tandem reaction.

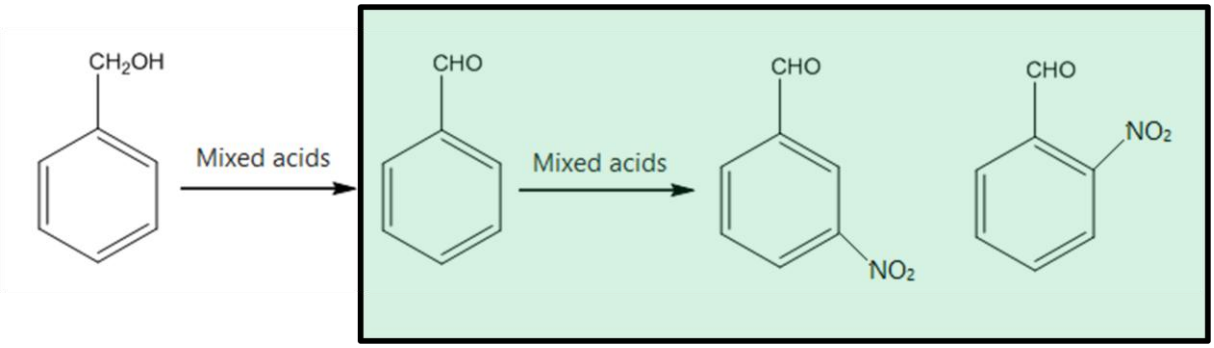

Fig. 8.1. Nitration of benzaldehyde in tandem oxidation-nitration process.

A detailed overview of nitration mechanism of organics was provided in Chapters 1 and 2. In this Chapter, suffice it to say that for the nitration of aromatic species Ar

$$Ar + NO_2^+ \overset{k_N}{\rightarrow} ArNO_2 + H^+ \qquad \text{r. 8.1}$$

it is possible to express the nitration rate as

$$r_N = k_N[NO_2^+][Ar] = k_N^0 exp\left(-\frac{E_{a,N}}{RT}\right)[NO_2^+][Ar] \quad \text{eq. 8.1}$$

In a wide range of concentrations, normally employed in nitrations (Section 5.2), the concentration of nitronium ion can be expressed according to the H_R acidity function. Therefore, equation 8.1 can be written as

$$r_N = k_N^0 exp\left(-\frac{E_{a,N}}{RT}\right) exp\left(\frac{\Delta H}{RT}\right) exp\left(\frac{\Delta S^*}{R}\right) \frac{\gamma_{HNO_3}}{\gamma_{H_2O}} \frac{[HNO_3]}{[H_2O]} 10^{-H_R}[Ar] \quad \text{eq. 8.2}$$

and thus

$$r_N = k_N^{0*} exp\left(-\frac{E_{a,N}^*}{RT}\right) \frac{\gamma_{HNO_3}}{a_{H_2O}} 10^{-H_R}[HNO_3][Ar] = k_N^g[HNO_3][Ar] \quad \text{eq. 8.3}$$

which is a reported simplified expression for nitration reaction rate (Di Somma et al., 2012) based on experimental evidence. In eq. 8.3 the following expressions were used

$$k_N^{0*} = k_N^0 \, exp\left(\frac{\Delta S^*}{R}\right) \quad \text{eq. 8.4}$$

$$E_{a,N}^* = E_{a,N} + \Delta H \quad \text{eq. 8.5}$$

The Arrhenius-like expression for the global constant k_N^g is observed since the term 10^{-H_R} has an exponential dependence on $-1/T$, too, and the dependence on temperature of $\frac{\gamma_{HNO_3}}{a_{H_2O}}$ can be generally neglected.
Therefore, equation 8.2. will be adopted in the following.

8.2. Results and discussion

The results of a standard experimental run of benzaldehyde in mixed acid, in the neighborhood of the standard mixed acid composition, are presented in Fig. 8.2. As a general result, meta- and ortho- nitrobenzaldehydes were the main reaction products with a higher occurrence of 3-nitrobenzaldehyde; this was in agreement with the orto-para deactivating

effect of the aldehydic group. Contrary to what was expected, 4-nitrobenzaldehyde was always absent or present at trace levels. In fact, the deactivating effect of the aldehydic group would result in an ortho- to para- molar isomer ratio of 2:1. This result suggests that a different mechanism from direct nitration of the aromatic ring is responsible for 2-nitrobenzaldehyde formation. The main literature indications (Sainz-Diaz, 2002; Di Somma et al., 2014) are presented in detail in Section 2.1.2. According to them, the ortho- nitration of 2-nitrobenzaldehyde is the result of an internal rearrangement of an intermediate species deriving from the coordination of a nitronium ion with the aldehydic group (Fig. 2.3).
Some oxidation products were also detected; specifically, 3-nitrobenzoic acid is the favored oxidation products. 2-nitrobenzoic traces were also detected (not shown in Fig. 8.1).

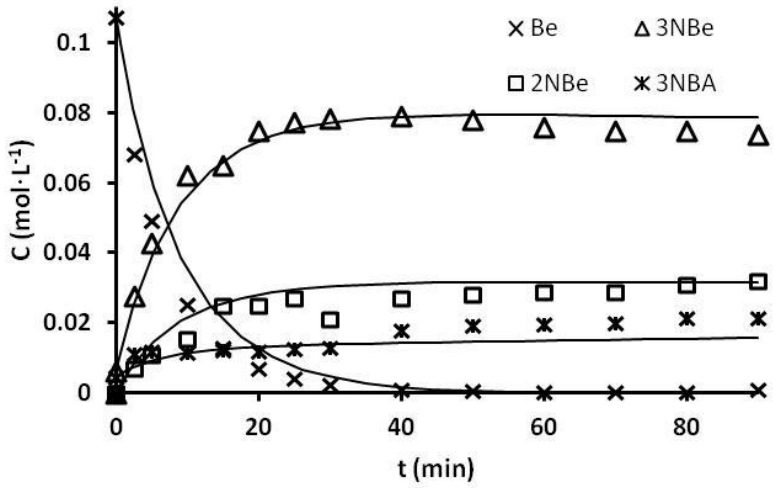

Fig. 8.2. Concentration profiles during benzaldehyde nitration in mixed acid [HNO_3] = 5.27 mol·L^{-1}; [H_2SO_4] = 9.38 mol·L^{-1}; T = 20 °C; experimental (symbols) and calculated (continuous lines) data; Be = Benzaldehyde; 3NBe = 3-nitrobenzaldehyde; 2NBe =2-nitrobenzaldehyde; 3NBA = 3-nitrobenzoic acid. Overall σ(%) = 7.0.

Poly-nitration reactions did not occur under all the investigated conditions up to 50 °C. On the basis of the experimental evidence of the oxidative capacity of nitric acid on the aldehydic group, additional experiments were carried out to take into account the effect of oxidations and nitration of the oxidized products. The direct oxidation product of benzaldehyde oxidation was benzoic acid. Some experiments were carried out starting from benzoic acid in mixed acids. An example is shown in Fig. 8.3. As expected, 2- and 3-nitrobenzoic acids were the only reaction products, with a higher occurrence of the meta substituted isomer. Contrary to what observed for benzaldehyde, benzoic acid takes a relatively long time to be completely

dissolved in concentrated mixed acids. For this reason, the time zero was assumed as that at which no solid was present in the mixture, this explaining the partially converted benzoic acid for t = 0.

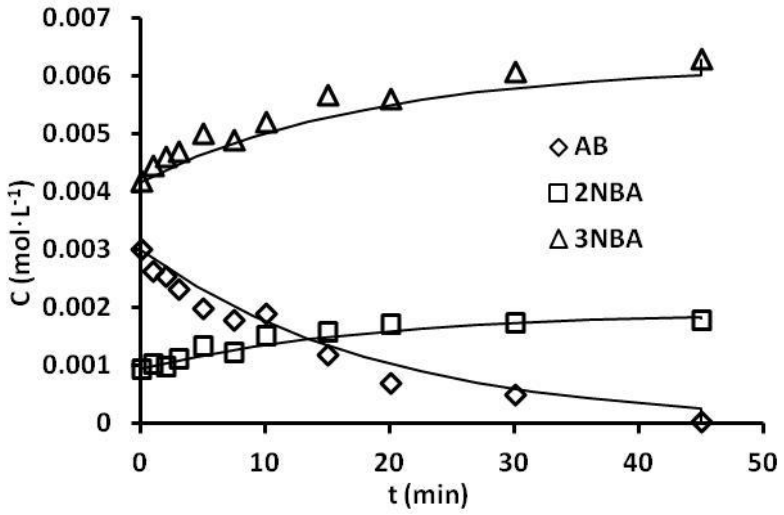

Fig. 8.3. Concentration profiles during the nitration of benzoic acid in mixed acid. [HNO_3] = 4.57 mol·L^{-1}; [H_2SO_4] = 9.28 mol·L^{-1}; T = 20 °C; experimental (symbols) and calculated (continuous lines) data; AB =benzoic acid; 3NBA = 3-nitrobenzoic acid; 2NBA=2-nitrobenzoic acid. Overall σ(%) = 5.3.

Under all the investigated conditions in the neighborhood of standard mixed acid composition, benzaldehyde oxidation was much slower than nitration or completely absent and nitrated products were the main ones.

In order to clarify the occurrence of oxidation reaction, other experiments were carried out starting from 2- and 3- nitrobenzaldehydes in mixed acid. As an example, the results of two experiments are presented in Fig. 8.4. Both experiments were carried out adding solid nitrobenzaldehydes to mixed acid at higher temperature than ambient, 50 °C and 40 °C for 2 and 3 nitrobenzaldehyde, respectively. The results show that formed 2- and 3-nitrobenzaldehydes can be efficiently oxidized to 2- and 3- nitrobenzoic acid in mixed acid. However, it is worth noting that both oxidation reactions were much slower than nitration reactions (Fig. 8.2) even at significantly higher temperature. Under the same conditions, nitration of benzaldehyde occurs much faster and oxidation products were detected only at trace levels (data not shown).

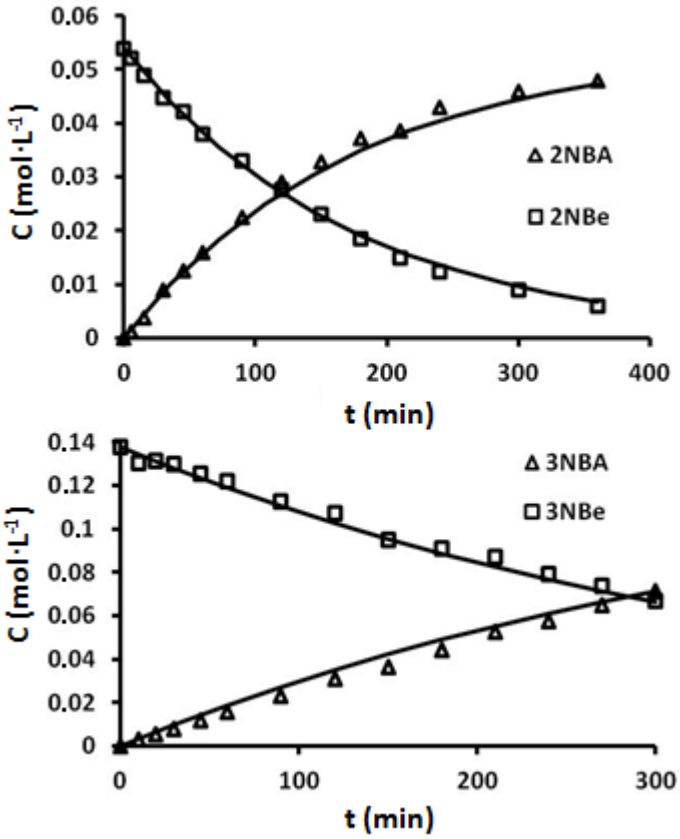

Fig. 8.4. Concentration profiles during the oxidation of 2- and 3-nitrobenzaldehyde in standard mixed acid. T = 50°C and 40 °C, respectively; experimental (symbols) and calculated (continuous lines) data; 3NBA = 3-nitrobenzoic acid; 3NBe=3-nitrobenzaldehyde; 2NBA = 2-nitrobenzoic acid; 2NBe=2-nitrobenzaldehyde. Overall σ(%) = 2.0; σ(%) = 3.0, respectively.

Once the relative occurrence of oxidation reactions was evaluated, the effect of the main process variables on nitrations was studied, i.e. nitric acid and sulfuric acid concentrations, and temperature. In Fig. 8.5 the effect of nitric acid concentration on benzaldehyde nitration rate is investigated. As expected, the reaction rate was faster when the nitric acid concentration was increased, being nitronium ion concentration higher. As previously observed (Di Somma et al., 2014), a small increase in the acidic concentration results in a great increase in the reaction rate. Reaction products distribution was deliberately omitted in Fig. 8.5. and it will be discussed later on. A similar effect was observed at varying sulfuric acid concentrations, Fig. 8.6.

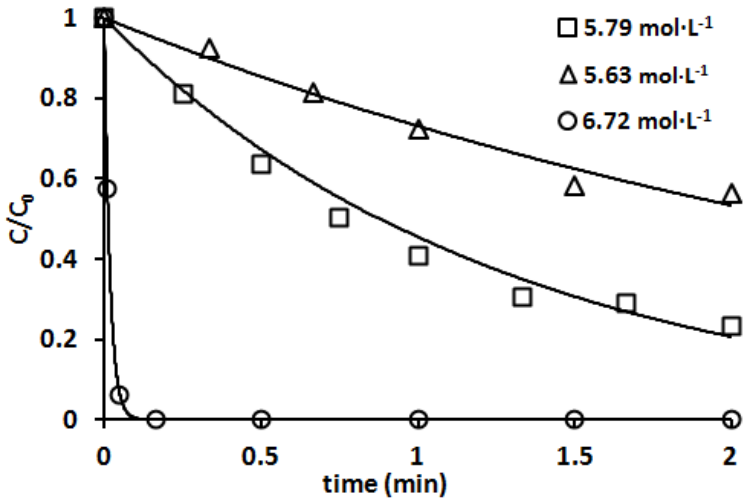

Fig. 8.5. Normalized concentration profiles of benzaldehyde in mixed acid at varying HNO_3 concentrations.[H_2SO_4] = 9.46 mol·L^{-1}; T = 20 °C.

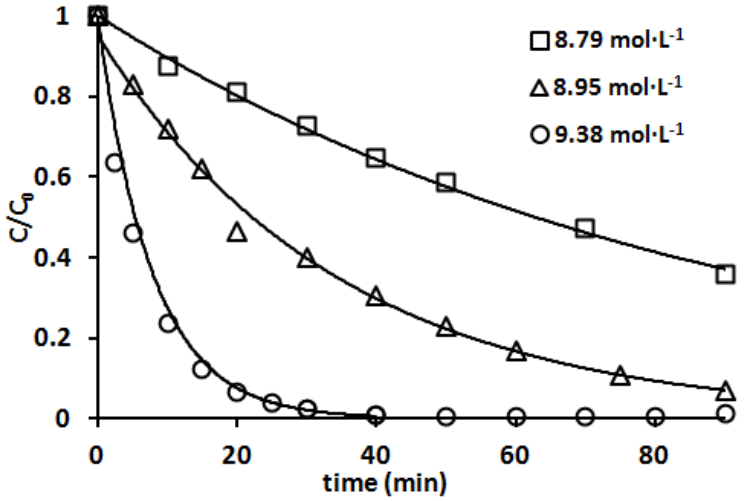

Fig. 8.6. Normalized concentration profiles of benzaldehyde in mixed acid at varying H_2SO_4 concentrations. [HNO_3] = 5.24 mol·L^{-1}; T = 20 °C.

The effect of temperature is reported in Fig. 8.7. As expected an increase in temperature results in higher nitration rates. According to equation 8.3, at low organic concentrations, nitric acid consume can be neglected and a pseudo first-order nitration kinetic is observed. Pseudo first-order kinetic constants have an Arrhenius-like dependence on temperature, Fig. 8.8.

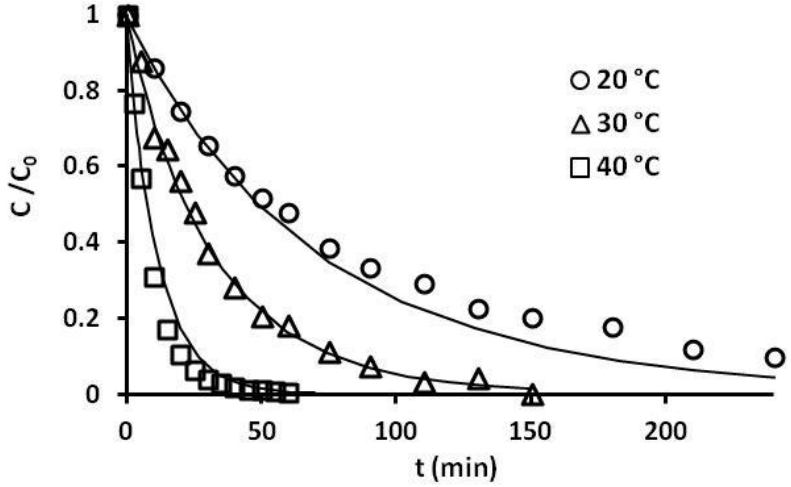

Fig. 8.7. Normalized concentration profiles of benzaldehyde in mixed acid at varying temperature. [HNO_3] = 4.54 mol·L^{-1}; [H_2SO_4] = 9.21 mol·L^{-1}. Experimental (symbols) and calculated (continuous lines) data. Overall σ(%)=7.0.

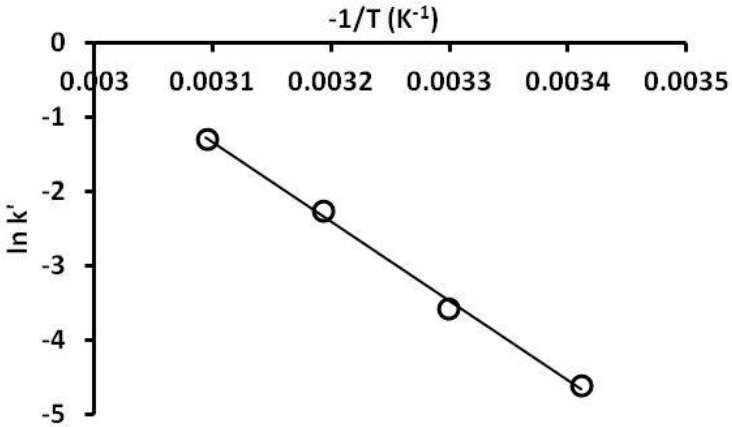

Fig. 8.8. Pseudo first-kinetic constant dependence on temperature. [HNO_3] = 4.54 mol·L^{-1}; [H_2SO_4] = 9.21 mol·L^{-1}.

Finally, the influence of mixed acid composition on selectivity towards the two isomers was investigated. Di Somma et al., (2014) highlighted the increase in the ortho-substituted isomer when increasing the nitric acid content. On the basis of previous investigations (Sainz-Diaz et al., 2002) this has been directly related to the higher nitronium ion concentration, that could favour the internal rearrangement of the species deriving from the coordination of a nitronium ion of the aldehydic group. This internal rearrangement is only possible on the ortho-position because of its spatial closeness to this reaction center (Chapter 2). Following these

considerations, the experimental selectivities to the two isomers were plotted against the estimated nitronium ion concentration (Fig.8.9) together with the prediction of the mathematical model that will be developed in the next Section. Under all the investigated conditions, 3-nitrobenzaldehyde is the main reaction product. However, results confirmed the observed increase in selectivity to the ortho-substituted isomer for higher nitric acid concentrations, and, consequently, nitronium ion levels. The highest obtained yield of 31.6 % is higher than the reported value of 27 % reported by Di Somma et al. (2014) for H_R = -5.4.

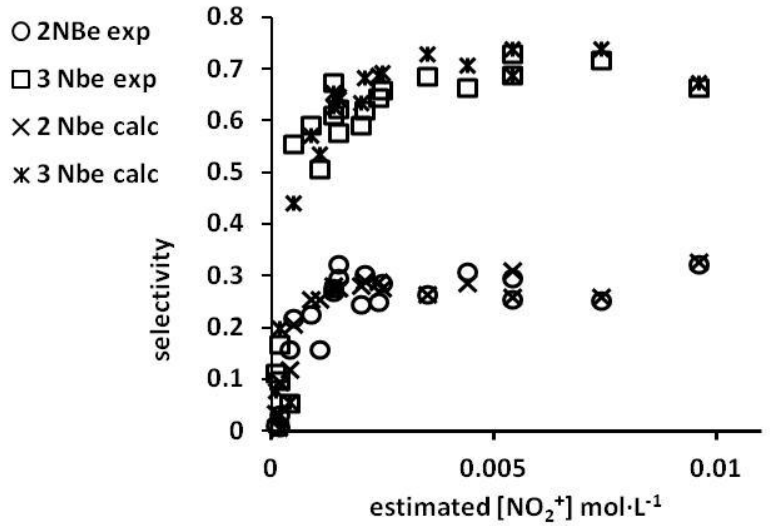

Fig. 8.9. Experimental (exp) and calculated (calc) selectivities to 2-nitrobenzaldehyde (2NBe) and 3-nitrobenzaldehyde (3NBe) at different mixed acid compositions. T = 20°C.

8.3. Kinetic model

The main results of the literature survey and the presented experimental campaign can be summarized as follows:

- Benzaldehyde reactivity is strongly dependent on mixed acid composition;
- Oxidation of benzaldehyde, 2-nitrobenzaldehyde and 3-nitrobenzaldehyde are secondary reaction pattern. Their influence is higher for less concentrated mixed acid, in which nitration kinetics are slower;
- 2-nitrobenzaldehyde yield was shown to vary between 18 and 31.6 % at varying nitric acid and sulfuric acid concentrations;

- the para-substituted isomer was never detected under all the adopted conditions (except at trace levels);
- The increase in the ortho-substituted isomer yield at higher nitronium ion concentrations was attributed to the formation and internal rearrangement of a coordination species deriving from the attack of a nitronium ion to the aldehydic group ($BeNO_2^+$).

On the basis of the above information, the following reaction scheme could be proposed (Fig. 8.10).

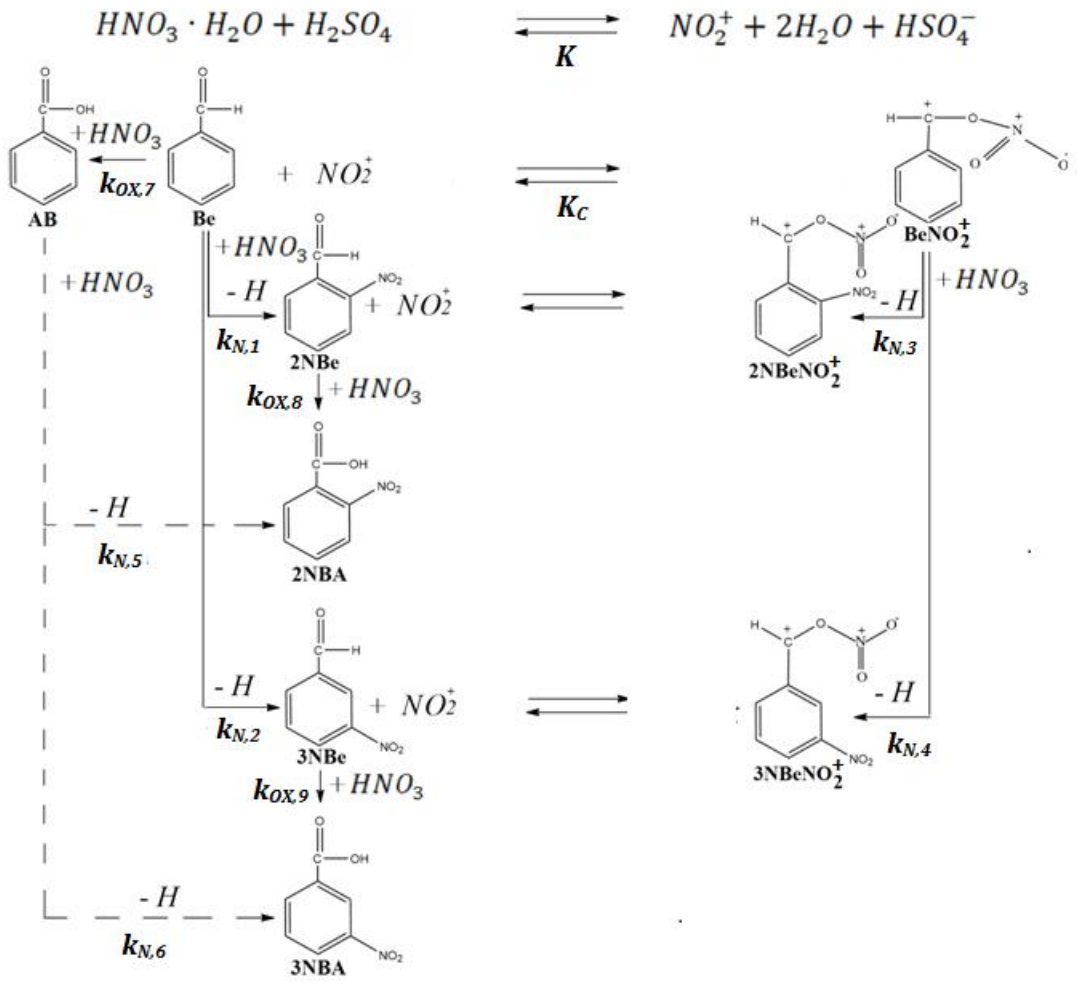

Fig. 8.10. Proposed reaction scheme for benzaldehyde nitration.

Nitronium ion is the real nitrating species. It can directly attack either the ortho-position ($k_{N,1}$ in Fig. 8.10) or meta-position ($k_{N,2}$ in Fig. 8.10) of the aromatic ring of benzaldehyde (Be).

Nitronium ion can also attack the aldehydic group of benzaldehyde to form $BeNO_2^+$ that is in equilibrium with benzaldehyde (equilibrium constant K_C). $BeNO_2^+$ can internally rearrange to give the ortho-nitrated form of the coordination species ($k_{N,3}$ in Fig. 8.10), which is in equilibrium with 2-nitrobenzaldehyde ($2NBe$). $BeNO_2^+$ can also be directly nitrated in position 3 ($k_{N,4}$ in Fig. 8.10). All the secondary oxidation reactions of benzaldehyde to benzoic acid (BA, $k_{OX,7}$ in Fig. 8.10), 2-nitrobenzaldehyde to 2-nitrobenzoic acid ($2NBA$, $k_{OX,8}$ in Fig. 8.10), and 3-nitrobenzaldehyde to 3-nitrobenzoic acid ($3NBA$, $k_{OX,9}$ in Fig. 8.10) were also included in the scheme. Finally, benzoic acid can be nitrated to form nitrobenzoic acid isomers ($k_{N,5}$ and $k_{N,6}$ in Fig. 8.10). The mathematical kinetic model was developed on the base of the reaction scheme presented in Fig. 8.10. For each organic species a differential mass balance was considered as follows

$$\frac{d[Ar_i]}{dt} = \sum_{k=1}^{n} (\pm k_{N,k}^{g} [Ar_j][HNO_3] \pm k_{OX,k}[Ar_j]) \qquad \text{eq. 8.6}$$

where the contribution of all the nitration and oxidation reactions to the formation or consume of Ar_i were taken into account.

In the previous Section, it was shown that, under all the adopted conditions, oxidation reactions are much slower than nitrations. Therefore, the contribution of these reactions to the global mass balance is almost always of minor importance. In a first attempt to model benzaldehyde oxidation to benzoic acid, literature indications were followed (Joshi et al., 2005). According to them, benzaldehyde oxidation reaction has a first-order dependence on benzaldehyde concentration with a molar benzaldehyde to nitric acid consume of 1:0.5. On the other hand, there is no information about oxidation kinetics of 2 and 3-nitrobenzaldehyde by nitric acid. To reduce the complexity of the kinetic scheme and the number of parameters to be determined a semi-empirical approach was followed. Several kinetic runs were carried out starting from 2- and 3-nitrobenzaldehyde, showing a pseudo first-order dependence on nitrobenzaldehydes concentration. Under the adopted conditions, the logarithm of pseudo first-order kinetic constants was found to vary linearly with the molar concentration of water, as shown in Fig. 8.11 at 40°C. Their intercepts were found to be a linear function of the absolute temperature (data not shown). The obtained empirical expressions to describe these secondary reaction pathways are reported together with the other adopted equation in the

mathematical description of the model (eq. 8.9 – 8.10). In Table 8.1 the adopted experimental conditions are summarized.

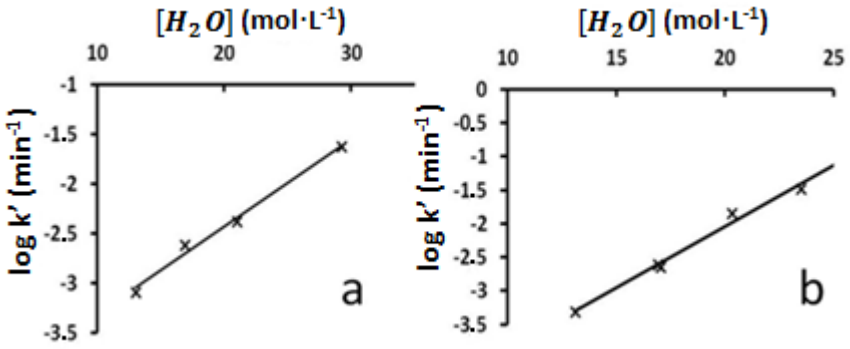

Fig. 8.11. Logarithm of pseudo first-order kinetic constants *vs.* molar water concentration in 2-nitrobenzaldehyde (a) and 3-nitrobenzaldehyde (b) oxidation at T = 40°C. Experimental condition are summarized in Table 8.1.

Run	HNO_3wt. %	H_2SO_4wt. %	H_2O wt. %	*log k* (min^{-1})	$[NBe]_0$(mol· L^{-1})
1	25	60	15	-3.1	0.053
2	20	60	20	-2.6	0.043
3	30	30	40	-1.6	0.043
4	26.1	50.3	26.1	-2.4	0.050
5	25	60	15	-3.3	0.138
6	20	60	20	-2.6	0.075
7	20	60	20	-2.6	0.137
8	25	50	25	-1.8	0.133
9	30	40	30	-1.5	0.140

Table. 8.1. Adopted experimental conditions for nitrobenzaldehydes oxidation. Runs 1-4 refers to 2-nitrobenzaldaldehyde; runs 5-9 to 3-nitrobenzaldehyde; T = 40°C.

The developed kinetic model relies on the following equilibrium reaction

$$HNO_3 \cdot H_2O + H_2SO_4 \rightleftarrows HSO_4^- + NO_2^+ + 2H_2O \qquad K \qquad \text{r. 8.2}$$

$$Be + NO_2^+ \rightleftarrows BeNO_2^+ \qquad K_C \qquad \text{r. 8.3}$$

$$2NBe + NO_2^+ \rightleftarrows 2NBeNO_2^+ \qquad \text{r. 8.4}$$

$$3NBe + NO_2^+ \rightleftarrows 3NBeNO_2^+ \qquad \text{r. 8.5}$$

and the following irreversible reactions

$$Be + HNO_3 \longrightarrow 2NBe + H_2O \qquad k_{N,1} \qquad \text{r. 8.6}$$

$$Be + HNO_3 \longrightarrow 3NBe + H_2O \qquad k_{N,2} \qquad \text{r. 8.7}$$

$$BeNO_2^+ + HNO_3 \longrightarrow 2NBeNO_2^+ + H_2O \qquad k_{N,3} \qquad \text{r. 8.8}$$

$$BeNO_2^+ + HNO_3 \longrightarrow 3NBeNO_2^+ + H_2O \qquad k_{N,4} \qquad \text{r. 8.9}$$

$$AB + HNO_3 \longrightarrow 2NBA + H_2O \qquad k_{N,5} \qquad \text{r. 8.10}$$

$$AB + HNO_3 \longrightarrow 3NBA + H_2O \qquad k_{N,6} \qquad \text{r. 8.11}$$

$$Be + HNO_3 \longrightarrow AB \qquad k_{OX,7} \qquad \text{r. 8.12}$$

$$2NBe + HNO_3 \longrightarrow 2NBA \qquad k_{OX,8} \qquad \text{r. 8.13}$$

$$3NBe + HNO_3 \longrightarrow 3NBA \qquad k_{OX,9} \qquad \text{r. 8.14}$$

for nitration reactions from r. 8.6 to r. 8.11 the reaction rate was expressed as

$$r_{N,i} = k_{N,i}^g [HNO_3][Ar_i] = k_{N,i}[NO_2^+][Ar_i] = k_{N,i}^0 exp\left(-\frac{E_{aN,i}}{RT}\right)[NO_2^+][Ar_i] \qquad \text{eq. 8.7}$$

whereas the following expressions were adopted for oxidation reactions from r. 8.12 to r. 8.14

$$r_{OX,7} = k_{OX,7}^0 exp\left(-\frac{E_{aOX,7}}{RT}\right)[Be] \qquad \text{eq. 8.8}$$

$$r_{OX,8} = \frac{10^{(0.088\cdot[H_2O]-4.19\cdot(T-313)*0.048)}}{60}\cdot[2NBe] \qquad \text{eq. 8.9}$$

$$r_{OX,9} = \frac{10^{(0.18\cdot[H_2O]-5.68\cdot(T-313)*0.032)}}{60}\cdot[3NBe] \qquad \text{eq. 8.10}$$

where $r_{OX,8}$, $r_{OX,9}$ are expressed in mol·L^{-1}·s^{-1} and eq.s 8.9 and 8.10 are the above-mentioned empirical equations.

The following material balances were considered. In the following equations, the pseudo-component theory presented in Section 7.4 was used to describe the global reaction consume of species in equilibrium.

$$\frac{d[H_2SO_4]_{tot}}{dt} = 0 \qquad \text{eq. 8.11}$$

$$\frac{d[H_2O]}{dt} = r_{N,1} + r_{N,2} + r_{N,3} + r_{N,4} + r_{N,5} + r_{N,6} \qquad \text{eq. 8.12}$$

$$\frac{d[HNO_3]_{TOT}}{dt} = -r_{N,1} - r_{N,2} - r_{N,3} - r_{N,4} - r_{N,5} - r_{N,6} - 0.5r_{N,7} - 0.5r_{N,8} - 0.5r_{N,9} \qquad \text{eq. 8.13}$$

$$[NO_2^+] = exp\left(\frac{\Delta H}{RT}\right) exp\left(\frac{\Delta S^*}{R}\right) \frac{\gamma_{HNO_3}}{\gamma_{H_2O}} \frac{[HNO_3]}{[H_2O]} 10^{-H_R} \qquad \text{eq.8.14}$$

$$[Be]_{TOT} = [Be] + [BeNO_2^+] \qquad \text{eq. 8.15}$$

$$[BeNO_2^+] = \frac{K_C \cdot [Be]_{TOT} \cdot [NO_2^+]}{(1 + K_C \cdot [NO_2^+])} \qquad \text{eq. 8.16}$$

$$\frac{d[BA]}{dt} = r_{OX,7} - r_{N,5} - r_{N,6} \qquad \text{eq. 8.17}$$

$$\frac{d[2NBA]}{dt} = r_{OX,8} + r_{N,5} \qquad \text{eq. 8.18}$$

$$\frac{d[3NBA]}{dt} = r_{OX,9} + r_{N,6} \qquad \text{eq. 8.19}$$

$$\frac{d[Be]_{TOT}}{dt} = -r_{N,1} - r_{N,2} - r_{N,3} - r_{N,4} - r_{OX,7} \qquad \text{eq. 8.20}$$

$$\frac{d[2NBe]_{TOT}}{dt} = r_{N,1} + r_{N,3} - r_{OX,8} \qquad \text{eq. 8.21}$$

$$\frac{d[3NBe]_{TOT}}{dt} = r_{N,2} + r_{N,4} - r_{OX,9} \qquad \text{eq. 8.22}$$

The total nitric acid consume in nitration was taken into account in equation 8.13. Moreover, at highly acidic mixed acid composition ($[H_2SO_4]$ > 9 mol·L^{-1}), for which nitrations occur, the conversion of nitric acid to nitrate can be ruled out since it is mostly undissociated. Simulations carried out with the model developed in Chapter 5 confirmed the literature indications (Fig. 8.12). The equilibrium between benzaldehyde and its nitronium coordinated

form is regulated by eq. 8.15 and 8.16. In equation 8.15, using the M_C function theory a value close to 0 was estimated for $n_{BeNO_2^+}$, that suggested a small influence of the activity coefficients in the investigated range of concentrations or a compensation effect in their ratio. Similar compensation effects in the ratio of activity coefficients has been already reported (Ross et al., 1986). For this reason, they were included in the equilibrium constant value. For the nitronium coordination equilibria of 2- and 3-nitrobenzaldehydes (r. 8.4 and 8.5), there was no need to distinguish between their coordinated and uncoordinated forms since the global balances eq.s 8.21 and 8.22 were considered; in addition the coordinated forms $2NBeNO_2^+$ and $3NBeNO_2^+$ are not directly involved in irreversibile reactions, whereas the oxidation reactions of $2NBe$ and $3NBe$ only have a minor importance in the global mass balance. Moreover, it must be considered that equilibria r. 8.3, 8.4, and 8.5 are mostly shifted to the left, as confirmed by the optimization results. This assumption was confirmed by several optimization procedures, carried out taking into account equilibria r. 8.4 and 8.5, that resulted in identical results, showing that the partition between the equilibrium forms has no influence on the kinetic model. On the contrary, equilibrium r. 8.3 is of crucial importance, being the coordinated form $BeNO_2^+$ directly involved in two irreversible reactions (r. 8.8 and 8.9).

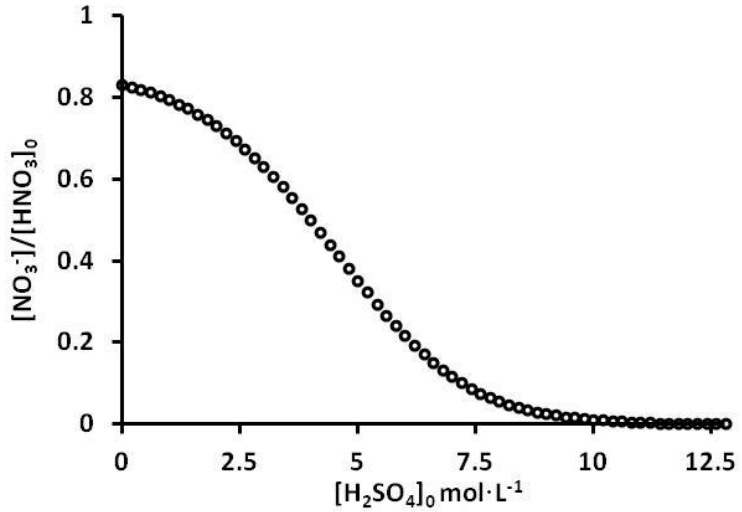

Fig. 8.12. Simulated nitric acid dissociation degree to nitrate ion in sulfuric acid. $[HNO_3]$ = 5 mol·L^{-1}.

Equations 8.11 - 8.22 were simultaneously solved using the Matlab Software in order to find the values of the parameters to minimize the following objective function

$$\sum_{g=1}^{h}\sum_{i=1}^{l}\sum_{m=1}^{n}\left(y_{g,i,m}-c_{g,i,m}\right)^2 \qquad \text{eq. 8.23}$$

were y and c are the calculated and experimental concentrations and h, l, and n respectively represents the number of experimental data recorded in each experiment, the number of the measured reacting species, and the number of experiments used in the optimization procedure. The parametric optimization was carried out using more than 50 different experimental runs at varying temperature, mixed acid composition, and initial benzaldehyde concentration. For each experimental run, the concentration profiles of at least 4 species were experimentally measured.

The optimized parameters, together with their 97 % intervals of confidence, are shown in Table 8.2. Irrespective of their numeric values, it is worth stressing that the mathematical model was independent on the value of the kinetic constant $k_{N,1}$, this suggesting that the direct nitration of benzaldehyde in ortho-position can be ruled out in the global reaction scheme. This can explain the apparent contradictory absence of the para-substituted isomer under all the investigated conditions. If the direct ortho-nitration of benzaldehyde was present, then a para- to ortho- molar ratio of about 0.5:1 would be expected, since the aldehydic group has the same deactivating influence on the two positions, and the probability of an ortho-substitution is double than a para-substitution reaction. According to the results, 2-nitrobenzaldehyde is only formed by the internal rearrangement of $BeNO_2^+$ when attacked by a second nitronium ion. This mechanism can also explain the observed increase in the selectivity to 2-nitrobenzaldehyde for higher nitric acid concentrations.

The results of the kinetic model calculations (continuous lines) were presented and compared with the experimental data (symbols) in Fig. 8.2 - 8.7, and 8.9 for some of the adopted experimental runs. Additional examples are presented in Fig. 8.13 – 8.17. Moreover, as an additional model verification, an example of the comparison between experimental and calculated data for an experimental run that was not included in the optimization procedure was shown in Fig. 8.18. As presented, the model is capable of predicting the behavior of the reacting system at varying conditions in the investigated ranges.

Nitration reactions		
N. Reaction	$k_{N,i}^{0}$ **(L·mol^{-1}·s^{-1})**	$E_{aN,i}$ **(J·mol^{-1})**
1	Not evaluable	Not evaluable
2	$(1.64\pm0.011)\cdot10^{18}$	$(1.118\pm0.002)\cdot10^{5}$
3	$(3.00\pm0.060)\cdot10^{20}$	$(9.213\pm0.008)\cdot10^{4}$
4	$(1.70\pm0.085)\cdot10^{19}$	$(8.318\pm0.008)\cdot10^{4}$
5	$(1.69\pm0.30)\cdot10^{16}$	$(9.410\pm0.046)\cdot10^{4}$
6	$(3.05\pm0.45)\cdot10^{15}$	$(8.820\pm0.035)\cdot10^{4}$
Oxidation reaction		
N. Reazione	$k_{OX,i}^{0}$ **(s^{-1})**	$E_{aOX,i}$ **(J·mol^{-1})**
7	$(9.40\pm0.88)\cdot10^{3}$	$(5.004\pm0.020)\cdot10^{4}$
Equilibrium constant		
	ΔS_C **(J·K^{-1}·mol^{-1})**	ΔH_C **(J·mol^{-1})**
	$-(3.89\pm0.032)\cdot10^{2}$	$-(1.015\pm0.001)\cdot10^{5}$

Table 8.2. Estimated model parameters.

The kinetic parameters in Table 8.2 were estimated at varying temperature, nitric acid concentration and sulfuric acid concentration in the ranges 10 – 50 °C, 2.41 – 6.72 mol·L^{-1}, and 8.9 – 10.0 mol·L^{-1}, respectively, which are their validity ranges. Moreover, as shown in Chapter 9, they are capable of predicting benzaldehyde nitration kinetic at nitric acid and sulfuric acid concentrations up to 8.3 mol·L^{-1} and 10.7 mol·L^{-1}, respectively.

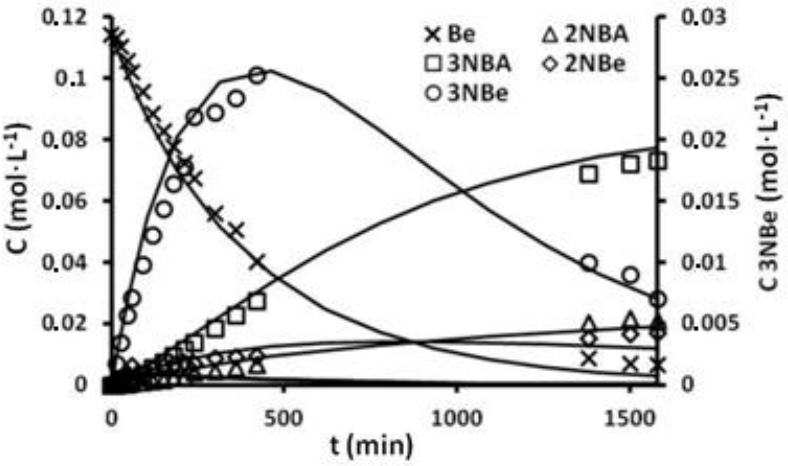

Fig. 8.13. Concentration profiles. Experimental (symbols) and calculated (continuous lines) data. [HNO_3] = 3.88 mol·L^{-1}; [H_2SO_4] = 9.19 mol·L^{-1}; T = 20 °C.

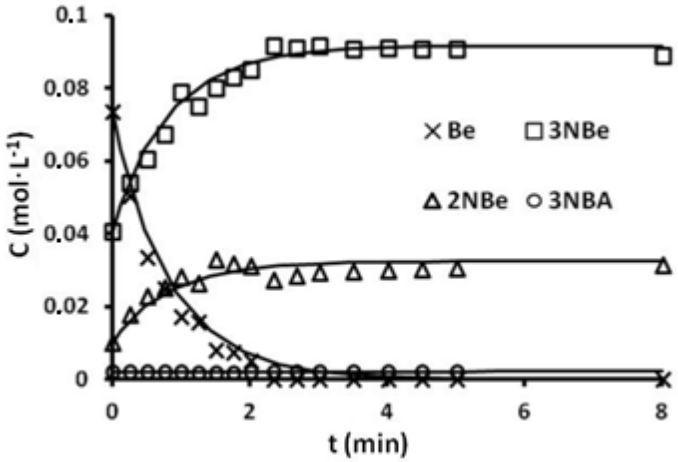

Fig. 8.14. Concentration profiles. Experimental (symbols) and calculated (continuous lines) data. [HNO_3] = 6.01 mol·L^{-1}; [H_2SO_4] = 9.52 mol·L^{-1}; T = 20 °C.

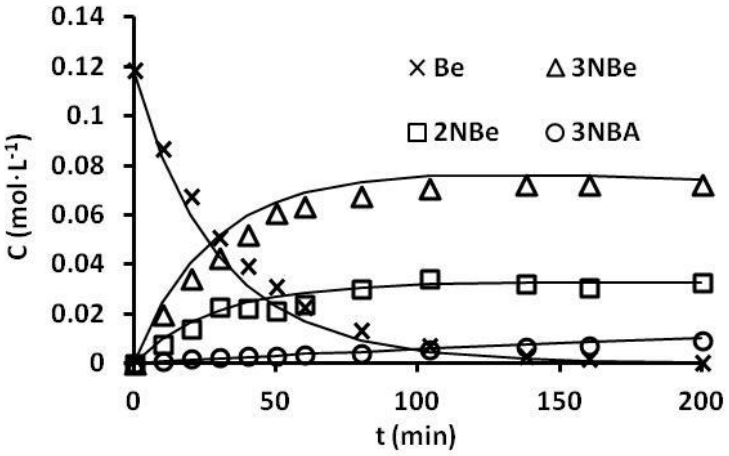

Fig. 8.15. Concentration profiles. Experimental (symbols) and calculated (continuous lines) data. [HNO_3] = 4.85 mol·L^{-1}; [H_2SO_4] = 9.34 mol·L^{-1}; T = 20 °C.

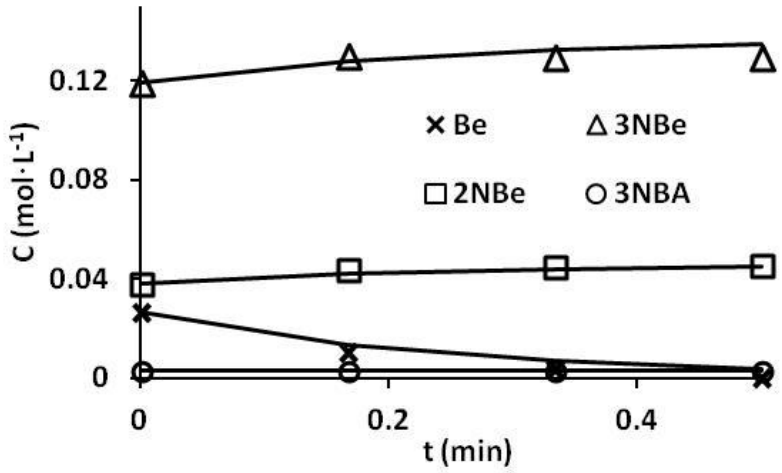

Fig. 8.16. Concentration profiles. Experimental (symbols) and calculated (continuous lines) data. [HNO_3] = 6.72 mol·L^{-1}; [H_2SO_4] = 9.45 mol·L^{-1}; T = 20 °C.

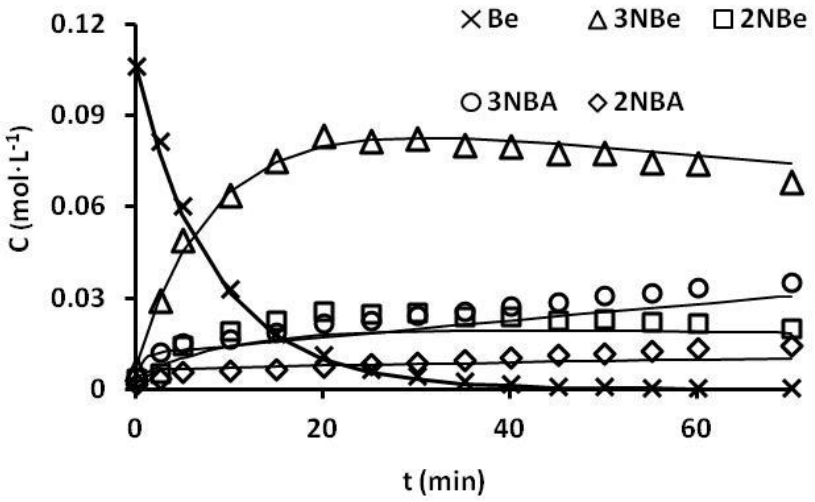

Fig. 8.17. Concentration profiles. Experimental (symbols) and calculated (continuous lines) data. [HNO_3] = 4.52 mol·L^{-1}; [H_2SO_4] = 9.14 mol·L^{-1}; T = 40 °C.

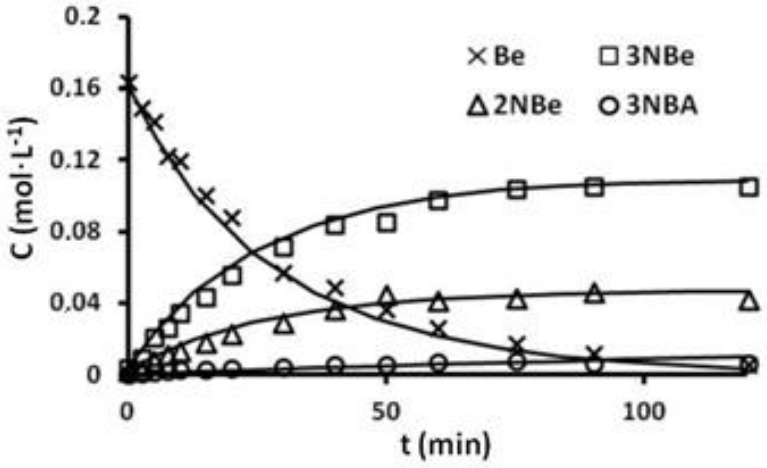

Fig. 8.18. Concentration profiles. Experimental (symbols) and calculated (continuous lines) data. [HNO_3] = 5.02 mol·L^{-1}; [H_2SO_4] = 9.20 mol·L^{-1}; T = 20 °C.

8.4. Towards the industry: heterogeneous system modeling

As previously presented, most nitration processes in mixed acid are carried out in heterogeneous liquid-liquid systems at industrial scale. In fact, the organic substrate, as well as the reaction products, are poorly soluble in the aqueous acidic phase where the reaction occurs. As a result, despite the determination of kinetic parameters is of crucial importance in selecting the most convenient operating conditions, the mass transfer limitations and the solubility of the organic compounds also need to be taken into account.

In this Section, an extension of the developed integrated kinetic model to the liquid-liquid heterogeneous reacting system is presented. The predictions of the model were in agreement with the experimental results.

8.4.1. Kinetic model extension

As explained in Chapter 4, there was no possibility to separately analyze the aqueous acidic and the organic phases during heterogeneous experiments. This is mainly due to the difficulties in separating two liquid reactive immiscible phases, keeping the system isothermal, and quenching the reaction at the same time. For this reason, only the overall moles consume can be experimentally determined for each organic compound. In order to further validate the kinetic model, different kinetic runs under heterogeneous conditions were carried out. The magnetic stirrer speed was regulated to run experiments under a kinetic regime. According to Danckwerts (1970), Doraiswamy, and Sharma (1984) theories on regimes of heterogeneous reactions (Joshi et al., 2005), when the rate of chemical reactions is much slower than the rate of mass transfer, the overall substrate consume is controlled by the chemical reaction (kinetic regime). In a liquid-liquid system, the mass transfer rate is dependent on the magnetic stirrer speed. At higher speeds, the turbulence, the spatial concentration equalization, and the surface between the partially miscible phases are significantly enhanced. As a result, in such heterogeneous systems the overall substrate consume increases at higher impeller speeds, up to a plateau value, which is representative of the kinetic regime. Several experimental runs, under different conditions, showed that for the investigated system the kinetic regime assumption is verified for impeller speeds higher than 700 rpm. An example is shown in Fig. 8.19; as presented, nitrobenzaldehydes concentration

profiles were independent on the stirrer speed (benzaldehyde profiles were omitted for convenience of the eye).

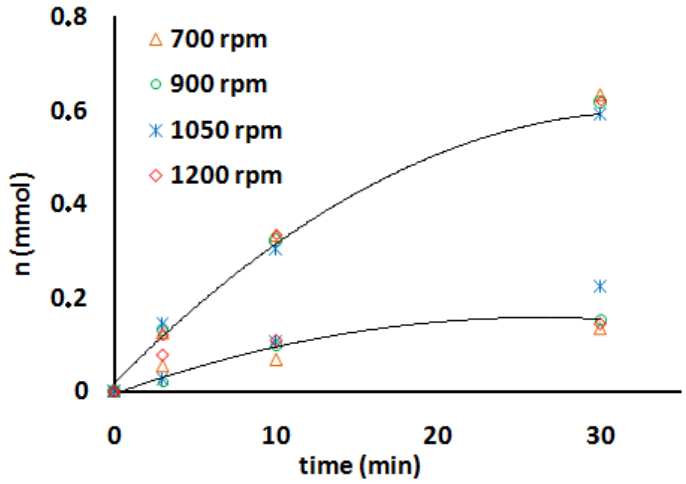

Fig. 8.19. Concentration profiles of 2- and 3-nitrobenzaldehyde at different stirrer speeds. [HNO_3] = 5.82 mol·L^{-1}; [H_2SO_4] = 10.41 mol·L^{-1}; T = 15 °C.

The kinetic nitration model, developed in the previous Section, was modified adopting the following expressions

$$\frac{dN_i}{dt} = \sum_i r^*_{N,i} \qquad \text{eq. 8.24}$$

$$r^*_{N,i} = k^0_{N,i} exp\left(-\frac{E_{aN,i}}{RT}\right)[NO_2^+][Ar_i]^{aq}V^{aq} = k^0_{N,i} exp\left(-\frac{E_{aN,i}}{RT}\right)[NO_2^+]N^{aq}_{Ar,i} \qquad \text{eq. 8.25}$$

where $[Ar_i]^{aq}$ is the concentration of the aromatic species *i* in the aqueous acidic phase and V^{aq} is the volume of the acidic phase. Equations 8.23 and 8.24 take into account the overall moles n_i consume which is controlled by the kinetics in the aqueous acidic phase, in which the reactions occur. The volume of the aqueous acidic phase and the solubility of the organics change during the reaction as nitric acid is being consumed, whereas water is being formed. In fact, in this case, for each mole of nitrated organic substrate one mole of nitric acid is consumed and one mole of water is formed according to the mechanisms presented in this Chapter. Moreover, dissolved organics can contribute to the acidic mixture volume changes. Even though the organic concentration in the acidic phase is almost always negligible with respect to the total molar concentration of water and acids, the additive volumes simplifying hypothesis was assumed for dissolved benzaldehyde, together with dissolved nitrobenzaldehydes according to equation 8.26

$$V^{aq}(t) = V^{mix}(t) + V^{Ar}_{diss}(t) \quad \text{eq. 8.26}$$

$$V^{Ar}_{diss}(t) = \sum_i \frac{N^{aq}_{Ar,i} MW_i}{\rho_i} \quad \text{eq. 8.27}$$

where V^{mix} is the volume of the nitrating mixture, V^{Ar}_{diss} the volume of the dissolved organics, and MW_i and ρ_i the molar weight and density of the i-th species, respectively. In equation 8.27, $N^{aq}_{Ar,i}$ are equal to the maximum dissolved moles of the organic species *i*, according to the solubility value in the mixture, until the amount of added organic is higher than its solubility, and becomes equal to the total moles of the species *i* in the system once its amount drops below the solubility value, because of the occurrence of the reactions.

Solubilities of the organics in mixed acid at varying composition and temperature where separately investigated as described in Chapter 4. Their values were found to be independent on the presence of the other organics in the system. The logarithm of the organic molar fraction was linearly dependent on the reciprocal of the absolute temperature as shown for some experimental runs in Fig. 8.20.

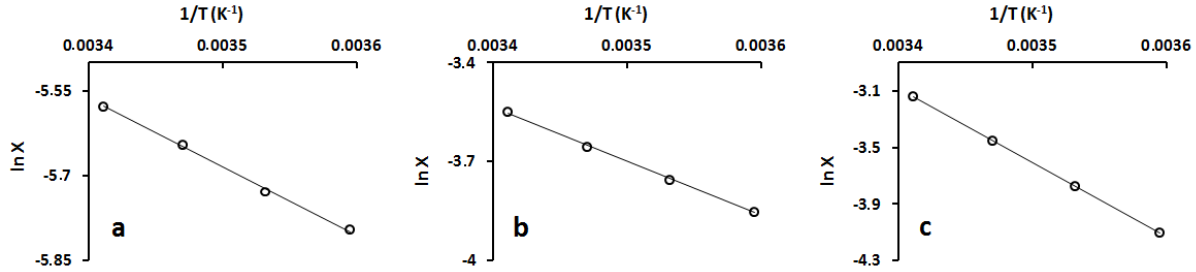

Fig. 8.20. Solubility dependence on temperature. a) benzaldehyde, [HNO_3] = 6.60 mol·L^{-1}, [H_2SO_4] = 6.76 mol·L^{-1}; b) 2-nitrobenzaldehyde, [HNO_3] = 1.90 mol·L^{-1}, [H_2SO_4] = 10.25 mol·L^{-1}; c) 3-nitrobenzaldehyde, [HNO_3] = 3.79 mol·L^{-1}, [H_2SO_4] = 11.32 mol·L^{-1}.

At a fixed temperature, empirical linear and quadratic correlations were found between the logarithm of the *i*-th organic species molar fraction and the total molar acid concentration, in the neighborhood of the investigated conditions. The empirical expressions can be summarized as follows

$$\ln X_{Be} = 0.593 \cdot ([HNO_3] + [H_2SO_4]) + 0.0108 \cdot T - 16.771 \quad \text{eq. 8.28}$$
$$if\ [HNO_3] + [H_2SO_4] > 12.9\ mol \cdot L^{-1}$$

$$\ln X_{2NBe} = 0.030 \cdot ([HNO_3] + [H_2SO_4])^2 + 0.0428 \cdot T - 20.729 \quad \text{eq. 8.29}$$

$$\ln X_{3NBe} = 0.403 \cdot ([HNO_3] + [H_2SO_4]) + 0.0492 \cdot T - 23.961 \quad \text{eq. 8.30}$$

The above equations were simultaneously solved to predict the molar consume of benzaldehyde and formation of 2-nitrobenzaldehyde and 3-nitrobenzaldehyde under heterogeneous liquid-liquid conditions. The calculated and experimental data were compared in Fig. 8.21 - 8.24. As shown, the model was capable of predicting the experimental consume rate without any further adjustment of the previously estimated kinetic parameters. The blue lines, reported in Fig. 8.21 - 8.24, represent the maximum amount of dissolved benzaldehyde in the acid mixture, calculated by equations 8.26 and 8.28; benzaldehyde was in a separated phase as long as the total benzaldehyde moles in the system were higher than this value.

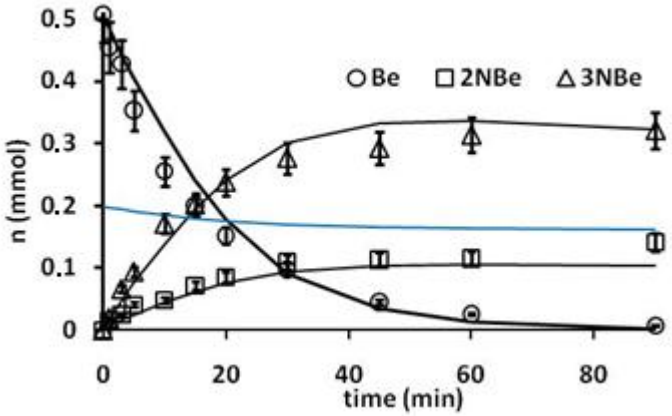

Fig. 8.21. Heterogeneous nitration experimental run. Experimental (symbols) and calculated (lines) data. Solubility value (blue line). $[HNO_3]_0$= 4.82 mol·L^{-1}, $[H_2SO_4]_0$= 9.32 mol·L^{-1}; T = 35 °C. n_{Be}^0= 0.51 mmol.

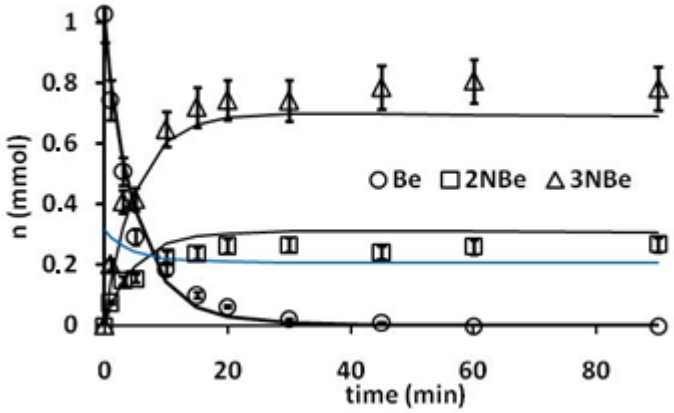

Fig. 8.22. Heterogeneous nitration experimental run. Experimental (symbols) and calculated (lines) data. Solubility value (blue line). $[HNO_3]_0$= 5.00 mol·L^{-1}, $[H_2SO_4]_0$= 10.44 mol·L^{-1}; T = 25 °C. n^0_{Be}= 1.03 mmol.

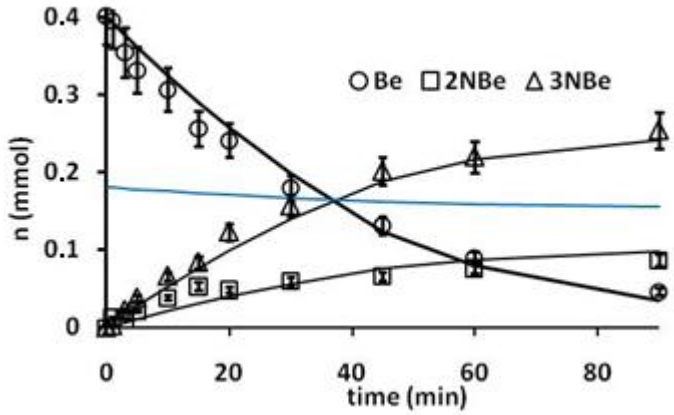

Fig. 8.23. Heterogeneous nitration experimental run. Experimental (symbols) and calculated (lines) data. Solubility value (blue line). $[HNO_3]_0$= 4.85 mol·L^{-1}, $[H_2SO_4]_0$= 9.30 mol·L^{-1}; T = 25 °C. n^0_{Be}= 0.4 mmol.

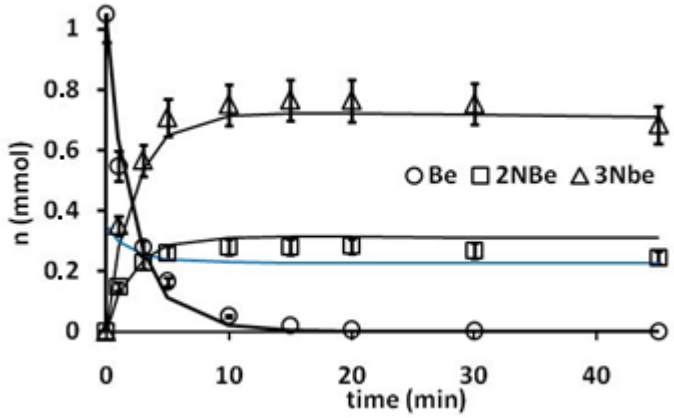

Fig. 8.2. Heterogeneous nitration experimental run. Experimental (symbols) and calculated (lines) data. Solubility value (blue line). $[HNO_3]_0$= 5.01 mol·L^{-1}, $[H_2SO_4]_0$= 10.43 mol·L^{-1}; T = 35 °C. n_{Be}^0= 1.05 mmol.

9. Results V: Benzaldehyde nitration in microreactors

9.1. Introduction

According to literature findings (Kulkarni et al., 2014), and on the basis of the experimental preliminary results and safety considerations presented in Section 6.2, benzaldehyde nitration and tandem oxidation-nitration of benzyl alcohol are suitable reactions for microreactor technology adoption. In this Chapter, some detailed investigations were carried out to evaluate microreactors performances in the management of the process. The results show the potentialities of microreactors to safely carry out the investigated reactions under hasher conditions, often impossible to be adopted in batch reactors, even at laboratory scale. The adoption of innovative reactor configurations was both used as a model verification and as an experimental tool to safely study the process intensification in harsh conditions.

In this respect, in the first part of the Chapter, the experimental results were used to validate the model predictions by adopting conditions different from those previously used in the model development. Successively, the kinetic model was used to identify conditions to maximize 2- and 3- nitrobenzaldehyde yields, respectively.

Some preliminary experiments were run to choose the most suitable microreactor configuration. To this regard, the choice was restricted to two experimental devices presented in Chapter 4: a tubular stainless-steel reactor (2 mm internal diameter) equipped with a cross mixer device in a thermostatic bath and a commercially available small-diameter borosilicate glass device with embedded mixer and heat exchanger. The two microreactor configurations are typical examples of the two most adopted approaches in the literature: bath-immersed flow reactors (Kulkarni et al., 2014) and integrated microreactors (Lowe et al., 2012; Kulkarni, 2014), being the former less sophisticated and cheaper, the latter more compact and easier to be used. It was already highlighted that in both cases the nature of heat transfer remains almost the same (Kulkarni, 2014).

The first comparison was made at 20°C in standard mixed acid. The fed flow rate of mixed acid and organics were adjusted in order to have an organic concentration of $5.0 \cdot 10^{-2}$ mol·L^{-1} and reaction times of 20, 40, and 60 min. Under those conditions the reacting mixture was

homogeneous during the experiments and the obtained results were not significantly different from each other and from the same experiment carried out in a refrigerated batch reactor. The similar obtained results can be attributed to the relatively long residence times and the low organics concentrations. Under these conditions the cross mixed and the embedded mixing system are equally efficient in dissolving the organics in the acid mixture and reaction times are sufficiently high to achieve an efficient radial mixing and homogeneous conditions along the axes of the channels. However, experiments carried out with shorter residence times and higher organics concentrations, even though lower than solubility, gave non-reproducible results in the cross-mixer and immersed channel configuration. This is probably due to the inefficiency of the cross mixer and radial equalization in these new conditions. Similar considerations were found in the literature when adopting a simpler T junction (Kulkarni et al., 2009). On the contrary, consistent and reproducible results were obtained with the integrated reactor with embedded static mixer under all the investigated conditions, which is why this reactor configuration was used for further experimental evaluations. Moreover, it is worth mentioning that a scaled-up version of the adopted microreactor with similar functionalities and properties is commercially available from Corning or Chemtrix, in different materials, which could be an attractive commercial application.

9.2. Model validation

The previously presented two kinetic models for benzyl alcohol oxidation and benzaldehyde nitration were integrated in a comprehensive kinetic model. At all the adopted temperatures and mixed acid concentrations, in order to obtain nitrobenzaldehydes, the kinetic model confirmed the experimental results concerning instantaneous conversion of benzyl alcohol to benzaldehyde so that no traces of unconverted benzyl alcohol were detected. Which is why benzyl alcohol concentrations profiles were omitted in the Figures presented in this Chapter, since they are not discernible on the adopted time scales. Some exceptions will be discussed later on. A simplified reaction scheme of the overall process is shown in Fig. 9.1.

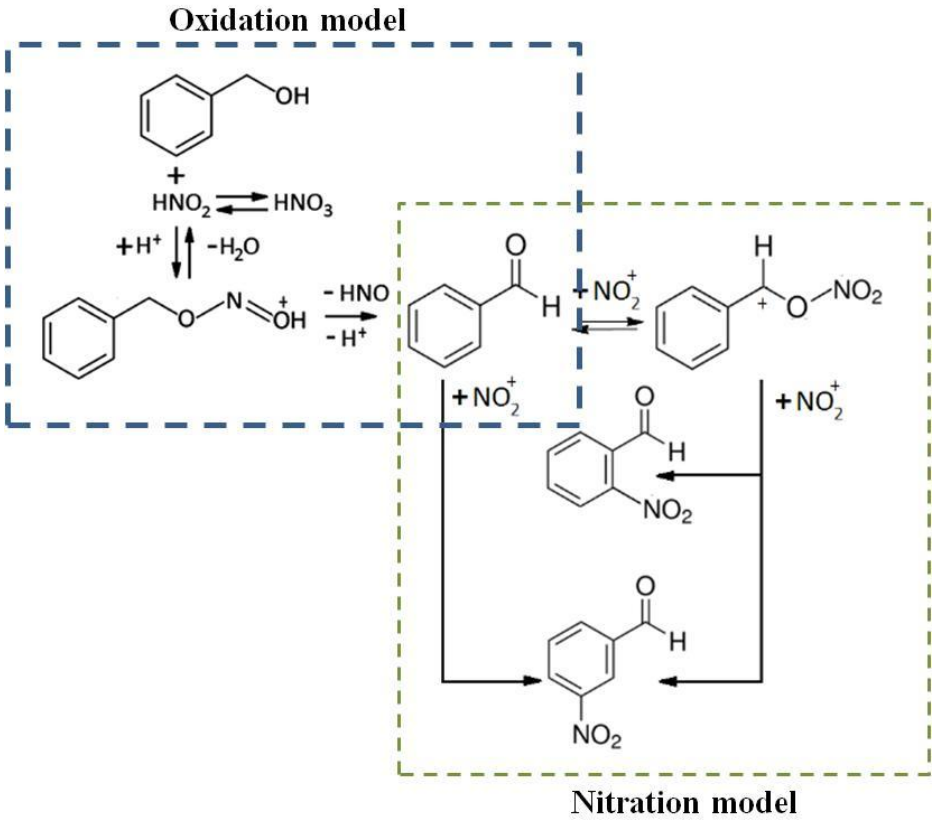

Fig. 9.1. Integrated model scheme for tandem oxidation-nitration of benzyl alcohol.

The previously obtained kinetic parameters were used to develop a new mathematical model for a continuous flow reactor. Assuming a plug flow reactor ideal behavior, which is consistent with the static embedded mixing system, the following mass balance can be adopted for each aromatic species Ar_i

$$\frac{d[Ar_i]}{d\tau} = \sum_j r_j \qquad \text{eq. 9.1}$$

were τ is the residence time defined as the ratio between the reactor volume V and the total flow rate Q_{tot}, and r_j is the generic positive reaction rate of formation or negative reaction rate of consume of the i-th species. The developed model, together with the ideal flow assumption was verified by running different experiments and comparing model predictions with experimental concentrations. The results of a first comparison are shown in Fig. 9.2 – 9.4. Other examples carried out in harsher conditions will be presented in the next Sections. The figures show a good agreement between model predictions and experimental data.

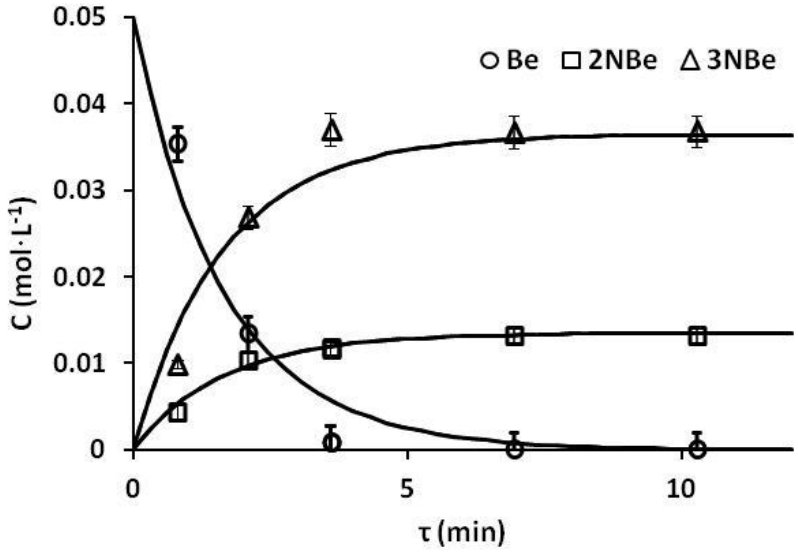

Fig. 9.2. Concentration *vs.* residence time. Predicted (lines) and experimental data (symbols). (Be) benzaldehyde; (2NBe) 2-nitrobenzaldehyde; (3NBe) 3-nitrobenzaldehyde; [HNO_3] = 5.70 mol·L^{-1}; [H_2SO_4] = 10.05 mol·L^{-1}; T = 6 °C; [Be]$_0$ = 0.05 mol·L^{-1}.

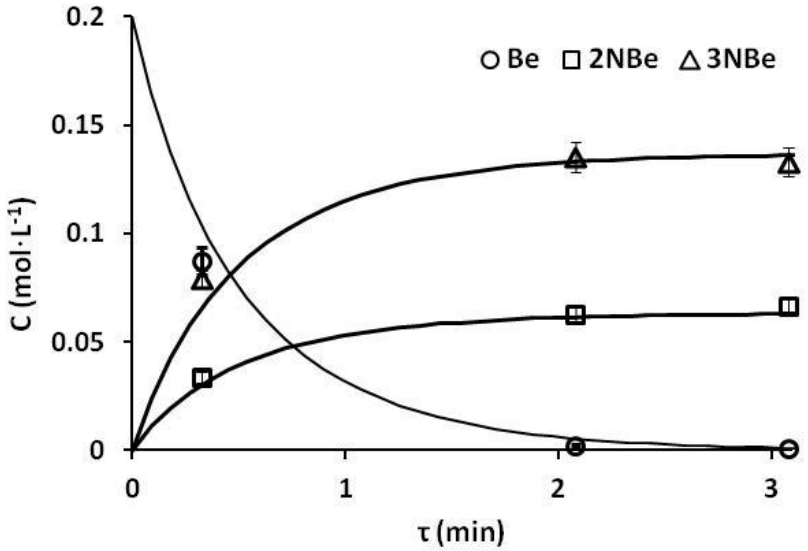

Fig. 9.3. Concentration *vs.* residence time. Predicted (lines) and experimental data (symbols). (Be) benzaldehyde; (2NBe) 2-nitrobenzaldehyde; (3NBe) 3-nitrobenzaldehyde; [HNO_3] = 5.67 mol·L^{-1}; [H_2SO_4] = 9.91 mol·L^{-1}; T = 25 °C; [Be]$_0$ = 0.2 mol·L^{-1}.

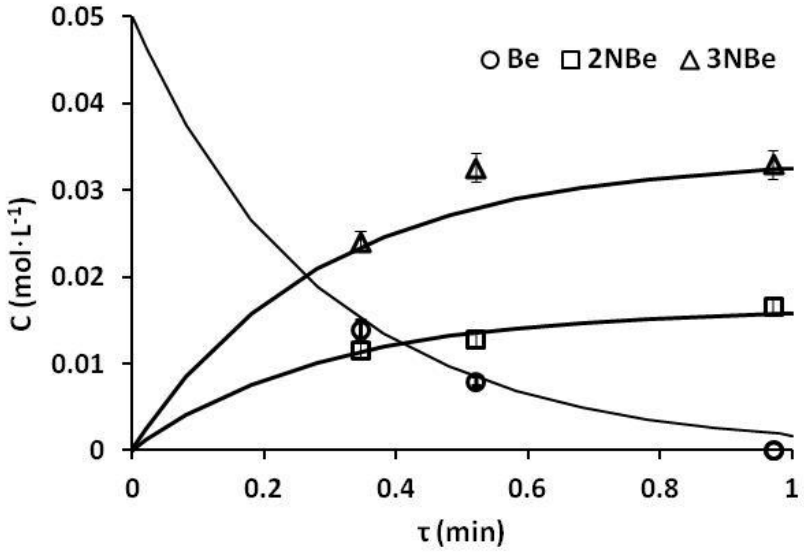

Fig. 9.4. Concentration *vs.* residence time. Predicted (lines) and experimental data (symbols). (Be) benzaldehyde; (2NBe) 2-nitrobenzaldehyde; (3NBe) 3-nitrobenzaldehyde; [HNO_3] = 5.61 mol·L^{-1}; [H_2SO_4] = 9.84 mol·L^{-1}; T = 35.5 °C; [Be]$_0$ = 0.05 mol·L^{-1}.

9.3. Intensification of nitrobenzaldehydes synthesis

9.3.1. Intensification of o-nitrobenzaldehyde synthesis

Using a microreactor it was possible to safely investigate tandem oxidation-nitration reactions in conditions that were impossible to be safely adopted in a batch reactor, namely higher acid concentrations and temperature. Once the model was validated, it was used to find new reaction conditions under which it is possible to maximize 2-nitrobenzaldehyde yield. An upper limit temperature was fixed at 70 °C (dashed vertical line in Fig. 9.5); in fact, for higher temperatures it is impossible to avoid a significant nitric acid decomposition, which is favored by sulfuric acid high concentrations (Di Somma et al., 2014a). Fig. 9.5 shows the predicted and experimental effect of the temperature on 2-nitrobenzaldehyde yield at fixed nitric acid and sulfuric acid molar fraction. As shown, at a fixed mixed acid composition an optimal temperature to maximize ortho-nitrobenzaldehyde yield can be found. This can be seen as the result of two conflicting effects of temperature. In fact, at higher temperature the gap between the formation rate of 3- and 2- nitrobenzaldehyde was reduced according to the estimated kinetic parameters in Chapter 8. However increasing temperature, the equilibrium between

benzaldehyde and the nitronium coordinated form of benzaldehyde is shifted to the former, reducing the influence of the ortho-substituted isomer formation mechanism.

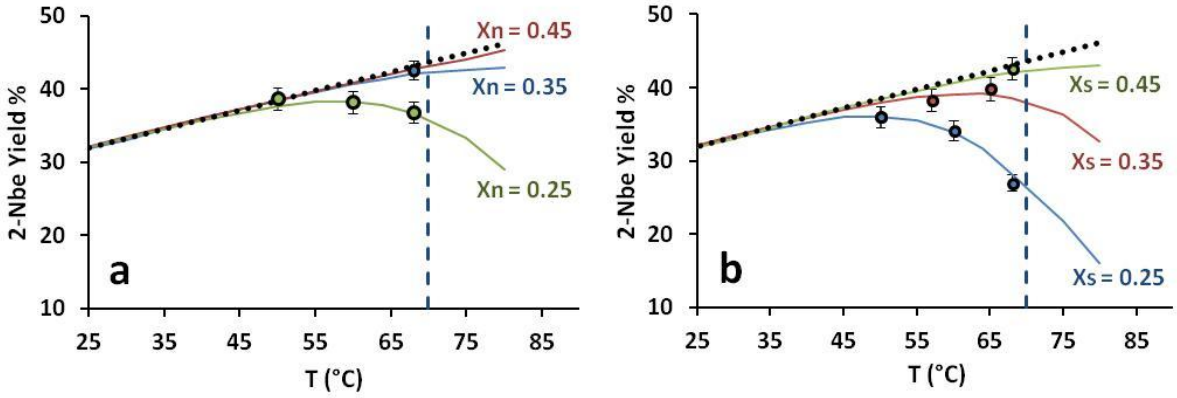

Fig. 9.5. Percentage yield of 2-nitrobenzaldehyde at varying conditions. (a) the effect of nitric acid molar fraction at fixed sulfuric acid molar fraction X_S = 0.45; (b) the effect of sulfuric acid molar fraction at fixed nitric acid molar fraction X_N = 0.35; experimental (symbols) and calculated (lines) data.

As a general result, an increase in acid concentrations shifts the optimum yield to higher temperature. In fact, higher nitronium ion concentrations due to more concentrated acidic media, can compensate for the shift of the abovementioned equilibrium. As reported in Fig. 9.5. the effect of sulfuric acid and nitric acid concentration is qualitatively similar. Moreover, considering the upper limit temperature of 70°C, no significant increase in 2-nitrobenzaldehyde yield can be achieved for nitric acid and sulfuric acid molar fractions higher than X_N = 0.35, and X_S = 0.45, respectively. This upper plateau is highlighted in Fig. 9.5. using dotted black lines. As a result of the presented considerations in the neighborhood of the optimum point, additional experimental runs were carried out under the following conditions: X_N = 0.35 ($[HNO_3]$ = 7.91 mol·L^{-1}); X_S = 0.45 ($[H_2SO_4]$ = 10.17 mol·L^{-1}); T = 68 °C; The nitronium ion concentration was calculated in agreement to the relations presented in Chapter 5, depending on the adopted conditions. It must be noted that under highly acidic conditions no extensive data on the effect of temperature on nitronium ion concentration could be found. As a general result (Albright et al., 1996; Edwards et al., 1994; Edwards et al., 1995), at a fixed mixed acid composition, nitronium ion concentration is reported to decrease when increasing temperature. This is taken into account in equation 5.5 for relatively low concentrated mixed acid, but not in empirical relation 5.2, which was adopted for highly

concentrated mixtures. Few experimental data by Edwards et al. (1994) in the range 20 – 40 °C showed a maximum decrease of nitronium ion concentration of about 9 %. However, in the range of interest it was verified that even doubling the percentage decrease, selectivities to nitrated isomers is only affect for less than 2%, which is lower than the maximum evaluated experimental error related to HPLC measurement. The results of two experimental runs carried out at different organic concentrations are reported in Fig. 9.6. The reaction is very fast and impossible to follow. According to the model prediction complete conversion of benzaldehyde is achieved in less than 60 ms. However, the lowest residence time obtainable with the available equipment was 9 s. As shown, up to 18 s the isomers yields is constant since oxidation reaction are too slow to affect them on this time scale. The average measured 2-nitrobenzaldehyde yield was 41 % and space-time yields were 0.33 and 3.29 $g \cdot L^{-1} \cdot s^{-1}$ for experiments in Fig. 9.6a and 9.6b, respectively. Finally, Fig. 9.6b shows that an increase in the organic concentration up to 0.5 $mol \cdot L^{-1}$ did not significantly affect the two isomers yields. However, it is worth mentioning that, under the higher concentrated conditions, a significant formation of gas bubbles was observed in the microreactor. Even though bubbles were efficiently carried by the liquid steam, their presence will necessarily affect the residence time distribution so that the experimental data attributed to residence times of 9 and 18 s are likely to have shorter residence times. In this specific case, this did not affect yields since they are constant at different times.

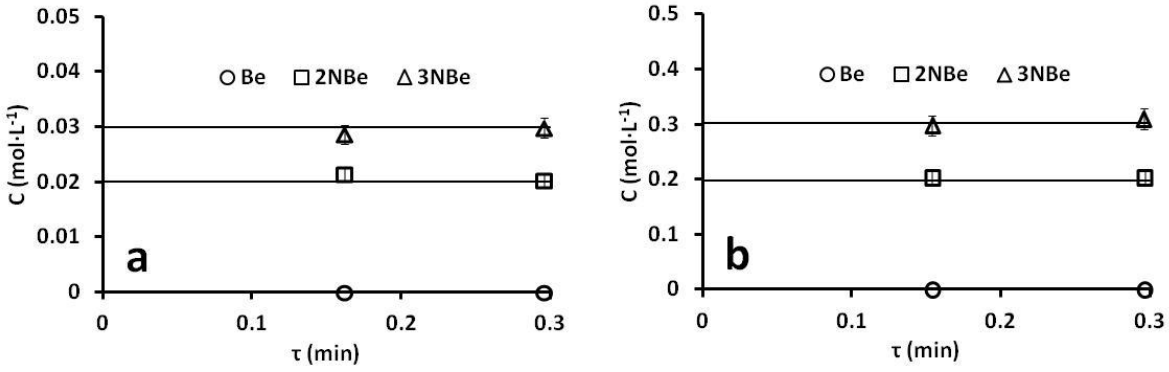

Fig. 9.6. Concentration *vs.* residence time. Predicted (lines) and experimental data (symbols). (Be) benzaldehyde; (2NBe) 2-nitrobenzaldehyde; (3Nbe) 3-nitrobenzaldehyde; $X_N = 0.35$; $X_S = 0.45$; T = 68 °C; $[Be]_0 = 0.05$ $mol \cdot L^{-1}$ (a) and 0.5 $mol \cdot L^{-1}$ (b).

Even though the best results were obtained under the above-mentioned conditions, it is worth noting that relatively high yield of about 38 % was obtained also under milder conditions: X_N = 0.3 ([HNO_3] = 7.41 mol·L^{-1}); X_S = 0.4([H_2SO_4] = 9.88 mol·L^{-1}); T = 52 °C (Fig. 9.7).

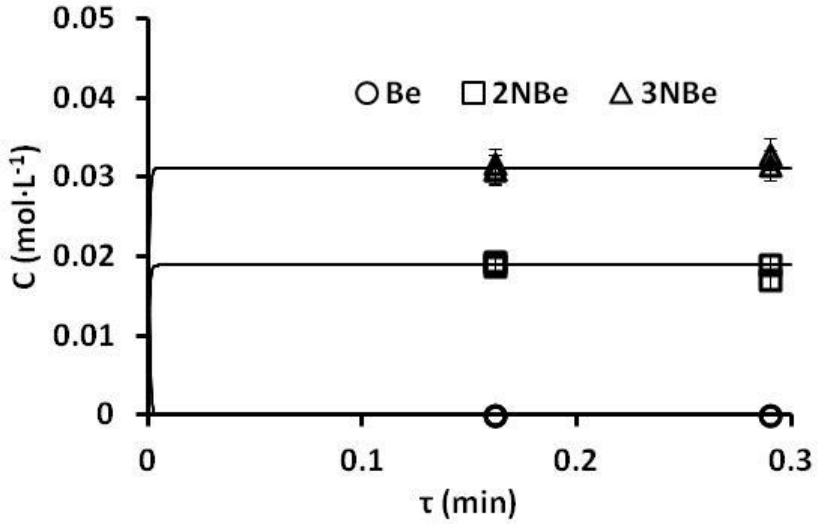

Fig. 9.7. Concentration *vs.* residence time. Predicted (lines) and experimental data (symbols). (Be) benzaldehyde; (2Nbe) 2-nitrobenzaldehyde; (3Nbe) 3-nitrobenzaldehyde; X_N = 0.300; X_S = 0.400; T = 52 °C; [Be]$_0$ = 0.05 mol·L^{-1}.

9.3.2. Intensification of m-nitrobenzaldehyde synthesis

A Matlab optimization routine was also used to find the experimental conditions to maximize 3-nitrobenzaldehyde yield. The optimum conditions, according to predictions, are: X_N = 0.130 ([HNO_3] = 3.90 mol·L^{-1}); X_S = 0.318 ([H_2SO_4] = 9.5453 mol·L^{-1}); T = 68 °C; in these conditions a 96 % yield was measured (Fig. 9.8). Also in this case, relatively high yield of 93 % was measured under milder conditions, namely X_N = 0.134 ([HNO_3] = 3.90 mol·L^{-1}); X_S = 0.35 ([H_2SO_4] = 10.19 mol·L^{-1}); T = 59 °C (Fig. 9.9).

Once defined the optimum conditions, simulations and experimental runs were carried out in order to investigate the behavior of the reacting system in the neighborhood of the local optimum, similarly to the previous presented study carried out for the ortho-substituted isomer. In Fig. 9.10 the maximum predicted yield was plotted against the temperature for different nitrating mixture compositions.

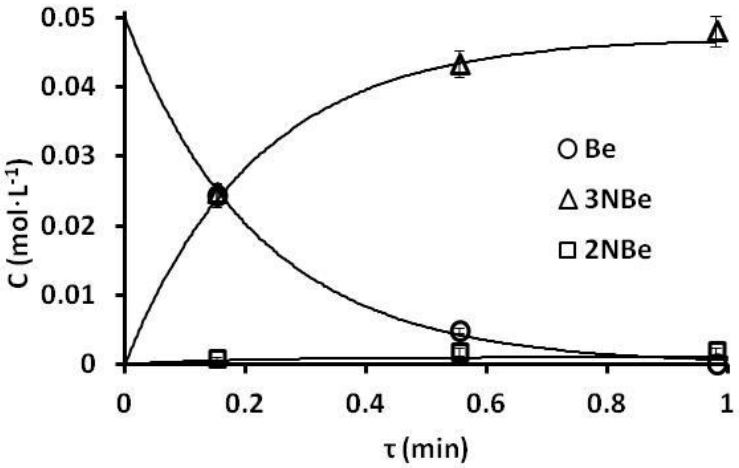

Fig. 9.8. Concentration *vs.* residence time. Predicted (lines) and experimental data (symbols). (Be) benzaldehyde; (2Nbe) 2-nitrobenzaldehyde; (3Nbe) 3-nitrobenzaldehyde; X_N = 0.130; X_S = 0.318; T = 68 °C; $[Be]_0$ = 0.05 mol·L^{-1}.

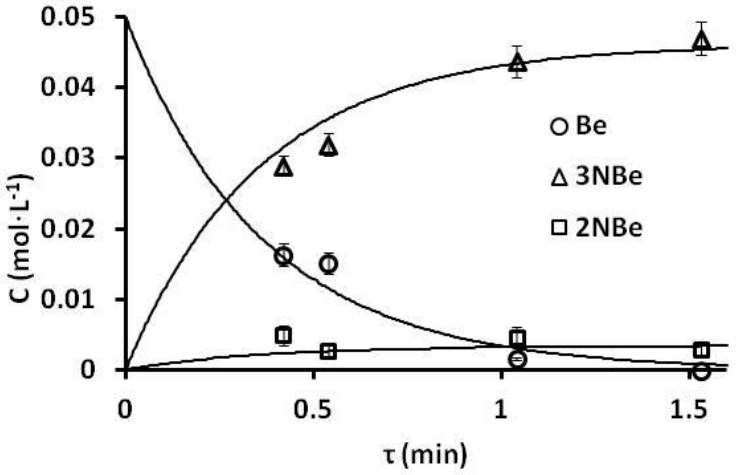

Fig. 9.9. Concentration *vs.* residence time. Predicted (lines) and experimental data (symbols). (Be) benzaldehyde; (2Nbe) 2-nitrobenzaldehyde; (3Nbe) 3-nitrobenzaldehyde; X_N = 0.134; X_S = 0.350; T = 59 °C; $[Be]_0$ = 0.05 mol·L^{-1}.

For less concentrated mixture and lower temperature nitration kinetics are slower and the significant occurrence of oxidation reactions reduce 3-nitrobenzaldehyde yield, being 3-nitrobenzoic acid the oxidation product detected at higher levels. On the contrary, using more acidic nitrating mixtures, 2-nitrobenzaldehyde yield increases, decreasing selectivity to 3-nitrobenzaldehyde. Finally, an increase in temperature, shift the equilibrium between benzaldehyde and its nitronium coordinated form to the former, favoring direct nitration of

the aromatic ring in meta- position. For all the above reasons, the qualitative and quantitative effect of the process variables on the meta-substituted isomer are significantly different from the ones observed in the case of 2-nitrobenzaldehyde. Unlike the ortho-isomer, at a fixed temperature and sulfuric acid molar fraction, a maximum yield can be achieved for an optimum value of nitric acid composition, as presented in Fig. 9.10c. This is in accordance with the previous investigations (Sainz-Diaz, 2002; Di Somma et al., 2014b) that showed a decrease in 3-nitrobenzaldehyde yield, and hence an increase in 2-nitrobenzaldehyde yield, for nitric acid concentrations corresponding to a molar fraction higher than 0.15.

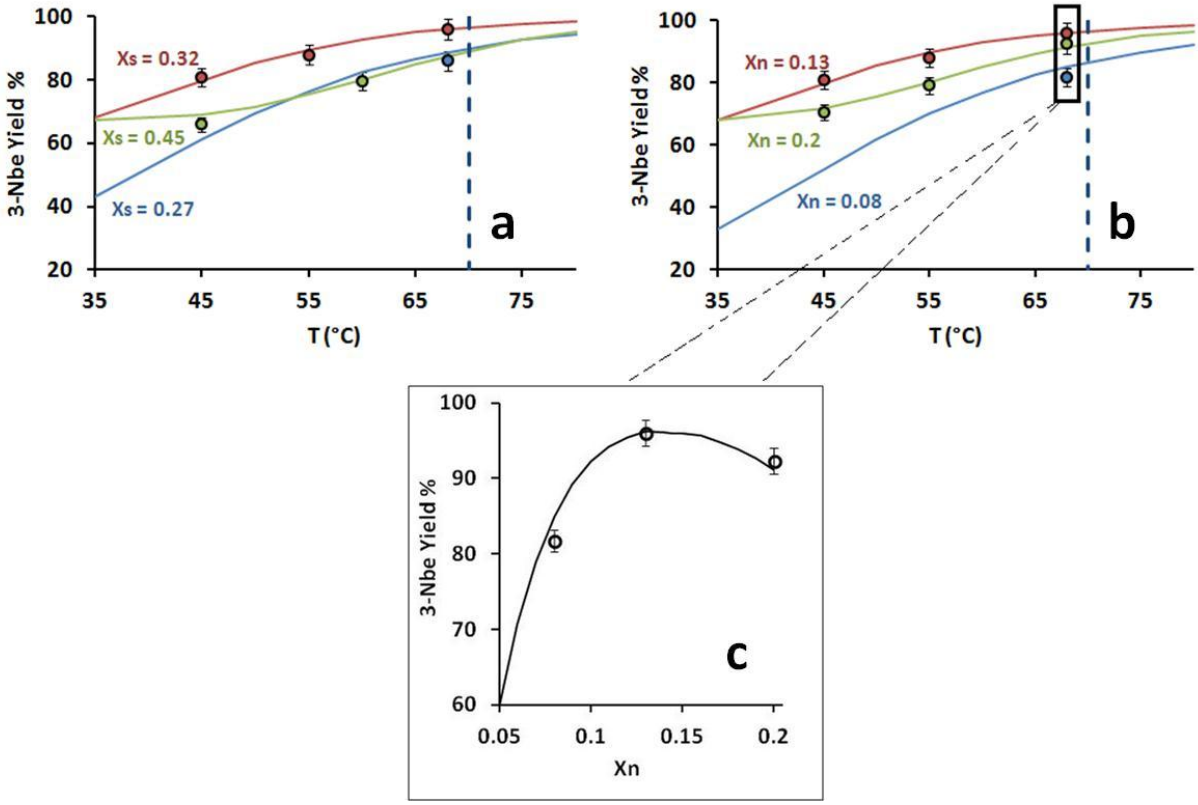

Fig. 9.10. Percentage yield of 3-nitrobenzaldehyde at varying conditions. (a) effect of nitric acid molar fraction at fixed sulfuric acid molar fraction X_S = 0.320; (b) effect of sulfuric acid molar fraction at fixed sulfuric acid molar fraction X_N = 0.130; (c) the effect of nitric acid at fixed X_S = 0.320 and T = 68 °C; experimental (symbols) and calculated (lines) data.

It must be stressed that, contrary to what was found for the ortho-substituted isomer, a full conversion of benzaldehyde, under the optimized conditions, was achieved for higher reaction times. Moreover, the time to achieve the maximum yield was strongly dependent on the adopted conditions. As a result, for lower temperature and acid concentrations, the residence

time necessary to achieve the maximum yield could be increased up to 2 orders of magnitude. Similarly to what was done for 2-nitrobenzaldehyde, some experiments were carried out under the experimental conditions of Fig. 9.8 and 9.9 with higher organic concentrations. In this case, the significant formation of gas bubbles affected the residence times and reduced the conversion of benzaldehyde. Since the gas formation is mainly ascribed to the oxidation reaction of benzyl alcohol, other experiments starting from benzaldehyde under the same experimental conditions were performed. Nevertheless, even though a higher conversion degree was achieved, it was always lower than the one measured for lower organic concentrations (data not shown). This is due to the fact that, in this less acidic media and for slower kinetics, an organic concentration of 0.5 $mol \cdot L^{-1}$ resulted in a liquid-liquid heterogeneous flow. Benzaldehyde is poorly soluble in the aqueous acidic phase and the conversion of benzaldehyde is limited by the solubility of the organic in the aqueous phase and the mass transfer between immiscible phases. It is worth noting that for the above described heterogeneous liquid-liquid phase experiments the average percentage selectivity was about 96 %, even though the conversion degree was lower. This is in agreement with the results obtained in homogeneous phase, since selectivity coincide with yield for a unitary conversion degree. The measured selectivities are reported in Table 9.1. In conclusion, under heterogeneous conditions, it is possible to conveniently carry out the reaction, but providing for higher residence times, that is equivalent to use higher volume microreactors to not reduce the inter-phase mass transfer and the productivity.

Run	**1**	**2**	**3**	**4**	**5**	**6**	**7**	**8**	**9**	**10**
Selectivity (%)	95.5	92.4	95.1	97.9	94.5	97.4	97.2	97.8	97.2	97.7

Table. 9.1. 3-nitrobenzaldehyde selectivities under heterogeneous conditions. X_N = 0.130; X_S = 0.318; T = 68 °C; C_0: 0.3 – 0.5 $mol \cdot L^{-1}$.

10. Conclusions

In this thesis, an extensive investigation of the production of nitrobenzaldehydes starting from benzyl alcohol and/or benzaldehyde is provided, as well as a deeper investigation on more general kinetic aspects concerning nitrations in mixed acid.

As a result, in the light of the previous works, a unitary vision of the problem of the determination of nitronium ion concentration in mixed acid was presented and practical empirical and semi-empirical approaches were provided to predict its concentration in a wide range of normally employed ternary aqueous mixtures of nitric and sulfuric acids in nitrations. The empirical approach was combined with a more rigorous simplified equilibrium model, based on the experimental evidence, to predict the speciation of the acids in mixtures at varying conditions, including the presence of nitrate and bisulphate ions. The results were in accordance with the previous investigations as well as with the successive results of this thesis. Even though the simplified approach is useful in verifying hypothesis and developing reliable integrated complex kinetic models, a further effort is recommended in the future to develop more rigorous and comprehensive equilibrium model, capable of reproducing experimental data in the whole range of concentrations. Despite the already published papers working in this direction, the identification of the parameters of complex models, i.e. Pitzer, eNRTL, *et cetera*, for a comprehensive description of such a common industrial reaction media is still an important object of study.

The results of this investigation were successfully used to develop kinetic models for benzyl alcohol oxidation and benzaldehyde nitration in mixed acid and could be of great importance in the description of other organic substrates reactions in such a media.

The development of kinetic models clarified the role of specific chemical intermediates in the mechanism of benzyl alcohol oxidation and benzaldehyde nitration by nitric acid. Specifically, benzyl nitrite formation was found to be in accordance with the experimental results obtained for benzyl alcohol oxidation. Moreover, the coordination of nitronium ion on the aldehydic group of benzaldehyde was found to be the only and preponderant effective mechanism for 2-nitrobenzaldehyde formation in mixed acid. The clarification of the formation pathway of the ortho-isomer, as well as the developed kinetic model, allowed to predict the conditions under which this mechanism could be either enhanced or inhibited. The experimental runs confirmed the predictions and the yields of nitrobenzaldehydes were significantly increased. However, harsher reaction conditions, namely higher temperature and

acids concentrations, were required for nitrobenzaldehydes synthesis intensification. The safety issues related to the managing of a tandem oxidation-nitration process carried out under atypical harsher conditions were successfully overcome with the adoption of commercially available microreactor devices. Using a microreactor, the reaction was easily and safely carried out under both homogeneous and heterogeneous conditions with exceptionally low residence times. This is a promising indication for highly priced materials productions, e.g. pharmaceutical drugs, since different scaled-up versions of the adopted device, with similar functionalities, are commercially available.

Finally, promising results were obtained when extending the kinetic model to the description of nitrobenzaldehydes formation under heterogeneous conditions. As a future recommendation, the development of a thermodynamic models for the prediction of organics solubility in mixed acid would be a surely useful tool in the heterogeneous phase reaction modeling.

Further future investigations should be devoted to a better characterization of the reacting system behavior under heterogeneous conditions in both batch and continuous reactors, also under non-isothermal conditions, to identify the limitations due to the interphase mass transfer. Preliminary investigations carried out in this regard, suggested that the adoption of microreactors could significantly enhance interphase mass transfer and perform under quasi-kinetic regime, which is rarely achieved in industrial-scale batch reactors.

Beyond the specific results obtained for the particular investigated chemical system, the kinetic modeling under homogeneous conditions, its extension to heterogeneous systems and the combination of the results for the process intensification in microreactors could represent a future benchmark as a characterization protocol, particularly suitable for the managing of hazardous reactions for pharmaceuticals and other low-throughput productions of highly priced materials.

References

Abubshait, S.A., Kassab, R.R., Al-Shehri, A.H., Abubshait, H.A, 2011. Synthesis and reactions of some novel 4-biphenyl-4-(2H)-phthalazin-1-one derivatives with an expected antimicrobial activity, Journal of Saudi Chemical Society 15, 59-65.

Aellig, C., Girard, C., Hermans, I., 2011. Aerobic alcohol oxidations mediated by nitric acid, Angew. Chem. Int. Ed. 50 (2011), 12355-12360.

Aellig, C., Neuenschwander, U., Hermans, I., 2012. Acid-catalyzed decomposition of the benzyl nitrite intermediate in HNO3-mediated aerobic oxidation of benzyl alcohol, Chem. Cat. Chem 4, 525-529.

Albright, L.F., Sood, M.K., Eckert, R.E., 1996. Modeling nitronium ion concentrations in HNO_3-H_2SO_4-H_2O mixtures. ACS Symposium Series. Washington DC.

Allinger, N.L., Cava, M.P., De Jongh, D.C., Johnson, C.R., Lebel, N.A., Stevens, C.L., 1972. Organic Chemistry. Worth Publishers, Inc.

Andreozzi, R., Aquila, T., Caprio, V., Insola, A., 1992. Adiabatic calorimetry for safety studies in nitration processes. Thermochimica Acta 199, 159-164.

Andreozzi, R., Marotta, R., Sanchirico, R., 2002. Thermal decomposition of acetic anhydride – nitric acid mixtures. Journal of Hazardous Materials 90, 111-121.

Andreozzi, R., Canterino, M., Caprio, V., Di Somma, I., Sanchirico, R., 2006. Salicylic acid nitration by means of nitric acid/acetic acid system: chemical and kinetic characterization. Organic Process Research & Development 10(6), 1199-1204.

Antes, J., Boskovic, D., Krause, H., Loebbecke, S., Lutz, N., Tuercke, T., Schweikert, W., 2003. Analysis and improvement of strong exothermic nitrations in microreactors. Chemical Engineering Research and Design 81(7), 760-765.

Arnett, E.M., Quirk, R.P., Burke, J.J., 1970. Weak bases in strong acids. III. Heat of ionization of amines in fluorosulfuric and sulfuric acids. A new general basicity scale.

Ball, R., Gray, B.F., 2013. Thermal instability and runaway criteria: the dangers of disregarding dynamics. Process Safety and Environmental Protection 91, 221-226

Barton, J.A., Nolan, P.F., 1989. Incidents in the chemical industry due to thermal-runaway chemical reactions. IChemE Symposium series no. 115, 3-17.

Barton, J., Rogers, R., 1997. Chemical Reaction Hazards: a guide to safety. Second Edition. Institution of Chemical Engineers. Warwickshire, UK.

Bernhardt, G., Petersen, E.N., Daum, G., 1979. Dynamit Nobel, DE-OS 2948058 Patent.

Bollas, G.M., Chen, C.C., Barton, P.I., 2008. Refined electrolyte-NRTL model: activity coefficient expressions for application to multi-electrolyte systems. AIChE Journal 54(6), 1608-1624.

Booth, G., 2003. Nitro Compounds, aromatic. Ullmann's Encyclopedia of Industrial Chemistry, Wiley-VCH.

Bretherick, L., 1990. Handbook of reactive chemical hazards, Butterworths, London.

Bruhne, F., 2003. Nitro Compounds, aromatic. Ullmann's Encyclopedia of Industrial Chemistry, Wiley-VCH.

Burns, J.R., Ramshaw, C., 2002. A microreactor for the nitration of benzene and toluene. Chemical Engineering Communications 189 (12).

Cantillo, D., Damm, M., Dallinger, D., Bauser, M., Berger, M., Kappe, C.O., 2014. Sequential Nitration/Hydrogenation Protocol for the Synthesis of Triaminophloroglucinol: Safe Generation and Use of an Explosive Intermediate under Continuous-Flow Conditions. Organic Process Research & Development 18(11), 1360-1366.

Cardillo, P., Girelli, A., 1982. Rivista dei Combustibili 36, 304-309.

Chandrasekar, D., Madhusudhana, K., Ramakrishna, S., Diwan, P.V., 2006. Determination of DPPH free radical scavenging activity by reverdes-phase HPLC: a sensitive screening method for polyherbal formulations. Journal of Pharmaceutical and Biomedical Analysis 40, 460-464.

Chen, C.Y., Wu, C.W., 1996. Thermal hazard aseessment and macrokinetics analysis of toluene mononitration in a batch reactor. Journal of Loss Prevention in the Process Industries 9(5), 309-316.

Chen, C.Y., Wu, C.W., Duh, Y.S., Yu, S.W., 1998. An experimental study of worst case scenarios of nitric acid decomposition in a toluene nitration process. Safety and Environmental protection 76, 211-216.

Chen, C.C., Song, Y., 2004. Generalized electrolyte-NRTL model for mixed-solvent electrolyte systems. AIChE Journa 50(8), 1928-1941.

Chen, L.P., Liu, T.T., Yang, Q., Chen, W.H., 2012. Thermal hazard evaluation for iso-octanol nitration with mixed acid. Journal of Loss Prevention in the Process Industries 25, 631-635.

Chen, C.-C., Wang, M., Yu, Y., 2016a. Modeling mixed-solvent electrolyte systems. Chemical Engineering Progress 112(2).

Chen, L., Zhou, Y., Chen, W., Yang, T., Xu, S., Rao, G., 2016b. T_{cf} and MTSR of toluene nitration in mixed acid. Chemical Engineering Transactions 48, 601-606.

Cherlo, S.K., Sreenath, K., Pushpavanam, S., 2009. Screening, selecting, and designing microreactors. Industrial & Engineering Chemistry Research 48, 8678-8684.

Chigorina, E.A., 2014. 1-cyanoacetyl-3,5-dimethylpyrazole, Synlett 25, 453-454.

Cho, S.G., No, K.T., Goh, E.M., Kim, J.K., Shin, J.H., Joo, Y.D., Seong, S., 2005. Optimization of neural networks architecture for impact sensitivity of energetic molecules. Bulletin of the Korean Chemical Society 26(3), 399-408.

Choudhary, V.R., Chaudhari, P.A., Narkhede, V.S., 2003. Solvent-Free Liquid-Phase Oxidation of Benzyl Alcohol to Benzaldehyde by Molecular Oxygen Using Nonnoble Transition Metal Containing Hydrotalcite-like Solid Catalysts. Catalysis Communications 4, 171-175.

Copelli, S., Derudi, M., Cattaneo, C.S., Nano, G., Raboni, M., Torretta, V., Rota, R., 2014. Synthesis of 4-chloro-3-nitrobenzotrifluoride: industrial thermal runaway simulation due to cooling system failure. Process Safety and Environmental Protection 92(6), 659-668.

Dakka, J., 1988. HBR Acid-Catalyzed Oxidation of Benzyl Alcohols by H2O2. Bulletin de la Societe Chimique de France 4, 756.

Das, B., Mondal, P., Kumar, S., 2011. Pressurization studies in a sealed autoclave for thermal decomposition of nitrated TBP and TiAP. Journal of Radionalytical and Nuclear Chemistry 288, 641-643.

Davey, W., Gwilt, J.R., 1950. The preparation of mononitrobenzaldehydes, Journal of the Chemical Society 204, 204-208.

Davis, W., De Bruin, H.J., 1964. New activity coefficients of 0-100 per cent aqueous nitric acid. Journal of Inorganic and Nuclear Chemistry 26(6), 1069-1083.

Deno, N.C., Peterson, H.J., Sacher, E., 1961. Nitric acid equilibria in water-sulphuric acid. The Journal of Physical Chemistry 65, 199-201.

di Miceli Raimondi, N., Olivier-Maget, N., Gabas, N., Cabassud, M., Gourdon, C., 2015. Safety enhancement by trans position of the nitration of toluene from semi-batch reactor to continuous intensified heat exchanger reactor. Chemical Engineering Research and Design 94, 182-193.

Di Somma, I., Marotta, R., Andreozzi, R., Caprio, V., 2012. Kinetic and safety characterization of the nitration process of methyl benzoate in mixed acid. Organic Process Research & Development 16(12), 2001-2007.

Di Somma, I., Marotta, R., Andreozzi, R., Caprio, V., 2014a. Nitric acid decomposition kinetics in mixed acid and their use in the modelling of aromatic nitration. Chemical Engineering Transactions 36, 127-132.

Di Somma, I., Marotta, R., Andreozzi, R., Caprio, V., 2014b. Increasing yield os 2-nitrobenzaldehyde during benzaldehyde nitration by mixed acid: chemical and safety investigation. Chemical Engineering Transactions 36, 181-186.

Di Somma, I., Russo, D., Andreozzi, R., Marotta, R., Guido, S., 2017. Kinetic modelling of benzyl alcohol selective oxidation in aqueous misture of nitric and sulfuric acids. Chemical Engineering Journal 308, 738-744.

de Queiroz, J.F., Carneiro, J.W.., Sabino, A.A., Sparrapan, R., Eberlin, M.N., Esteves, P.M., 2006. Electrophilic aromatic nitration: understanding its mechanism and substituent effects. The Journal of Organic Chemistry 71(16), 6192-6203.

Ducry, L., Roberge, D.M., 2005. Controlled autocatalytic nitration of phenol in a microreactor. Angewandte Chemie 117(48), 8186-8189.

Edwards, H.G.M., Fawcett, V., 1994. Quantitative Raman spectroscopic studies of nitronium ion concentrations in mixtures of sulphuric and nitric acids. Journal of Molecular Structure 326, 131-143.

Edwards, H.G.M., Turner, J.M., Fawcett, V., 1995. Raman spectroscopic study of nitronium ion formation in mixtures of nitric acid, sulfuric acid and water. Journal of the Chemical Society, Faraday Transactions 91(10), 1439-1443.

Ertel, W., 1978. Bayer, DE-OS 2808930 Patent.

Ertel, W., 1991. Bayer, US Patent

Etchells, J.C., 1997. Why reactions run away. Organic Process Research & Development 1(6), 435-437.

Fraenkel, D., 2015. Sctructure and ionization of sulfuric acid in water. New Journal of Chemistry 39, 5124-5136.

Galabov, B., Nalbantova, D., Schleyer, P., Schaefer, H.F., 2016. Electrophilic aromatic substitution: new insights into an old class of reactions. Accounts of Chemical Research 49(6), 1191-1199.

Gasparrini, F., Giovannoli, M., Misiti, D., 1988. Nitric acid facile oxidation of mono and diarylcarbinols to carbonyl compounds in a biphasic system, Synth. Commun. 18, 69.

Gosteli, J., 1977. Ciba-Geigy, DE-OS 2829346 Patent.

Grewer, T., Rogers, R., 2015. Thermal hazards of chemical reactions. Second Edition. Vol. 4. Industrial Safety Series, Elsevier.

Gygax, R., 1988. Chemical reaction engineering for safety. Chemical Engineering Science 43(8), 1759-1771.

Gu, Y., Zhang, J., Duan, Z., Deng, Y., 2005. Pechmann reaction in non-chloroaluminate acidic ionic liquid under solvent-free conditions. Advanced Synthesis & Catalysis 347(4), 512-516.

Gustin, J.L., 1993. Thermal stability screening and reaction calorimetry. Application to runaway reaction hazard assessment and process safety management. Journal of Loss Prevention in the Process Industries 6(5), 257-291.

Gustin, J.L., 1998. Runaway reaction hazards in processing organic nitro compounds. Organic Process Research & Development 2, 27-33.

Hagedorn, F., Imre, L., Wedemeyer, K., 1978. Bayer, DE-OS 2805402 Patent.

Halder, R., Lawal, A., Damavarapu, R., 2007. Nitration of toluene in a microreactor. Catalysis Today 125(1-2), 74-80.

Hammett, L.P., Feyrup, A.J., 1932. A series of simples base indicators. I. The acidity functions of mixtures of sulfuric and perchloric acids with water. Journal of the American Chemical Society 54, 2721-2739.

Hammett, L.P., Paul, M.A., 1934. The relation between the rates od some acid catalyzed reactions and the acidity function, H_0. Journal of the American Chemical Society 56(4), 830-832.

Hoggett, J.G., Moodie, R.B., Penton, J.R., Schofield, K., 1971. Nitration and aromatic reactivity. Cambridge University Press, Rhadon.

Huang, X.I.A.N., Chan, C.C., 1982. Synthetic and Applications of Bis[benzyltriethylammonium] Dichromate: A New Selective Oxidation Reagent. Synthesis 1091.

Hughes, E.D., Ingold, C.K., Reed, R.I., 1950. Kinetics and mechanism of aromatic nitration. Part II. Nitration by the nitronium ion, NO_2^+, derived from nitric acid. Journal of the Chemical Society 0, 2400.

Joshi, S.R., Kataria, K.L., Sawant, S.B., Joshi, J.B., 2005. Kinetics of oxidation of benzyl alcohol with dilute nitric acid. Industrial & Engineering Chemistry Research 44, 325-333.

Johnson, C.D., Katritzky, A.R., Shakir, N., Viney, M., 1967. The mechanism of the electrophilic substitution of heteroarometic compouns. Part VIII. The α-, β- and γ-nitration of pyridine 1-oxides. Journal of the Chemical Society B, 1213-1219.

Kawamoto, H., Saito, S., Hatanaka, W., Saka, S., 2007. Catalytic pyrolisis of cellulose in sulfolane with some acidic catalysts. Journal of Wood Science 53, 127-133.

Khudhairy, D., Zaldivar, J.M., 1989. Activity coefficients in HNO_3-H_2SO_4-H_2O mixtures. Commission of European Communities, Joint Research Centre – Ispra Sita. Technical note I.89.90.

Klais, O., Hoffmann, H., Naing, E.K., 2009. Nitration of alkyl benzoates with mixed acid. Chemical Engineering & Technology 32(2), 319-327.

Knapkiewicz, P., 2013. The silicon-glass microreactor with embedded sensors-technology and results of preliminary qualitative tests, toward intelligent microreaction plant. Journal of Micromrchanics and Microengineering 23.

Kockmann, N., Roberge, D.M., 2009. Harsh reaction conditions in continuous-flow microreactors for the pharmaceutical production. Chemical Engineering & Technology 32, 1682-1694.

Koleva, G., Glabov, B., Hadjieva, B., Schaefer, H.F., Schleyer, P., 2015. An expretimentally established key intermediate in benzene nitration with mixed acid. Angewandte Chemie International Edition 54(47), 14123-14127.

Kotoyoti, T., 1991. Investigation of a thermal runaway reaction involving a nitration process. Journal of Loss Prevention in the Process Industries 4, 120-124.

Kowalczyk, B.A., Roberts, P.N., McEwen, G.K., Robinson, J., 1997. Scale-up of the nitration of 1-acetyl-3,4-dichloro-1,2-(ethylenedioxy)benzene using nitric acid/trifluoroacetic acid. Organic Process Research & Development 1, 355-358.

Kroschwitz, J.I., Kirk, O, 1992. Encyclopedia of Chemical Technology, 4th ed, Wiley-Interscience, New York, Vol. 4, 64-72.

Kulkarni, A.A., Nivangune, N.T., Kalyani, V.S., Joshi, R.A., Joshi, R.R., 2008. Continuous flow nitration of salicylic acid. Organic Process Research & Development 12(5), 995-1000.

Kulkarni, A.A., Kalyani V.S., Joshi, R.A., Joshi, R.R, 2009. Continuous flow nitration of benzaldehyde. Organic Process Research & Development 13, 999-1002.

Kulkarni, A.A., 2014. Continuous flow nitration in miniaturized devices. Beilstein Journal of Organic Chemistry 10, 405-424.

Lee, G.A., Freedman, H.H., 1976. Phase Transfer Catalyzed Oxidations of Alcohols and Amines By Aqueous Hypochlorites. Tetrahedron Letters 20, 1641.

Li, L., Yao, C., Jiao, F., Han, M., Guangwen, C., 2017. Experimental and kinetic study of the nitration of 2-ethylhexanol in capillary microreactors. Chemical Engineering & Processing: Process Intesification 117, 179-185.

Li, W.S., Liu, L.K., 1989. A Convenient Oxidation of Benzylic Methyl, Methylene, and Methine Groups with Potassium Permanganate/Triethylamine Reagent. Synthesis 293.

Liu, X., Qui, A., Sawyer, D.A., 1993. The Bis(bipyridine)copper-(II)-Induced Activation of Dioxygen for the Catalytic Dehydrogenation of Alcohols. Journal of the American Chemical Society 115, 3239.

Lowe, H., Wei, G., Jiang, M., Hofmann, C., Kost, H.J., Schutt, C., 2012. Multi-step processing in a microstructured flow reactor: direct nitration of propane – a proof of principle. Green Processing and Synthesis 1, 439-448.

Lunghi, A., Alos, M.A., Gigante, L., Feixas, J., Sironi, E., Feliu, J.A., Cardillo, P., 2002. Identification of the decomposition products in an industrial nitration process under thermal runaway conditions. Organic Process Research & Development 6(6), 926-932.

Maddirala, A.R., Andreana, P.R., 2016. Synthesis of 3-substituted 2-indolinones by a multicomponent coupling isocyanide-dependent microwave-assisted intramolecular transamidation process, European Journal of Organic Chemistry, 196-209

Maestri, F., Dionigi, L.R., Rota, R., Gigante, L., Lunghi, A., Cardillo, P., 2006. Safe and productive operation of homogeneous semibatch reactors. II. The nitration of N.(2-phenoxyphenyl) methane sulphonamide. Industrial & Engineering Chemistry Research 45, 8014-8023.

Maestri, F., Copelli, S., Rota, R., 2009. Simple procedure for optimal scale-up of fine chemical processes. II. Nitration of 4-chlorobenzotrifluoride. Industrial & Engineering Chemistry Research 48, 1316-1324.

Markofsky, S.B., 2003. Nitro Compounds, aliphatic. Ullmann's Encyclopedia of Industrial Chemistry, Wiley-VCH.

Marziano, N.C., Cimino, G.M., Passerini, R.C., 1973. The M_C activity coefficient function for acid-base equilibria. Part I. New methods for estimating pKa values for weak bases. Journal of the Chemical Society, Perkin Transactions 2, 1915-1922.

Marziano, N.C., Traverso, P.G., Cimino, G.G., 1980. Thermodynamic nitration rates of aromatic compounds. Part 1. The nitration of benzene and some benzene derivatives in aqueous sulphuric and perchloric acids. A comparison of the results referred to water as standard state. Journal of the Chemical Society, Perkin Transactions 2, 574-578.

Marziano, N.C., Tomasin, A., Traverso, P.G., 1981. The M_C activity coefficient function for acid-base equilibria. Part 5. The M_C activity coefficient for a reliable estimate of thermodynamic values. Journal of the Chemical Society, Perkin Transactions 2 7, 1070-1075.

Marziano, N.C., Sampoli, M., Gonizzi, M., 1986. On the Mc activity coefficient function describing solute and solvent equilibria: methanesulfonic acid aqueous solutions. The Journal of Physical Chemistry 90(18), 4347-4353.

Marziano, N.C., Tomasin, A., Sampoli, M., 1991a. Nitric acid equilibrium in concentrated trifluoromethanesulfonic acid studied by Raman spectroscopy. Journal of the Chemical Society, Perkin Transactions 2, 1995.1998.

Marziano, N.C., Tomasin, A., Tortato, C., 1991b. Equilibria and nitration of sulphonic acids in concentrated sulphuric acid. Journal of the Chemical Society, Perkin Trasactions 2, 1575-1580.

Marziano, N.C., Tortato, C., Ronchin, L., Martini, F., Bianchi, C., 1999. On the acidity of liquid and solid catalysts. Part 2. A thermodynamic and kinetic study for acid-catalysed nitrations. Catalysis Letters 58, 81-87.

Medard, L.A., 1989. Accidental explosions. Ellis Horwood Limited. Chichester, England.

McMullen, J.P., Jensen, K.F., 2010. Integrated microreactors for reaction automation: new approaches to reaction development. Annual Review of Analytical Chemistry 3, 19-42.

Minkwitz, R., Seelbinder, R., Schobel, R., 2002. Protonated sulfuric acid: preparation of trihydroxyoxosulfonium hexafluoroantimonate $H_3SO_4^+SbF_6^-$. Angewandte Chemie International Edition 41(1), 111-114.

Minogue, N., Riordan, E., Sodeau, J.R., 2003. Raman spectroscopy as a probe of low-temperature ionic speciation in nitric acid and sulfuric acid stratospheric mimic systems. The Journal of Physical Chemistry A 107, 4436-4444.

Mitscherlich, E., 1834. Annalen der Physik un Chemie 31, 625; 12, 305.

Morimoto, T., Hirano, M., Aikawa, Y., Zhang, X., 1988. Ready Oxidation of Alcohols to Carbonyl Compounds by Sodium Bromite in Methylene Dichloride in the Presence of Aluminium Oxide. Journal of the Chemical Society, Perkin Transactions 1, 2423.

Mosier, N.S., Ladisch, C.M., Ladisch, M.R., 2002. Characterization of acid catalytic domains for cellulose hydrolysis and glucose degradation. Biotechnology and Bioengineering 79(6), 610-618.

Neelakandan, K., Manikandan, H., Prabhakaran, B., Santosha, N., Chaudhari, A., Kulkarni, M., Mannathusamy, G., Titirmare, S., 2014. Synthesis, isolation and use of a common key intermediate for calcium antagonist inhibitors. Der Pharmacia Sinica, 5(1), 11-17.

Nemethne-Sovago, J., Benke, M., 2014. Microreactors: a new concept for chemical synthesis and technological feasibility (review). Materials Science and Engineering 39, 89-101.

Nishiguchi, T., Okamoto, H., 1990. Oxidation of ethers by nitrous dioxide in the presence of silica gel. Chemical Communications 22, 1607-1608.

Ogata, Y., Sawaki, Y., Matsunaga, F., Tezuka, H., 1966. Kinetics of the nitric acid oxidation of benzyl alcohols to benzaldehydes. Tetrahedron 22, 2655-2664.

Olah, G.A., 1971. Aromatic substitution. XXVIII. Mechanism of electrophilic aromatic substitutions. Accounts of Chemical Research 4(7), 240-248.

Olah, G.A., Malhotra, R., Narang, S.C., 1989. Nitration methods and mechanisms. VCH. New York.

Panke, G., Schwalbe, T., Stimer, W., Taghavi-Moghadam, S., Wille, G., A practical approach of continuous processing to high energetic nitration reactions in microreactors. Synthesis, 2827-2830.

Patil, L.K., Gaikar, V.G., Kumar, S., Mudali, U.K., Natarajan, R., 2012. Thermal decomposition of nitrated tri-n-butyl phosphate in a flow reactor. ISRN Chemical Engineering.

Perrin, D.D., 1982. Ionisation constants of inorganic acids and bases in aqueous solution. International Union of Pure and Applied Chemistry, second edition, Pergamon Press, 76.

Redlich, O., Duerst, R.W., Merbach, A., 1968. Ionization of strong electrolytes. XI. The molecular states of nitric acid and perchloric acid. The Journal of Chemical Physics 49, 2986–2994.

Roberge, D.M., Ducry, L., Bieler, N., Cretton, P., Zimmermann, B., 2005. Microreactor technology: a revolution for the fine chemical and pharmaceutical industries?. Chemical Engineering & Technology 28, 318-323.

Roberge, D.M., Zimmermann, B., Rainone, F., Gottsponer, M., Eyholzer, M., Kockmann, N., 2008. Microreactor technology and continuous processes in the fine chemical and pharmaceutical industry: is the revolution underway?. Organic Process Research & Development 12, 905-910.

Roberge, D.M., Gottsponer, M., Eyholzer, M., Kockmann, N., 2009. Industrial design, scale-up, and use of microreactors. Chemistry Today 27, 8-11.

Robertson, E.B., Dunford, H.B., 1964. The state of the proton in aqueous sulfuric acid. Journal of the American Society 86(23), 5080-5089.

Ross, D.S., Gu, C.L., Hum, G.P., Malhotra, R., 1986. Oxidation of benzyl alcohols by nitrous and nitric acids in strong sulfuric acid media. International Journal of Chemical Kinetics 18, 1277-1288.

Russo, D., Onotri, L., Marotta, R., Andreozzi, R., Di Somma, I., 2017a. Benzaldehyde nitration by mixed acid under homogeneous condition: a kinetic modeling. Chemical Engineering Journal 307, 1076-1083.

Russo, D., Di Somma, I., Marotta, R., Tomaiuolo, G., Andreozzi, R., Guido, S., Lapkin, A.A., 2017b. Intensification of nitrobenzaldehydes synthesis from benzyl alcohol in a microreactor. Organic Process Research & Development 21(3), 357-364.

Saada, R., Patel, D., Saha, B., 2015. Causes and consequences of thermal runaway incidents – will they ever be avoided?. Process Safety and Environment Protection 97, 109-115.

Sainz-Diaz, C.I., Hernandez-Laguna, A., 1999. Trans-2,2’-dinitrostilbene as a precursor of o-nitrobenzaldehyde, a key intermediate for pharmaceuticals: reactivity and molecular structure studies, Journal of Chemical Society, Perkin Transaction 2, 1489-1496.

Sainz-Diaz, C.I., 2002. A new approach to the synthesis of 2-nitrobenzaldehyde. Reactivity and molecular structure studies, Monatshefte fur Chemie 133, 9-22.

Sampoli, M., De Santis, A., Marziano, N.C., 1985a. On the relationship between the dissociation of indicators in non-ideal acid solution and the dissociation of the acid itself. Journal of the Chemical Society, Chemical Communications, 110-111.

Sampoli, M., De Santis, A., Marziano, N.C., Pinna, F., Zingales, A., 1985b. Equilibria of nitric acid in sulfuric and perchloric aid at 25 °C by Raman and UV Spectroscopy. The Journal of Physical Chemistry 89, 2864-2869.

Santaniello, E., Milani, F., Casati, R., 1983. Tetrabutylammonium Chlorochromate, a new mild and selective oxidizing agent. Synthesis 749.

Sato, K., Aoki, M., Takgi, J., Noyori, R., 1997. Organic Solventand Halide-Free Oxidation of Alcohols with Aqueous Hydrogen Peroxides. Journal of the American Chemical Society 119, 12386.

Sauer, W., Goldner, H., Heidrich, H.J., Faust, G., Fiedler, W., Carstens, E., Heine, G., 1976. VEB Arzneimittelwerk Dresden, DE-OS 2708115 Patent.

Schofield, K., 1981. Aromatic nitration. Cambridge University Press.

Sebej, P., Solomek, T., Hroudnà, L., Brancovà, P., Klàn, P., 2009. Photochemistry of 2-Nitrobenzylidene Acetals, The Journal of Organic Chemistry 74, 8647-8658.

Semmelhack, M.F., Schmid, C.R., Cortes, D.A., Chou, C.S., 1984. Oxidation of Alcohols to Aldehydes with Oxygen and Cupric Ion, Mediated by Nitrosonium Ion. Journal of the American Chemical Society 106, 3374.

Shin, T.R., Jung, S.M., Jeon, I.Y., Baek, J.B., 2013. The oxidation mechanism of highly ordered pyrolytic graphite in a nitric acid/sulfuric acid mixture. Carbon 52, 493-498.

Song, Y., Chen, C.C., 2009. Symmetric electrolyte nonrandom two-liquid activity coefficient model. Industrial & Engineering Chemistry Research 48, 7788-7797.

Squadrito, G.L., Pryor, W.A., 1998. Oxidative chemistry of nitric oxide: the roles of superoxide, peroxynitrite, and carbon dioxide. Free Radical Biology and Medicine 25(4-5), 392-403.

Stock, L.M., 1976. The Mechanism of Aromatic Nitration Reactions. ACS Symposium Series, Vol. 22, Chapter 2, 48-72.

Strazzolini, P., Runcio, A., 2003. Oxidation of benzylic alcohols and ethers to carbonyl derivatives by nitric acid in dichlorometane. European Journal of Organic Chemistry, 526-536.

Suh, Y.K., Kang, S., 2010. A review on mixing in microfluidics. Micromachines 1, 82-111.

Susana, L., Beatriz, I., Norma, A., 2001. Oxidation of toluene to benzaldehyde over VSb0.8TiO2O4: effect of operating conditions. Catalysis Today 64, 179-187.

Taft, R.W., 1952. The dependence of the rate of hydration of isobutene on the acidity function, H_0, and the mechanism for olefin hydration in aqueous acids. Journal of the American Chemical Society 74(21), 5372-5376.

Thomazeau, C., Olivier-Bourbigou, H., Magnam L., Luts, S., Gilbert, B,M., 2003. Determination of an acidic scale in room temperature ionic liquids. Journal of the American Chemical Society 125(18), 5264-5265.

Tomikawa, K., Kanno, H., 1998. Raman study of sulfuric acid at low temperatures. Journal of Physical Chemistry A 102, 6082-6088.

Traverso, P.G., Marziano, N.C., Passerini, R.C., 1977. The M_C activity coefficient function for acid-base equilibria. Part 4. Limitations of empirical relationships involving observed nitration rates and acidity functions. Journal of the Chemical Society, Perkin Transactions 2, 845-847.

Tromans, D., 1998. Oxygen solubility modelling in inorganic solutions: concentration, temperature and pressure effects. Hydrometallurgy 50, 279-296.

Urbanski, T., 1964. Chemistry and Technology of Explosives; Pergamon Press, PWN-Polish Scientific Publishers: Warszawa, Vol. 1.

van Woezik, B.A.A., Westerterp, K.R., 2001. Runaway behaviour and thermally safe operation of multiple liquid – liquid reaction in the semi-batch reactor. The nitric acid oxidation od 2-octanol. Chemical Engineering and Processing 41, 59-77.

Venkatesan, H., Hocutt, F.M., Jones, T.K., Rabinowitz, M.H., 2010. A one-step synthesis of 2,4-unsubstituted quinoline-3-carboxylic acid esters from o-nitrobenzaldehydes, Journal of Organic Chemistry Note 75, 3488-3491.

Walrafen, G.E., Yang, W.H., Chu, Y.C., 2002. High-temperature raman investigation of concentrated sulfuric measurement of H-bond ΔH values between H_3O^+ or $H_5O_2^+$ and HSO_4^-. Journal of Physical Chemistry A 106, 10162-10173.

Wang, Y., Tam, W., Stevenson, S.H., Clement, R.A., Calabrese, J., 1988. New organic non-linear optical materials of stilbene and diphenylacetylene derivatives. Chemical Physics Letters 148, 136-141.

Wang, M., Kaur, H., Chen, C.C., 2017. Thermodynamic modeling of HNO_3-H_2SO_4-H_2O ternary system with symmetric electrolyte NRTL model. AIChE Journal 63(7), 3110-3117.

Watts, P., Haswell, S.J., 2005. The application of microreactors for small scale organic synthesis. Chemical Engineering & Technology 28, 290-301.

Westerterp, K.R., Molga, E.J., 2006. Safety and runaway prevention in batch and semibatch reactors – a review. Chemical Engineering Research and Design 84(7), 543-552.

Wheland, G.W., 1942. A quantum mechanical investigation of the orientation of substituents in aromatic molecules. Journal of the American Chemical Society 64, 900-908.

Wiss, J., Fleury, C., Fuchs, V., 1995. Modelling and optimization of semi-batch and continuous nitration of chlorobenzene from safety and technical viewpoints. Journal of Loss Prevention in the Process Industries 8(4), 205-213.

Wong-Hawkes, S.Y., Matteo, J.C., Warrington, B.H., White, J.D., 2006. Microreactors ad new tools for drug discovery and development. Ernst Schering Foundation Symposium Proceedings 3, 39-55.

Yan, R., Yang, P., Li, Z., Wang, H., Diao, Y., Wang, L., Zhang, S., 2011. Synthesis of 2-Nitrobenzaldehyde in the Presence of Ionic Liquids, Advanced Materials Research 233-235, 1146-1151

Zaldivar, J.M., Barcons, C., Hernandez, H., Molga, E., Snee, T.J., 1992. Modelling and optimization of semibatch toluene mononitration with mixed acid from perfomance and safety viewpoints. Chemical Engineering Science 47(9-11), 2517-2522.

Zaldivar, J.M., Hernandez, H., Nieman, H., Molga, E., Bassani, C., 1993. The FIRES project: experimental study of thermal runaway due to agitation problems during toluene nitration. Journal of Loss Prevention in the Process Industries 6(5), 319-326.

Zaldivar, J.M., Molga, E., Alos, M.A., Hernandez, H., Westerterp, K.R., 1995. Aromatic nitrations by mixed acid. Slow liquid – liquid reaction regime. Chemical Engineering and Processing 34, 543-559.

Zaldivar, J.M., Cano, J., Alos, M.A., Sempere, J., Nomen, R., Lister, D., Maschio, G., Obertopp, T., Gilles, E.D., Bosch, J., Strozzi, F., 2003. Journal of Loss Prevention in the Process Industries 16, 187-200.

Zhang, X., Stefanick, S., Villani, F.J., 2004. Application of microreactor technology in process development. Organic Process Research & Development 8, 455-460.